

# RL-MPC for Autonomous Greenhouse Control

Combining RL and MPC to maximize  
the economic benefit of a Greenhouse

Systems and Control Masters Thesis  
Murray Harraway

# RL-MPC for Autonomous Greenhouse Control

Combining RL and MPC to maximize  
the economic benefit of a Greenhouse

by

Murray Harraway

Student Name	Student Number
Murray Harraway	5827973

Supervisor: Tamas Keviczky  
Daily Supervisor: R.D. McAllister  
Project Duration: November 2023–August 2024  
Faculty: Delft Center for Systems and Control, Delft



# Preface

*A preface...*

*Murray Harraway  
Delft, June 2024*

# Abstract

- *Background*
- *Aim*
- *Method*
- *Results*
- *Conclusion*

# Contents

<b>Preface</b>	i
<b>Summary</b>	ii
<b>Nomenclature</b>	v
<b>1 Introduction</b>	1
1.1 Problem Statement . . . . .	2
1.2 Thesis Contribution . . . . .	3
1.3 Recent and Related Developments . . . . .	3
1.4 Thesis Outline . . . . .	3
<b>2 Background</b>	5
2.1 Greenhouse Model . . . . .	5
2.1.1 Model Description . . . . .	6
2.1.2 Model State Equations . . . . .	7
2.1.3 Uncertainty in this Thesis . . . . .	10
2.1.4 Optimization Goal . . . . .	11
2.2 Reinforcement Learning . . . . .	12
2.2.1 The RL problem . . . . .	13
2.2.2 Q learning . . . . .	15
2.2.3 Policy Optimization . . . . .	15
2.2.4 Actor-Critic . . . . .	15
2.2.5 SAC . . . . .	16
2.3 MPC . . . . .	16
2.3.1 The General MPC problem . . . . .	16
2.3.2 Economic Model Predictive Control (EMPC) . . . . .	17
2.4 RL and MPC in tandem . . . . .	18
2.4.1 The Optimality . . . . .	19
2.4.2 Computational Effort . . . . .	19
2.4.3 The Prediction Horizon . . . . .	19
<b>3 Reinforcement Learning Setup</b>	21
3.1 Environment Description . . . . .	21
3.2 Experimental Setup . . . . .	23
3.3 Hyper-parameter Tuning . . . . .	24
3.4 Deterministic Results . . . . .	25
3.4.1 Discount Factor . . . . .	25
3.4.2 Activation Function . . . . .	28
3.4.3 Final Results and Conclusion . . . . .	28
3.5 Stochastic Results . . . . .	30
3.5.1 Conclusion . . . . .	31
3.6 Trained Value Function . . . . .	31
3.6.1 Temporal Difference Learning . . . . .	31
3.6.2 Expected Return Learning . . . . .	34
3.6.3 Results . . . . .	37
3.7 Conclusion . . . . .	41
<b>4 Model Predictive Control Setup</b>	42
4.1 Greenhouse MPC problem formulation . . . . .	42
4.2 Deterministic Results . . . . .	43

4.3 Stochastic Results . . . . .	45
4.4 Conclusion . . . . .	47
<b>5 Deterministic RL-MPC</b>	<b>48</b>
5.1 Implementation . . . . .	48
5.1.1 RL-MPC problem formulations . . . . .	48
5.1.2 Initial RL and MPC performance . . . . .	51
5.2 Results - Implementations 1 . . . . .	51
5.3 Results - Implementations 2 . . . . .	52
5.4 Results - Implementation 3 . . . . .	53
5.5 Results - Implementation 4 . . . . .	54
5.6 Results - Implementation 5 and 6 . . . . .	55
5.7 Final Result and Conclusion . . . . .	56
<b>6 Stochastic RL-MPC</b>	<b>58</b>
6.1 Initial RL and MPC Performance . . . . .	58
6.2 Results - VF and Terminal Region . . . . .	60
6.3 Conclusion . . . . .	61
<b>7 Computational Speed Up of RL-MPC</b>	<b>63</b>
7.1 Reducing Neurons and Hidden Layers . . . . .	63
7.2 Taylor Approximation . . . . .	66
7.3 Combined . . . . .	66
7.4 Discussion and Conclusion . . . . .	67
<b>8 Discussion and Conclusion</b>	<b>69</b>
8.1 Discussion . . . . .	69
8.2 Conclusion . . . . .	69
8.3 Recommendations & Future Work . . . . .	69
<b>References</b>	<b>70</b>
<b>A RL &amp; RL Training</b>	<b>74</b>
A.1 Overview of RL Algorithms . . . . .	74
A.2 Selection of RL Algorithm . . . . .	74
A.3 Agent Training . . . . .	76
A.4 Value Function Training . . . . .	76
<b>B RL-MPC</b>	<b>77</b>

# Nomenclature

If a nomenclature is required, a simple template can be found below for convenience. Feel free to use, adapt or completely remove.

## Abbreviations

Abbreviation	Definition
ISA	International Standard Atmosphere
...	

## Symbols

Symbol	Definition	Unit
$V$	Velocity	[m/s]
...		
$\rho$	Density	[kg/m <sup>3</sup> ]
...		

# 1

## Introduction

The world population is set to increase to a staggering 10 billion people in the year 2050 [1], increasing food demand substantially. Currently, 800 million people are chronically hungry, with 2 billion people suffering from micronutrient deficiencies [2]. The situation is compounded by the anticipated rise in food demand, which is expected to increase from 30% to 62% between the years 2010 and 2050, resulting in 30% of the population being at risk of hunger [3]. As such, there is a pressing need to enhance food production by at least 70% [4]. Although large investments have been made to increase food productivity, food losses, waste, and climate change continue to serve as significant constraints [2]. To meet these food demands, agriculture space has drastically increased [5]; however, an increase in agriculture land space has led the sector to account for almost 15% of the world's energy consumption while also accounting for more than 70% of water consumption [4]. The need for more efficient use of space and resources is clear to increase food demands while limiting space and resource usage. Although greenhouses have been extensively used to combat these problems and have been shown to reduce the environmental burden as compared to typical open-land production [6], they still require about 10 times more energy consumption compared to traditional farming [4]. This increase in energy is owed to the drastic increase in greenhouse operating costs. Moreover, with the soaring operating energy costs associated with greenhouses and a global trend indicating an increase in gas and electricity prices [7], growers are under increasing pressure to adopt more effective growing methods. As a result, agreement policies have been signed to reduce the CO<sub>2</sub> emissions of these greenhouses to an acceptable level [8].

These structures are designed to enhance crop yield per hectare by utilizing climate-controlled environments [9]. These smart greenhouses are essential in combating the degrading effects of climate change on crop quality and yield. However, efficiently maintaining such an environment, especially for economic profit, requires advanced control methods. These control methods must be able to adjust factors such as temperature, humidity, lighting, and CO<sub>2</sub> levels to accommodate ideal conditions for crop growth [10] whilst keeping energy costs at a minimum. Growing crops in a controlled environment can ensure the extension of their growing season as well as protection from outside temperature and weather changes. The advent of smart and advanced greenhouses necessitates skilled labor for operation, contributing to a scarcity of qualified personnel [11]. Coupled with the escalating labour costs, the move to autonomous greenhouses is an attractive idea.

Common controllers nowadays is the use of computers for the control of actuators, adjusting conditions based on set points manually specified by the grower [12]. While these techniques exist, often called automatic greenhouses, the growth of crops still heavily relies on the expertise of the grower. Due to the numerous factors that affect crop growth, determining the optimal set-points becomes highly complex. The complexity is further intensified by the fact that the development of a plant is highly influenced by the control inputs taken days or even weeks in advance. Therefore, it is crucial to strategically choose control inputs now in order to maximise future rewards, such as economic profit. In order to achieve

this, control strategies such as Reinforcement Learning (RL) and Model Predictive Control (MPC) can be implemented [12]. Both strategies provide optimal control to pursue the same goal, which is optimizing a reward/cost function. Both control schemes have their own advantages and disadvantages. However, there is a notable similarity between the two, suggesting that combining them could lead to a more efficient solution for autonomous greenhouse control.

While both RL and MPC are used for optimal control, RL focuses on learning from interactions with an environment to maximize long-term rewards, while MPC leverages model-based predictions and optimization to determine optimal control actions over a finite time horizon. Several methods are available that seek to integrate the two control schemes, shedding light on the strengths and weaknesses of the resulting controller with respect to its specific application. There are two main methods for combining RL and MPC: using MPC as the function approximator for the RL agent, or modifying the MPC's objective function and terminal constraints to incorporate RL knowledge. The latter approach allows the learned knowledge from RL to guide and improve the performance of the MPC controller, potentially leading to more effective and adaptive control strategies. It is this approach that will be investigated in this thesis.

## 1.1. Problem Statement

RL's ability to learn from interactions with a highly complex environment leads to its ability to learn the optimal behaviour, even in the presence of uncertainty. However, the quality of control is strongly influenced by the training of the RL algorithm. Moreover, RL does not directly impose state constraints. While it is possible to indirectly incorporate these constraints in the reward function with penalty functions, such an approach does not ensure that the optimal policy obtained will always adhere to these constraints. Moreover, the value function obtained through RL is only an approximation, this becomes an issue when the problem at hand is safety critical. Finally, RL faces a limitation in online flexibility due to its reliance on a feed-forward pass for policy evaluation.

In contrast, the quality of the solution obtained through MPC is subject to the accuracy of the prediction model, which is often simplified to reduce the computational burden, especially with non-convex dynamics, which may lead to sub-optimal control. Nevertheless, MPC is recognized for its sample efficiency, robustness and constraint handling. However model mismatch and uncertainties in forecasted disturbances can lead to a significant deterioration in control effectiveness.

Arguably, the most crucial characteristic of both control strategies lies in their respective prediction horizon. Both controllers utilise future information to determine the optimal control actions. MPC achieves this by employing explicit optimization over a finite prediction horizon, while RL explores and interacts with its environment to optimise for both immediate and long-term rewards. Hence, a shortcoming of MPC is the finite prediction horizon. This limitation becomes even more pronounced when dealing with sparse rewards and slow system dynamics. In such cases, actions taken at the current time step may only yield rewards past the prediction horizon, causing the MPC controller to be myopic. It is possible to counteract this drawback with an extended prediction horizon, but at the detriment of simplicity and computational efficiency of the controller. In general, there are no closed-loop performance guarantees for an MPC that optimises for economic benefit (EMPC). Importantly, two main methods exist to assure closed-loop performance: to use a sufficiently large horizon or the application of an appropriate terminal constraint and/or terminal cost function.

While MPC's prediction horizon is finite, RL utilizes a discounted infinite prediction horizon which allows the RL agent to weigh the benefit of future rewards on current actions. The exploration present in RL allows it to discover patterns and optimal policies, that a typical MPC might not be able to achieve, particularly in environments characterised by non-linear dynamics. A synergistic approach to combining the two control strategies would be to have a MPC controller optimize a short prediction horizon while propagating future information provided by RL. This integration of the two controllers is further justified in the context of greenhouse dynamics, where actions executed at the current time step may result in rewards that manifest over the long term. The terminal cost function in the MPC formulation, which must encapsulate information beyond the prediction horizon, underscores the clear connection with the value function obtained through RL to supply the necessary information for achieving the desired system performance. Notably, this may also be viewed as unrolling the value function  $N$

times, and performing an N-step look-ahead minimization on the resulting equation. Nevertheless, incorporating the learned value function (typically a neural network RL) in the MPC's formulation introduces additional complexity to the problem due to its highly non-linear nature. Consequently a naive implementation of this control strategy could have severe detrimental effects. Alternatively, the RL policy can also provide the MPC with a terminal region or constraint to more effectively guide it towards a control policy that is closer to the optimal solution.

Therefore, in the development of the RL-MPC algorithm, for greenhouse control, the following research questions will be answered:

- *How does the economic performance of the RL-MPC algorithm compare to the standalone RL and MPC algorithms?*
  - *In a deterministic environment*
  - *In a stochastic environment*
- *What modifications and/or approximations can be employed to reduce the computational time of the RL-MPC algorithm?*

## 1.2. Thesis Contribution

In answering the above questions leads to several contributions in the field. Notably, among the existing works, there is a scarcity of algorithms that independently train a RL agent and subsequently employ MPC for the N-step look-ahead minimization. Specifically, none of the algorithms identified in the related literature utilize MPC for the specified N-step look-ahead minimization on the pretrained value function during online play, particularly in scenarios involving continuous state and action spaces. Lastly, it's worth noting that all the proposed RL-MPC algorithms are applied in the context of set-point or tracking regulation and are not explicitly geared towards maximizing economic benefits. Therefore, the main contribution of this thesis will involve developing and implementing a framework that incorporates a learned value function of RL into a economic non-linear model predictive controller (ENMPC) for a continuous state and action space, and making such an algorithm generate on-time control actions. A greenhouse poses as a suitable environment and system for the development of such an algorithm due to its non-linear dynamics and continuous state and action spaces. Importantly, the objective of a greenhouse is to maximize profits from the cultivation and sale of crops. In the context of greenhouse operations, it is noteworthy that the primary objective is to maximize profits. This goal typically does not entail specific setpoint and/or tracking regulations for crop growth.

## 1.3. Recent and Related Developments

Various literature exists that explores the implementation of RL and MPC [13]–[17] as well as some that delve into the theoretical background of such a controller [14], [18]–[20]. Most notably, the works in [13], [17], [18], [20] are the most similar to what is proposed in this thesis. Whereby a RL agent is trained and resulting learned value function is unrolled with the bellman equation. During online play, the optimal action to take is computed by performing an l-step look-ahead minimization on the unrolled equation. However works from [13], [14], [20] are the only that incorporate a MPC for the l-step look-ahead minimization. However the authors propose that the reinforcement learning process could be learned assisted with MPC, however this might impact the agents exploratory nature. Nonetheless, in all cases, the RL-MPC algorithm has shown to outperform its RL counterpart. A more comprehensive analyses of the related literature may be found in the literature review.

## 1.4. Thesis Outline

The subsequent sections of the thesis are outlined as follows. This thesis begins by discussing the necessary background knowledge in chapter 2. This chapter presents the greenhouse model that will be utilised and the rationale behind its selection. It also outlines the optimisation objective of the RL, MPC, and the combined RL-MPC controllers. In addition, this chapter will present the concepts of RL, MPC, and RL-MPC to the readers. chapter 3 explores the procedure of establishing and training the RL agent in two different environments: one without uncertainty (the nominal case) and one

with uncertainty (the stochastic case). The chapter also examines the performance of the resulting agent in its respective environments. Moreover, this chapter explores the process of training accurate value functions using a fixed RL policy and discusses the obtained outcomes. Chapter 4 entails the formulation of the optimal control problem for the MPC and discusses the performance of the MPC in an environment with and without uncertainty. Chapter 5 examines the various implementations of the RL-MPC controller and evaluates their performance on the nominal case. Chapter 6 applies the best RL-MPC implementations from Chapter 5 to a stochastic environment and discusses the findings. The penultimate chapter, Chapter 7, explores the ways in which the RL-MPC implementation can be optimised for computational efficiency and emphasises the significance of these optimisations. The thesis concludes with a presentation of the conclusion and future research in Chapter 8, along with a draft research paper provided in Appendix C.

# 2

## Background

This chapter provides an overview of the relevant background information used in completing this thesis. This chapter centres around the chosen greenhouse model and the rationale behind its selection. It delves into the principles of RL and MPC, and finally provides information on the necessity of combining these algorithms.

### 2.1. Greenhouse Model

The accuracy and complexity of the model at hand directly impacts the quality of the control. The dynamics of a greenhouse can be characterized through various modeling approaches depending on its application. Methods such as Computational FLuid Dynamics (CFD) are used to develop numerical models of the indoor climate of a greenhouse using partial differentiable equations. In recent years, CFD simulations have become increasingly more accurate in simulating indoor greenhouse climate [21], however extensive knowledge and computational power of the system is required. Their complexity makes them intractable for mathematical solvers such as MPC and they present substantial challenges for learning in model-free methods, resulting in a demanding and laborious training process [22]. Simplified models of greenhouse dynamics are developed by assuming homogeneity in the greenhouse climate and neglecting the impact of wall effects. Additional assumptions about  $CO_2$  and humidity are incorporated to yield a model conducive to control applications, as discussed in [22], [23]. While these simplified models sacrifice some accuracy in representing the system, they significantly reduce computational demands, thereby making them tractable for mathematical solvers. These mechanistic process models are often derived from first principles and use ordinary differential or difference equations to represent the system dynamics. In contrast, Data-drive models such as in [24] and [25] have also been used to create a black box model of the greenhouse dynamics. Although such models may yield accurate results, they do so only in the environment wherein the data originates from, whereas mechanistic process models often generalize better to different environments and situations. Although such black box models may be used for RL, they could pose challenges for mathematical solvers due to their potential complexity and/or unknown mathematical makeup. Similar models and scenarios exist for crops. In some cases, it is possible to model crops with a single variable (namely the crop dry weight) given the climate conditions for simple crops, such as lettuce [26]. However, for more complicated crops such as tomatoes and cucumber additional information is required to describe their growth behaviour and life cycle stages [27].

Although accurate models may seem appealing, they are often exhibit complexity and entail a high-dimensional state-space. Both factors have adverse effects on model-free RL algorithms and MPC, making such models impractical for the development of optimal control policies. This arises from the fact that, in the case of MPC, finding a tractable solution within the given time constraints may prove challenging. Consequently, it might fail to meet timing requirements and constraints, or even find no solution at all. Similarly, in the context of model-free RL algorithms, the use of highly accurate models could destabilize the learning procedure, making it a more difficult and time-consuming task to learn a policy [28], [29]. Therefore, for optimal control, is it desirable to use a low-dimensional simplified

model whereby the most important dynamics of the system is still captured. Moreover, the control law obtained from the simplified model may be adjusted and applied to the more accurate models in order to validate them. If however, the control law is not satisfactory, the simplified model must be adapted and a new control policy obtained. Often this leads to an iterative cycle of updating the model and validating the obtained control policy until a satisfactory performance on the high-accurate model is obtained [30]. Since the thesis focuses on the impact and implementation of merging RL and MPC for optimal control, it is outside of the scope to design and develop a model. Therefore a validated simplified mechanistic model of a greenhouse with lettuce crops will be selected. Although data driven models may mimic a simplified mechanistic process, a mechanistic process is required for a model predictive controller. Due to the relative simplicity of lettuce crop models, they find utility alongside a greenhouse model that assumes an indoor homogeneous climate. A model, which encapsulates the fundamental dynamics of the greenhouse and crops, is detailed in [31] and has been explicitly developed for optimal control applications. More importantly, the model proposed in [31] has been validated in [32], and has been extensively utilised in obtaining optimal control policies such as in [9], [16], [22], [33], [34]. Therefore, the choice was made to utilise the model suggested in [31] for this thesis.

### 2.1.1. Model Description

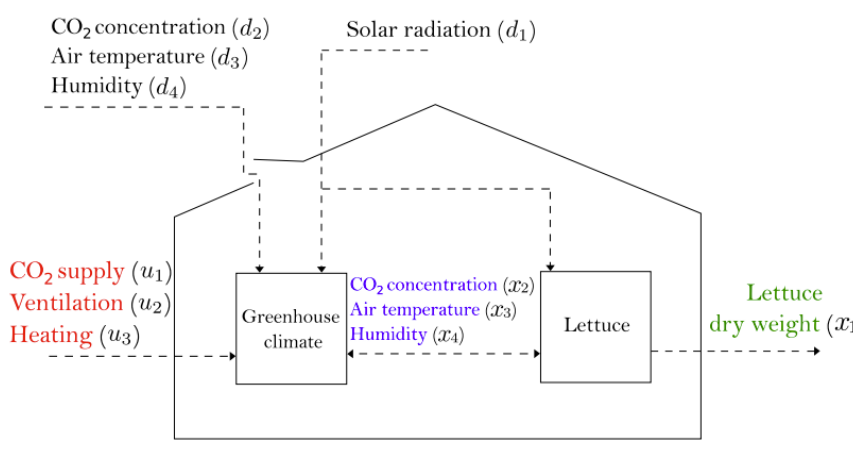


Figure 2.1: Graphical representation of the greenhouse crop production process [31]

Figure 2.1 displays a graphical representation of the used greenhouse model from the works of [31]. The control inputs are highlighted in red, the states of the indoor climate in blue, the state of the crops in green and the external disturbances given in black. The states of the system, control inputs, disturbances and outputs are described in Equation 2.1 where  $x \in \mathbb{X}^4$ ,  $u \in \mathbb{U}^3$ ,  $d \in \mathbb{D}^4$  and  $y \in \mathbb{Y}^4$ .

$$\begin{aligned} x(k) &= [x_d \quad x_{CO_2} \quad x_T \quad x_h]^T \\ u(k) &= [u_{CO_2} \quad u_v \quad u_q]^T \\ d(k) &= [d_{Io} \quad d_{CO2} \quad d_T \quad d_h]^T \\ y(k) &= [y_d \quad y_{CO_2} \quad y_T \quad y_{RH}]^T \end{aligned} \tag{2.1}$$

The state of the system includes Crop dry mass,  $C0_2$  density within the greenhouse, the temperature inside the greenhouse and the absolute humidity within the greenhouse. Crop dry mass is used since it is a more reliable and accurate measure of the biomass of the plant. Unlike fresh weight, which varies with the plant's water content which is in turn influenced by weather conditions, crop dry mass provides a more stable and consistent metric. The control vector encapsulates the  $C0_2$  injection rate, ventilation rate and the heating supply. Furthermore, the disturbances from the weather include the incoming solar radiation, ambient  $C0_2$  density, ambient temperature and the ambient humidity content. The measured output is largely the same as the state of the system however the units of the indoor

$\text{CO}_2$  density and relative humidity differ in that they report in units as used in standard measurement sensors. The non-linear continuous time dynamics is modelled by Equation 2.2

$$\begin{aligned}\dot{x} &= f(x(t), u(t), d(k), p) \\ y(k) &= g(x(k), u(k), d(k), p)\end{aligned}\quad (2.2)$$

where  $p$  are the value of the parameters used in the model and displayed in Table 2.2,  $x$  is the model state,  $y$  is the measurement outputs and  $d$  is the weather disturbance. The next section delves deeper into the model's state equations.

### 2.1.2. Model State Equations

**State Equations** The model described in [31] is fully described by the crop dry weight, temperature, humidity and  $\text{CO}_2$  levels of the indoor climate. All variables and their units are given in Table 2.1 and model constants in Table 2.2. These states are modeled through a set of ordinary differentiable equations where the change of crop state is represented as

$$\frac{dX_d}{dt} = c_{\alpha\beta}\phi_{phot,c}(t) - \phi_{resp,d}(t) \quad (2.3)$$

where  $c_{\alpha\beta}$  is the crop yield factor,  $\phi_{phot,c}$  is the gross carbon dioxide uptake from canopy photosynthesis (also referred to as canopy photosynthesis rate) and  $\phi_{resp,d}$  is the maintenance respiration rate of the respired dry matter. The greenhouse  $\text{CO}_2$  density is described through

$$\frac{dX_{\text{CO}_2}}{dt} = \frac{1}{c_{cap,c}}(-\phi_{phot,c}(t) + \phi_{resp,c}(t) + u_{\text{CO}_2}(t) \cdot 10^{-6} - \phi_{vent,c}(t)) \quad (2.4)$$

where  $c_{cap,c}$  is the volumetric  $\text{CO}_2$  capacity of the greenhouse,  $\phi_{resp,c}$  is the respiration rate of  $\text{CO}_2$  of the crop and  $\phi_{vent,c}$  is the leakage of  $\text{CO}_2$  through the vents of the greenhouse. Similarly, the change in greenhouse temperature is modeled by the following ODE:

$$\frac{dX_{\text{Temp}}}{dt} = \frac{1}{c_{cap,q}}(u_q(t) - Q_{vent,q}(t) + Q_{Io,q}(t)) \quad (2.5)$$

where  $c_{cap,q}$  is the effective heat capacity of the greenhouse,  $Q_{vent,q}(t)$  describes the heat energy exchange between the outside climate and the indoor climate through the greenhouse cover and vents and lastly  $Q_{Io,q}(t)$  denotes the heat energy received from the incoming irradiance.

Finally, the humidity of the greenhouse is described by

$$\frac{dX_H}{dt} = \frac{1}{c_{cap,h}}(\phi_{transp,h}(t) - \phi_{vent,h}(t)) \quad (2.6)$$

whereby  $c_{cap,h}$  is the volumetric humidity capacity of the greenhouse,  $\phi_{transp,h}$  models the transpiration rate of the canopy and  $\phi_{vent,h}$  is the leakage of water vapour through the vents of the greenhouse.

**Process Equations** The gross canopy photosynthesis rate  $\phi_{phot,c}$  is defined as below:

$$\phi_{phot,c}(t) = (1 - e^{-C_{LAI,d}x_d(t)}) \frac{c_{Io}^{phot} d_{Io}(t) \cdot \phi(t)}{c_{Io}^{phot} d_{Io}(t) + \phi(t)} \quad (2.7)$$

where  $C_{LAI,d}$  is the effective canopy surface and  $c_{Io}^{phot}$  is the light use efficiency.  $\phi(t)$  is unit-less as is calculated below as:

$$\phi(t) = (-c_{\text{CO}_2,1}^{phot} x_T(t)^2 + c_{\text{CO}_2,2}^{phot} x_T(t) - c_{\text{CO}_2,3}^{phot})(x_{\text{CO}_2}(t) - c^{phot}) \quad (2.8)$$

where  $c_{C0_2,1}^{phot}$ ,  $c_{C0_2,2}^{phot}$ ,  $c_{C0_2,3}^{phot}$  indicate the effect of temperature on the gross canopy synthesis rate and  $c^{phot}$  is the  $C0_2$  compensation point. The maintenance respiration rate of the crop dry matter is described as:

$$\phi_{resp,d}(t) = c_{resp,d} \cdot \phi_{resp}(t) \quad (2.9)$$

where  $c_{resp,d}$  is the respiration rate coefficient of the crop dry matter respiration,  $\phi_{resp}(t)$  is the respiration maintenance and can be calculated by:

$$\phi_{resp}(t) = x_d(t) \cdot c_{Q_{10},resp}^{(x_T(t)-25)/10} \quad (2.10)$$

where  $c_{Q_{10},resp}$  indicates the maintenance respiration factor and shows how the respiration maintenance of the crops doubles for every increase of  $10^{\circ}\text{C}$  and vice versa. Similarly. the  $C0_2$  respiration rate of the crop is calculated by:

$$\phi_{resp,c}(t) = c_{resp,C0_2} \cdot \phi_{resp}(t) \quad (2.11)$$

where  $c_{resp,C0_2}$  is the respiration rate coefficient of  $C0_2$  release of the crop. Furthermore, the mass exchange of  $C0_2$  is calculated by:

$$\phi_{vent,c}(t) = (u_v(t) \cdot 10^{-3} + c_{leak})(x_{C0_2}(t) - d_{C0_2}(t)) \quad (2.12)$$

where  $c_{leak}$  represents the ventilation leakage through the greenhouse cover. Heat energy exchange through the greenhouse cover and vents is described by:

$$Q_{vent,q}(t) = (c_{cap,v}u_v(t) + c_{go})(x_T(t) - d_T(t)) \quad (2.13)$$

where  $c_{cap,v}$  is the heat capacity per volume of greenhouse air and  $c_{go}$  is the heat energy exchange through the greenhouse cover. The heating provided by the irradiance is described by:

$$Q_{I_o,q}(t) = c_{og}^{rad}d_{I_o}(t) \quad (2.14)$$

Here,  $c_{og}^{rad}$  serves as an indicator of the proportion of heating supplied by the irradiance within the greenhouse. Finally. the canopy transpiration rate  $\phi_{transp,h}(t)$  and the mass exchange of water vapour through the vents and leaks,  $\phi_{vent,h}(t)$  can be expressed:

$$\phi_{transp,h}(t) = c_{ca}^{evap}(1 - e^{-C_{LAI,d}x_d(t)}) \cdot \left( \frac{c_{H_2O,1}^{sat}}{c_R(x_T(t) + c_T)} e^{\frac{c_{H_2O,2}x_T(t)}{x_T(t) + c_T}} - x_h(t) \right) \quad (2.15)$$

$$\phi_{vent,h}(t) = (u_v(t) \cdot 10^{-3} + c_{leak})(x_h(t) - d_h(t)) \quad (2.16)$$

**Output Measurement Equations** The output measurements for the indoor humidity and  $C0_2$  levels are reported in different units via the function  $g_{C0_2}(\cdot)$  and  $g_h$ . respectively. The output measurements for crop dry mass and indoor temperature correspond to the state variables, as illustrated below:

$$\begin{aligned} y_d(t) &= x_d(t) \\ y_{C0_2}(t) &= g_{C0_2}(x_T(t), x_{C0_2}(t)) \\ y_T(t) &= x_T(t) \\ y_{RH} &= g_h(x_T(t), x_h(t)) \end{aligned} \quad (2.17)$$

$$g_{C0_2}(z_T(t), z_{C0_2}(t)) = 10^3 \cdot \frac{R(z_T(t) + c_T)}{PM_{C0_2}} \cdot z_{C0_2}(t) \quad (2.18)$$

$$g_h(z_T(t), z_h(t)) = \frac{R(z_T(t) + c_T)}{c_{H_20,4}^{sat} \cdot \exp(\frac{c_{H_20,5}^{sat} z_T(t)}{z_T(t) + c_{H_20,6}^{sat}})} \cdot z_h(t) \quad (2.19)$$

where  $R, c_T, P, M_{CO_2}, c_{H_20,4}, c_{H_20,5}, c_{H_20,6}$  are constants and their descriptions and units given in Table 2.2. To facilitate the use of MPC and RL on this model, the greenhouse was discretized in time. The fourth-order Runge Kutta method was used and results in the system equations below:

$$\begin{aligned} x(k+1) &= f(x(k), u(k), p) \\ y(k) &= g(x(k), u(k), p) \end{aligned} \quad (2.20)$$

[35] states that discretizing the van Henten model using a time-step between 15 minutes and 1 hour is recommended. Therefore, a time interval of 30 minutes was selected for the purpose of this study. The initial interval of 30 minutes was originally set at 15 minutes. However, this decision was revised due to the excessive computational burden it imposed on the MPC solver, with minimal benefits. Consequently, extending the time step enables an exponential speedup in the simulation of the 40-day period, while causing only minor deterioration in performance. As a consequence of this, there is a noticeable increase in the rate at which RL training occurs, thereby allowing for a larger quantity of training episodes.

Category	Symbol	Description	units
State Variables	$x_d$	crop dry matter	$kg \cdot m^{-2}$
	$x_{CO_2}$	Indoor CO <sub>2</sub> density	$kg \cdot m^{-3}$
	$x_T$	Indoor air temperature	°C
	$x_h$	Indoor absolute humidity content	$kg \cdot m^{-3}$
Control Inputs	$u_{CO_2}$	CO <sub>2</sub> injection rate	$mg \cdot m^{-2} \cdot s^{-1}$
	$u_v$	ventilation rate	$mm \cdot s^{-1}$
	$u_q$	Heating supply	$W \cdot m^{-2}$
Disturbance	$d_{I_o}$	Outside irradiation	$W \cdot m^{-2}$
	$d_{CO_2}$	Outdoor CO <sub>2</sub> density	$kg \cdot m^{-3}$
	$d_T$	Outside ambient air temperature	°C
	$d_h$	Outside absolute humidity content	$kg \cdot m^{-3}$
Outputs	$y_d$	Lettuce dry weight	$kg \cdot m^{-2}$
	$y_{CO_2}$	Indoor CO <sub>2</sub> concentration	ppm
	$y_T$	Indoor air temperature	°C
	$y_{RH}$	Indoor relative humidity content	%
Processes	$\phi_{phot,c}$	gross canopy rate	$kg \cdot m^{-2} \cdot s^{-1}$
	$\phi_{resp,d}$	Respired dry matter from maintenance respiration of the crop	$kg \cdot m^{-2} \cdot s^{-1}$
	$\phi_{resp,c}$	Crop CO <sub>2</sub> respiration rate	$kg \cdot m^{-2} \cdot s^{-1}$
	$\phi_{vent,c}$	Mass exchange of CO <sub>2</sub> between indoor and outdoor climate	$kg \cdot m^{-2} \cdot s^{-1}$
	$Q_{vent,c}$	Heat energy exchange between indoor and outdoor climate	$W \cdot m^{-2}$
	$Q_{I_o,q}$	Incoming Heat energy from outside irradiation	$W \cdot m^{-2}$
	$\phi_{transp,h}$	Canopy transpiration rate	$kg \cdot m^{-2} \cdot s^{-1}$
	$\phi_{vent,h}$	Mass exchange of water vapour between indoor and outdoor climate	$kg \cdot m^{-2} \cdot s^{-1}$

Table 2.1: Model Variables

Symbol	Description	Value	units
$c_{\alpha\beta}$	yield factor	0.544	-
$c_{cap,c}$	Volumetric $\text{CO}_2$ capacity of indoor air	4.1	$\text{m}^3[\text{air}] \cdot \text{m}^{-2}[\text{gh}]$
$c_{cap,q}$	Effective heat capacity of indoor air	30000	$\text{J} \cdot \text{m}^{-2}[\text{gh}] \cdot {}^\circ\text{C}$
$c_{cap,h}$	Volumetric humidity capacity of indoor air	4.1	$\text{m}^3[\text{air}] \cdot \text{m}^{-2}[\text{gh}]$
$c_{LAI,d}$	Effective canopy surface	53	$\text{m}^{-2}[\text{L}] \cdot \text{kg}^{-1}[\text{dw}]$
$c_{I_0}^{phot}$	Light use efficiency	$3.55 \cdot 10^{-9}$	$\text{kg}[\text{CO}_2] \cdot \text{J}^{-1}$
$c_{C0_2,1}^{phot}$	Influences temperature gross canopy photosynthesis	$5.11 \cdot 10^{-6}$	$\text{m} \cdot \text{s}^{-1} \cdot {}^\circ\text{C}^{-2}$
$c_{C0_2,2}^{phot}$	Influences temperature gross canopy photosynthesis	$2.30 \cdot 10^{-4}$	$\text{m} \cdot \text{s}^{-1} \cdot {}^\circ\text{C}^{-1}$
$c_{C0_2,3}^{phot}$	Influences temperature gross canopy photosynthesis	$6.29 \cdot 10^{-4}$	$\text{m} \cdot \text{s}^{-1}$
$c_{\text{CDCP}}$	Carbon dioxide compensation point	$5.2 \cdot 10^{-5}$	$\text{kg}[\text{CO}_2] \cdot \text{m}^{-3}[\text{air}]$
$c_{resp,d}$	Respiration rate of the dry crop matter	$2.65 \cdot 10^{-7}$	$\text{s}^{-1}$
$c_{Q10,resp}$	Maintenance respiration factor	2	-
$c_{resp,c}$	$\text{CO}_2$ release rate factor from respiration	$4.87 \cdot 10^{-7}$	$\text{s}^{-1}$
$c_{leak}$	greenhouse cover ventilation leakage	$7.5 \cdot 10^{-6}$	$\text{m} \cdot \text{s}^{-1}$
$c_{cap,v}$	heat capacity of indoor temperature per volume	1290	$\text{J} \cdot \text{m}^{-3}[\text{gh}] \cdot {}^\circ\text{C}^{-1}$
$c_{g^0}$	heat transmission through cover factor	6.1	$\text{W} \cdot \text{m}^{-2}[\text{gh}] \cdot {}^\circ\text{C}^{-1}$
$c_{rad}^{rad}$	solar heat load coefficient	0.2	-
$c_{ca}^{evap}$	vapour mass transfer factor between leaf and air	$3.6 \cdot 10^{-3}$	$\text{m} \cdot \text{s}^{-1}$
$c_{ca}^{sat}$	Influences water vapour saturation point	9348	$\text{J} \cdot \text{m}^{-3}$
$c_{H_2O,1}^{sat}$	Influences water vapour saturation point	17.4	-
$c_{H_2O,2}^{sat}$	Influences water vapour saturation point	239	${}^\circ\text{C}$
$c_{H_2O,3}^{sat}$	Influences water vapour saturation point	610.48	Pa
$c_{H_2O,4}^{sat}$	Influences water vapour saturation point	17.2694	-
$c_{H_2O,5}^{sat}$	Influences water vapour saturation point	238.3	${}^\circ\text{C}$
$c_{H_2O,6}^{sat}$	Influences water vapour saturation point		
$c_R$	Gas Constant	8314	$\text{J} \cdot \text{K}^{-1} \cdot \text{kmol}^{-1}$
$c_T$	For conversion between Kelvin and Celsius	273.15	K
$R$	Molar Gas constant	8.3144598	$\text{J} \cdot \text{mol}^{-1} \cdot \text{K}^{-1}$
$P$	Pressure at 1 atmospheric pressure	101325	Pa
$M_{\text{CO}_2}$	Molar Mass of $\text{CO}_2$	0.0441	$\text{kg} \cdot \text{mol}^{-1}$

Table 2.2: Model Constants

### 2.1.3. Uncertainty in this Thesis

In reality, uncertainty is present in all aspects of the model. In the case of the greenhouse environment, uncertainty may arise in the weather predictions, there may be measurement noise on the outputs and the control inputs may not be exact. Additionally, the simplified model leads to a model mismatch, which may result in significant prediction errors. As was done in [16], [36], the source of uncertainty in the stochastic environment is modeled as parametric uncertainty which aims to largely capture all of this uncertainty. Moreover, in the objective function (discussed further in subsection 2.1.4), the pricing of energy and the lettuce may also be stochastic, however it is assumed to be fixed, along with the weather predictions. It is not the focus of this thesis to accurately model the uncertainty in a greenhouse crop environment. However, it is important to observe the impact of uncertainty on the generated policy for each algorithm. This will help determine the performance of these controllers in a more realistic scenario. Thus, the parameters of the environment are represented as uncertain parameters with well-defined probabilistic properties. It is assumed that the uncertain parameters  $\hat{p}$  follow the uniform probabilistic distribution:

$$\hat{p} \sim U(\mu_p, \delta_p) \quad (2.21)$$

where  $\mu_p$  is the mean value of the parameters  $p$  (shown in Table 2.2), and  $\delta_p$  is expressed as a percentage where the upper and lower bounds of the distribution is expressed as  $p(1 - \delta_p)$  and  $p(1 + \delta_p)$ . It must be noted that since all parameters are perturbed, including parameters of the output measurement equations, output noise is also introduced. The uniform distribution was chosen for its higher level

of aggressiveness compared to the normal distribution. While it may not accurately represent the uncertainty at hand, it is a useful tool for evaluating the potential variability and risks associated with the various policies generated especially at higher degrees of uncertainty. Introducing this uncertainty results in the following system dynamics:

$$\begin{aligned}\hat{x}(k+1) &= f(\hat{x}(k), u(k), d, \hat{p}) \\ \hat{y}(k) &= g(\hat{x}(k), u(k), d, \hat{p})\end{aligned}\quad (2.22)$$

where the states and output measurements of the system are uncertain and  $\hat{p}$  denotes the uncertain parameters.

#### 2.1.4. Optimization Goal

Maximising the economic profit of the greenhouse is highly desirable. This concept essentially involves maximising the lettuce's size while minimising the resources used throughout its entire growth period. The optimisation goal can be modeled and is referred to by the economic profit indicator (EPI), as demonstrated below:

$$EPI = \sum_{ts}^{tf} (c_{price_1} \cdot u_1(t) + c_{price_2} \cdot u_2(t)) - c_{price_3} \cdot y_1(tf) \quad (2.23)$$

where  $t_s$  denotes the starting time,  $t_f$  the end time,  $c_{p1}, c_{p2}$  the pricing coefficients of injecting CO<sub>2</sub> and heating respectively and  $c_{p3}$  as the price of lettuce. These pricing factors are shown in Table 2.3. It is important to highlight that ventilation, such as opening windows, does not incur any costs and therefore does not have a pricing factor. Although it is also possible to optimize  $t_f$ , i.e. when is the best time to sell the lettuce, it is decided to keep the growing period fixed. The duration of the growing period for lettuce typically falls within the range of 30 to 50 days. Therefore, a fixed growing period of 40 days was selected. As a result, over a duration of 40 days (1 episode or 1 complete simulation), there is a total of:

$$k_{total} = \frac{\frac{40}{growing\ period} \cdot 24 \frac{hrs}{day} \cdot 60 \frac{min}{hr}}{30 \frac{min}{timestep}} = 1920 \frac{time\ steps}{growing\ period}$$

Moreover, this optimization goal is subject to constraints where the control constraints are:

$$\begin{aligned}u_{min} &= (0 \ 0 \ 0)^T \\ u_{max} &= (1.2 \ 7.5 \ 150)^T \\ \delta u_{max} &= \frac{1}{10} u_{max}\end{aligned}\quad (2.24)$$

and the state constraints are defined as:

$$\begin{aligned}y_{min} &= (0 \ 500 \ 10 \ 0)^T \\ y_{max} &= (\infty \ 1600 \ 20 \ 100)^T \\ \delta_u &= \frac{1}{10} u_{max}\end{aligned}\quad (2.25)$$

The values in question were obtained from typical horticultural practices. In many papers, such as in [36], the lower and upperbound of the indoor temperature is time-varying in order to aid MPC in making better decisions. It was decided to keep the lower and upper bounds of the temperature constant in order to fully test the RL and specifically the MPC in an economic optimization setting.

$c_{price_1}$	$3.4308 \cdot 10^{-4}$
$c_{price_2}$	$6.405 \cdot 10^{-5}$
$c_{price_3}$	22.285

**Table 2.3:** Pricing factors

The pricing factors includes the discrete time interval  $h$ , as well as the required conversions from  $mg$  to  $kg$  and joules to  $kWh$  for the C0<sub>2</sub> injection and heating, respectively. Furthermore,  $c_{p_3}$  incorporates the factor of harvestable fresh weight, which quantifies the amount of fresh weight relative to dry weight. Finally, the pricing of the C0<sub>2</sub> in €/kg, the price of heating in €/kWh and the pricing of lettuce in €/kg is also incorporated as shown in Equation 2.26

$$\begin{aligned} c_{p1} &= h \cdot C0_{2price} = 1800 \cdot \frac{0.1906}{10^6} \\ c_{p2} &= h \cdot Heating_{price} = 1800 \cdot \frac{0.1281}{3.6 \cdot 10^6} \\ c_{p3} &= (1 - c_\tau) \cdot c_{fw} \cdot Let_{price} = (1 - 0.07) \cdot 22.5 \cdot 1.065 \end{aligned} \quad (2.26)$$

The prices for  $C0_{2price}$ ,  $Heating_{price}$ , and  $Let_{price}$  were sourced from [37], while the factors for harvestable fresh weight,  $c_\tau$  and  $c_{fw}$ , were obtained from [31]. While these factors may not accurately reflect the present economic conditions, it is important to keep these factors constant when comparing the algorithms MPC, RL, and RL-MPC. This ensures a meaningful comparison between algorithms which aligns with one of the objectives of this thesis. This optimisation goal as shown in Equation 2.23 makes the reward incredible sparse, making it difficult to optimise this directly with both MPC and RL. Consequently, both algorithms utilise a stage costs/rewards received at every time interval, whereby the total sum of these stage costs over the duration of growth corresponds to the optimisation objective in Equation 2.23. section 3.1 and section 4.1 further discusses the implementation of Equation 2.23 for RL and MPC respectively.

## 2.2. Reinforcement Learning

With the surge in AI development, the demand for optimal greenhouse control has brought RL into the spotlight. Although AI algorithms are widely used in the farming and Horticulture industry, most of the application is centered around the detection and protection of plant and crop quality such as plant stress, pest, disease and weed detection [38]. Moreover, the prediction of crop yield and growth has also been an area of focus for AI owing to its unparalleled non-linear approximation capabilities [24]. Additionally, recent advancements in RL has displayed its ability to far outperform humans in decision making when presented with large complex problem spaces [39] due to its ability in finding the optimal control. Because of RL's ability to evaluate optimal control actions for large state spaces, it has shown great success such as in Google DeepMind's chess engine, AlphaZero, creating ones of the most powerful chess engines in the world. Furthermore, reinforcement learning has demonstrated exceptional proficiency in handling uncertainty and disturbances [40]. This makes it an ideal control strategy for greenhouse management, particularly considering the uncertainties inherent in weather conditions and crop growth.

Recently, research has focused on the optimization of crop growth and yield in greenhouse control, with studies such as [22], [41]–[46] employing reinforcement learning to address this challenge. This momentum has been fueled by initiatives like the Autonomous Greenhouse Challenge hosted by Wageningen University and Research first held in 2018 in which the challenge was designed to further push the limits of AI in fresh food production. In this competition, teams vie against each other to employ AI for optimizing cucumber crop growth in a climate-controlled greenhouse. Specifically, deep reinforcement learning policies have been applied and measured against each other, current control strategies and expert growers, showing promising results and in some cases, outperforming expert growers [37], [42]. As the years have progressed, an increasing number of teams have succeeded in

outperforming expert growers [37], [38]. Such achievements using reinforcement learning in a real-world application has displayed its potential in achieving complete autonomous greenhouse control.

### 2.2.1. The RL problem

Reinforcement Learning consists of four main components that define its nature: a policy, a reward signal, a value function and a model of the environment [47]. To further conceptualize the idea of RL, there exists an agent, environment and a reward signal that outlines the goal of the optimization problem (Figure 2.2). This agent explores and takes actions in the environment where at time  $k$  follows a policy  $\pi_k$  and the agent receives a reward  $R_k$  from the environment based on the action taken and the state of the agent. This policy is defined as a control law that maps the agent's states to probabilities of selecting each possible action that an agent can take [47]. The only objective of the agent is to maximize **this** reward, therefore the agent learns to make decisions and take actions that lead to favourable outcomes, as measured by the received rewards in the environment. Finally, the value function is defined as the expected future rewards based on the current state of the agent. Therefore the reward received is a measure of the immediate desire for an state, and the value function indicates the long-term desirability of a state. [47].

This interaction between agent and environment in Reinforcement Learning is modeled as a Markov Decision Process (MDP). The agent-environment interaction is as shown in Figure 2.2 and depicts the agents taking actions  $A_t$  in the environment and receiving reward  $R_{t+1}$  and transitioning to the next state  $S_{t+1}$  with probability  $P$  at every discrete time step  $k$ .

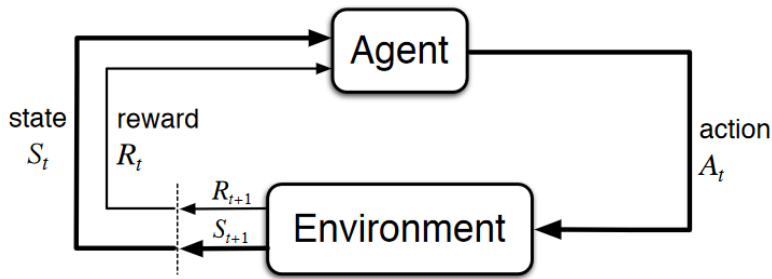


Figure 2.2: Agent-Environment Interface [47]

This interaction between agent and environment in Reinforcement Learning is modeled as a Markov Decision Process (MDP). This mathematical framework formalizes the decision process that satisfies the condition whereby future states depend only on the current state and action taken.

The agent-environment interaction is as shown in Figure 2.2 and depicts the agents taking actions  $A_t$  in the environment and receiving reward  $R_{t+1}$  and transitioning to the next state  $S_{t+1}$  with probability  $P$  at every discrete time step  $k$ . It is these cumulative rewards that the agent seeks to maximize over a specific time horizon. Furthermore the MDP problem can be characterized as a tuple of states, actions, rewards and a state transition function (model). Such that:

- states:  $(s \in S)$  where  $S$  is the finite state space.
- Actions  $(a \in A)$  where  $A$  is the finite action space
- Transition probability:  $P(s_{t+1}, r | s_t, a_t)$  where  $f : X \times U \rightarrow X$  is the state transition function
- Rewards:  $r : S \times A \rightarrow \mathbb{R}$  where  $r(s, a) = \mathbb{E}[R_t | S_{t-1} = s, A_{t-1} = a]$  is the reward function.

Furthermore, the agent follows a deterministic policy  $\pi$  that establishes a mapping from states to actions,  $\pi : S \rightarrow A$ . The optimal policy seeks to maximize the total expected return (cumulative reward) of the agent where the return,  $G_t$ , is defined as some specific function of the reward sequence [47] as shown in Equation 2.27.

$$G_t = R_{t+1} + R_{t+2} + R_{t+3} + \dots + R_T = \sum_{k=0}^T R_{t+k+1} \quad (2.27)$$

However this is only relevant for scenarios where there is a time horizon and/or an idea of a final time step  $T$  such as a task with some defined end point or events that are episodic in nature. This does not however extend to the greenhouse control problem as it does not necessarily follow naturally identifiable episodes, and therefore the notion of an infinite time horizon with discounted returns is introduced. Where the return function now becomes:

$$G_t = R_{t+1} + \gamma R_{t+2} + \gamma^2 R_{t+3} + \dots = \sum_{k=0}^{\infty} \gamma^k R_{t+k+1} = R_{t+1} + \gamma G_{t+1} \quad (2.28)$$

and the discount factor  $\gamma \in [0, 1]$ . Although the return (??) is a sum of an infinite number of terms, it is still finite if the reward is nonzero and constant if  $\gamma < 1$  [47]. As the discount factor,  $\gamma$ , approaches one, the more future rewards are considered. In contrast, values approaching zero render the agent "myopic", focusing solely on maximizing immediate rewards. The discount factor,  $\gamma$ , commonly fall within the range of 0.9 to 0.995 [37]. This is an important concept since it can be shown that if the rewards are bounded (i.e.  $\in \mathbb{R}$ ) and a discount value of  $\gamma < 1$  is used, then a stable optimal policy can be found [19]. There follows that a value function exists, under a specific policy  $\pi$  of a state  $s$ , denoted as  $v_\pi$  and defined as the expected return starting in state  $s$  and following the policy  $\pi$  thereafter. This value function is depicted below in Equation 2.29.

$$V_\pi(s) = \mathbb{E}_\pi [G_t | S_t = s] = \mathbb{E}_\pi \left[ \sum_{k=0}^{\infty} \gamma^k R_{t+k+1} | S_t = s \right], \forall s \in S \quad (2.29)$$

Given the absence of transition dynamics in a standard reinforcement learning (RL) problem, this can be extended for a state-action pair value function as in Equation 2.30 whereby  $Q_\pi$  denotes the expected return starting from state  $s$  and taking action  $a$ , under the policy  $\pi$  [41].

$$Q_\pi(s, a) = \mathbb{E}_\pi [G_t | S_t = s, A_t = a] = \mathbb{E}_\pi \left[ \sum_{k=0}^{\infty} \gamma^k R_{t+k+1} | S_t = s, A_t = a \right] \quad (2.30)$$

Important to note, that from ?? and Equation 2.29, a value function under a generic stationary policy  $\pi$  satisfies the Bellman equation as shown in Equation 2.31 [19], [48].

$$V_\pi(s) = \mathbb{E}[r(s, a) + \gamma V_\pi(s')] = \mathbb{E}[r(s, \pi(s)) + \gamma V_\pi(f(x, \pi(s)))] \quad (2.31)$$

Moreover, the value function under the optimal policy,  $\pi^*$  can be represented as shown in Equation 2.32 and for the state-action value function in Equation 2.33, where the relation between the value function and state-action value function is shown in Equation 2.34 and Equation 2.35.

$$V^*(s) = \max_a \mathbb{E}[r(s, a) + \gamma V^*(f(x, a))] \quad (2.32)$$

$$Q^*(s, a) = \mathbb{E} \left[ r(s, a) + \gamma \max_{a'} Q^*(s', a') \right] \quad (2.33)$$

$$V^*(s) = \max_{a \in A} Q^*(s, a) \quad (2.34)$$

$$Q^*(s, a) = r(s, a) + \gamma V^*(s') \quad (2.35)$$

Finally, if the optimal state-action value function (also known as Q-value) is known, then the optimal policy,  $\pi^*$  can be found by Equation 2.36 [49], whereby the optimal policy greedily selects an action that maximizes the Q-value function. Various methods exist to approximate this Q-value function, and it is

this goal that reinforcement seeks to achieve. However it also possible to directly optimize the policy,  $\pi$  to find the optimal policy  $\pi^*$ .

$$\pi^*(s) = \arg \max_{a \in A} Q^*(s, a), \forall s \in S \quad (2.36)$$

### 2.2.2. Q learning

These family of algorithms learn an approximating to the Q value function (Equation 2.33). Moreover, these algorithms are “off-policy” algorithms whereby each update can use data collected at any point during training. Q learning offers a deterministic policy, whereby in each state, the action is selected based on Equation 2.36. In order to find the optimal Q value function, the update rule in Equation 2.37 is used in combination with a Q-table (a table that holds all possible combinations of states and actions). This iterative update rule aims to approximate the bellman equation in Equation 2.33. Once the Q-function converges to the optimal Q-function, the optimal policy can be determined [50].

$$Q^{new}(s, a) = (1 - \alpha) \underbrace{Q(s, a)}_{\text{old value}} + \alpha \overbrace{(R_{t+1} + \gamma \max_{a'}(Q(s', a'))}^{\text{Learned value}} \quad (2.37)$$

where the temporal difference error is

$$TD_{error} = (R_{t+1} + \gamma \max_{a'}(Q(s', a')) - Q(s, a) \quad (2.38)$$

Where TD error equals zero when optimality has been achieved (Equation 2.33). However, this is only feasible for small problems, where the state and action space are small and discrete. In order to accommodate a continuous state space, the Deep-Q Network (DQN) was developed. In this approach, a neural network is utilized to estimate the Q-function, enabling the learning of a deterministic policy from data with high-dimensional features [51]. However, DQN still outputs a discrete policy and therefore does not accommodate a continuous action space [51]. Nevertheless, recent advancements have extended DQN’s applicability to continuous action spaces.

### 2.2.3. Policy Optimization

Policy optimization offers a more direct approach in learning the optimal policy as apposed to Q-learning. Such algorithms represent a policy as  $\pi_\theta(a|s)$ , whereby  $\pi_\theta(a|s)$  is a stochastic policy that gives the probabilities of choosing action  $a$  given state  $s$ . The vector  $\theta$  parameterize the policy, and it is these parameters that are optimized, by gradient ascent on the performance objective  $J(\pi_\theta)$  such as an Equation 2.39.

$$\theta_{t+1} = \theta_t + \alpha \nabla J(\hat{\theta}_t) \quad (2.39)$$

Here,  $\nabla J(\hat{\theta}_t)$  represents a stochastic estimate, where its expected value approximates the gradient of the performance objective function with respect to the policy’s parameters,  $\theta$  [47]. Such algorithms are called “on-policy” algorithms, which mean that each update is performed from data that was collected from the most recent version of the policy. All RL algorithms that follow this update rule on the policy are considered policy gradient/optimization methods, whether or not they also learn an approximation to a value function. However, such algorithms are often called actor-critic methods [47]. Policy Optimization algorithms are also naturally able to handle continuous state and action spaces.

### 2.2.4. Actor-Critic

Perhaps a more interesting class of RL algorithms combines both q-learning and policy optimization. Policy optimization methods directly optimize the policy, therefore they tend to be more stable and reliable in contrast to Q-learning and are better for continuous and stochastic environments [47]. However, because Q-learning learns “off-policy”, it has a substantially higher sample efficiency than

that of policy optimizations methods [47]. Actor-critic methods often incorporate the strengths from both policy gradient methods and q-learning, in order to achieve stable and fast learning. The critic learns a value function and the actor learns a policy. The critic provides feedback on how good an action was and uses this to update the policy. In this way, the actor can learn from both its own experience and the critic's feedback. Moreover, actor-critic algorithms are also suitable in tackling continuous state and action spaces [47]. It is worth mentioning that these algorithms can include both the critic and actor in the MPC's framework to enhance its performance in an economic optimisation setting. A commonly used actor-critic algorithm is Soft-Actor-Critic which will be the selected RL algorithm in this thesis. Numerous actor-critic algorithms exist and for a more in depth explanation on the various algorithms and the decision on why SAC was selected for this thesis see section A.1 and section A.2 respectively.

### 2.2.5. SAC

*A brief explanation of how SAC works and how it learns*

## 2.3. MPC

MPC demonstrates exceptional proficiency in managing constrained Multiple Input, Multiple Output (MIMO) systems, making it highly effective in applications like greenhouse control. Moreover, MPC's ability to handle non-linear dynamics and its optimality has contributed to its widespread adoption and has become the standard approach for implementing constrained multivariable control in the process industry [52]. Nearly every application introduces constraints, whether it be on the state of the system or the control inputs. Actuators, constrained by physical and safety limits such as temperature or pressure control, makes it necessary for controllers to handle such constraints. While the online computational time for such controllers may be expensive, for slow dynamics such as a greenhouse, sufficient computational time is available to accommodate this. Furthermore, the ongoing trend of faster computation mitigates this concern, making it less of a problem.

Although many control schemes exist in controlling greenhouses, it has been shown that an MPC controller outperforms an adaptive PID controller for greenhouse air control in [34]. Even though the control of a greenhouse is inherently non-linear, non-linear Model Predictive Control schemes have demonstrated effectiveness in handling this complexity, as evidenced in [53], [54] specifically for temperature control in a greenhouse. Furthermore, [55] shows insight of the performance of MPC when optimized for energy savings of a greenhouse, displaying impressive results over set-point tracking controllers. Further, [36] successfully implements a robust MPC to control the economic benefit of a greenhouse with parametric uncertainty, displaying its potential in greenhouse control. Moreover, as confirmed by [55], MPC stands out as the most effective control approach in smart greenhouses for energy savings. The study concludes that MPC is particularly advantageous when the system's dynamics can be reasonably approximated by a model and are sufficiently slow relative to the required time needed to perform the optimization.

Additionally, MPC has been shown to have a strong theoretical foundation. Researches have developed rigorous methods in analysing performance and stability on a MPC under certain conditions, including the optimality and robustness of the implemented controller. Indeed, if the system dynamics are known, it is possible to design an MPC to fulfill specific design requirements [56]. Nevertheless, while a solid mathematical framework exists for set-point tracking MPC, the same level of assurance cannot be provided for economic MPCs (EMPC), which aim to optimise for economic benefits.

### 2.3.1. The General MPC problem

MPC is an advanced method of control that uses a model of the system to predict the behaviour of the system over a finite horizon, known as the prediction horizon. The MPC controller aims to solve the infinite-horizon optimal control problem (OCP) as a series of finite-horizon problems in order to make the problem computationally tractable [14]. At each discrete time interval, the MPC solves the optimisation problem over this prediction horizon to compute the optimal inputs that minimize a given cost function, subject to constraints such as the system dynamics, initial state and state and control constraints. Each optimisation yields a sequence on control actions to take over this prediction horizon. The first control input is applied to the system, and at the subsequent time step, the system is sampled again and the entire process is recalculated providing an updated control sequence. While

this approach is not optimal, it is an approximation of the infinite time horizon problem and has been shown to yield excellent results in practice as discussed above. The choice of prediction horizon length is often a trade-off between computational efficiency and the desired control performance.

While MPC can be used for both continuous and discrete time system dynamics, continuous time system must be discretized to render the optimal control problem (OCP) tractable. This is necessary since a continuous time system gives rise to an infinite-dimensional problem. Therefore the discrete case will be considered as illustrated in Equation 2.20. It is possible that the state may be unknown (as in Equation 2.22), and therefore a state estimation is required, however we will further assume that the state is fully measurable or perfectly estimated, i.e.  $\hat{x}(k) = x(k)$  and therefore  $\hat{p} = p$ . When considering a finite-time horizon,  $N_p$ , the OCP problem can be formulated as in Equation 2.40.

$$\begin{aligned}
 & \min_{x(k_0:N_p+1), u(k_0:N_p)} J(x(k), u(k)) = \\
 & \quad \min_{x(k_0:N_p+1), u(k_0:N_p)} \sum_{k=k_0}^{N_p} l(x(k), u(k)) + V_T(x(N_p + 1)) \\
 \text{s.t. } & x(k_0) = x_{k_0} & \forall k = k_0, \dots, N_p, \\
 & x(k + 1) = f(x(k), u(k), d, p) & \forall k = k_0, \dots, N_p, \\
 & y(k) = g(x(k), u(k), d, p) & \forall k = k_0, \dots, N_p, \\
 & x_{\min} \leq x(k) \leq x_{\max} & \forall k = k_0, \dots, N_p, \\
 & u_{\min} \leq u(k) \leq u_{\max} & \forall k = k_0, \dots, N_p,
 \end{aligned} \tag{2.40}$$

where  $x(k_0 : N_p + 1)$  denotes a sequence of states, i.e.  $[x(k_0), x(k_0 + 1), \dots, x(N_p + 1)]^T$  and may be denoted as  $\mathbf{x}$  and similarly for the control actions  $\mathbf{u}$  and known disturbances  $\mathbf{d}$ . The cost function  $J(\cdot)$  may be explained by a stage cost  $l(\cdot)$ , where  $l : \mathbb{X} \times \mathbb{U} \rightarrow \mathbb{R}$ , which is the cost incurred at every time step  $k$  based on the current state and input applied and a terminal cost,  $V_T(\cdot)$ , which accounts for the cost associated with the state at the end of the prediction horizon. [36], [52]. The state and control constraints as shown. In the case of a setpoint tracking MPC, the stage cost and terminal cost function would commonly be represented as a quadratic term that penalizes the deviation between the state and the desired setpoint. Additionally, a setpoint tracking MPC would include a terminal constraint to guarantee performance and stability. This terminal constraint is typically set to the desired setpoint. However in economic optimisation, selecting an appropriate terminal constraint and/or cost function is difficult.

It is noted that the more accurate the model, the better the prediction and thus the better the actions. In the case of greenhouse control, if the model accurately captured all crop and greenhouse phenomena, state constraints would not be needed, since these constraints would be naturally incorporated into the dynamics. However, in practice, such dynamics are often still captured by explicit constraints. Moreover, an increasing complexity in the prediction model often leads to an increase in computational time and power which may exceed the time-scale of the system. This can make control actions impractical or infeasible within the required time frame [56]. Greenhouse environments are known to be complex and highly non-linear in nature. Hence, for control purposes, it is necessary to have simplified models that accurately predict system dynamics such as the model presented by van Henten [31] and as discussed in section 2.1 for greenhouse control.

Moreover, uncertainties in the model may greatly impact the performance of the MPC and the relation between a deterministic model and an uncertain model is explored in [36] and shown that even when a robust MPC strategy is used a 20% in relative parametric uncertainty decreased the crop yield by 11%.

### 2.3.2. Economic Model Predictive Control (EMPC)

The primary objective of an EMPC is to maximise economic benefit, whereby the economic benefit could refer to the profitability, efficiency and/or sustainability of the controlled process [57]. Typical processes that maximise for economic benefit would be in chemical and greenhouses processes with the objective of optimising profitability. In both processes it is difficult to define a steady state to which the MPC

must control the system to. In the case of a greenhouse the notion of a steady state is nonsensical, since it is desirable for the crop to grow with as little energy consumption. In the case of chemical processes it has become common practice to rely on a separate layer of control called real-time optimisation (RTO) to determine the steady state. This layer ensures that the current steady-state brings the greatest economic benefit. Subsequently, MPC is employed to steer the process towards this optimized steady state. However, this separation in control information is not necessarily desirable and/or optimal in regards to maximizing economic benefit. Thus, EMPC is introduced, wherein the economic objective is directly incorporated as the objective function of the optimal control problem that the MPC aims to minimize [58]. Here, the stage cost  $l(x, u)$  encapsulates an economic model of the process, and in this thesis the MPC aims to optimise Equation 2.23.

By adopting EMPC, it becomes feasible that dynamic, transient or time varying operation of the process could lead to higher economic benefit as compared to controlling the process to an optimal (time-varying) steady-state. As stated in [58], incorporating the economic model directly into the cost function does not assume the same structure of the stage costs of a traditional set-point tracking MPC and has therefore no stability guarantees. Furthermore, since the EMPC optimizes the process economics over a finite time horizon, it does not guarantee optimal closed-loop performance over an extended period. In general no closed-loop performance guarantees under EMPC exist[57].

[58] further showed in the case of a chemical process, despite the increase in economic benefits, the EMPC resulted in unstable plant dynamics which is highly undesirable for such a process. While a greenhouse may not experience this, it is still possible to encounter undesirable transient effects. For example, during the initial stages of the growth phase, the EMPC may not find it advantageous to expend energy due to the minimal growth, which could potentially cause irreparable harm to the plant. Nevertheless, this stage could arguably be considered the most crucial phase of the crop cycle in order to achieve optimal economic gain, as maximising crop growth in the early stages may have cumulative effects throughout the entire growth period.

In order to achieve performance and stability, a terminal constraint in the optimal control problem is introduced [59]. This terminal constraint must be selected carefully to achieve the desired performance and stability [58]. However, [59], introduces a terminal cost function with a terminal region constraint and demonstrates its superiority over a terminal constraint in terms of performance while maintaining system stability. Although, it is possible to develop a terminal cost/constrain to achieve desired closed-loop performance and stability, authors of [58], [59] and [57] acknowledge the difficulties in constructing such an appropriate terminal cost/constrain and a corresponding terminal region. Limited works provide theoretical analysis in order to construct an appropriate terminal cost in the absence of stability constraints. Most often, simulations are performed to design cost functions suitable for the specific application. Importantly, two main methodologies exist to assure closed-loop performance: to use a sufficiently large prediction horizon or the application of an appropriate terminal region and cost function [57]. Stability of the system's dynamics is not necessarily a concern, due to the nature of the greenhouse control system.

## 2.4. RL and MPC in tandem

MPC is recognized for its sample efficiency, robustness and constraint handling. However its prediction horizon, especially for economic prediction horizon is a shortfall. Moreover, large and complex systems may lead to a non-convex optimization problem which are computationally expensive to solve and may lead to sub-optimal control. Finally, model mismatch and uncertainties in forecasted disturbances can lead to a significant deterioration in control effectiveness [13].

While RL is predominantly explored within the machine learning community, its usefulness in the control space is undeniable. Although RL might suffer from the curse of dimensionality, necessitating a reduction of states and control action, the introduction of neural networks and actor-critic algorithms addresses this issue.

To differentiate this thesis from the concept of employing MPC as a function approximator, a concise explanation will be provided. This aims to clarify to the reader what the thesis does not focus on. As discussed in ??, the DQN is usually implemented as a neural network and is parameterized by a vector  $\theta$ . The approximated value of a state  $s$ , parameterized by a weight vector  $\theta$  is then given as  $\hat{v}(s, \theta) = v^*(s)$

where  $\hat{v}$  [16]. However, it is possible to use a MPC scheme instead of a neural network to facilitate parametrization for approximating the value function and policy. This is the goal of using MPC as a function approximator for RL. This thesis does not explore this concept. It instead explores the design and implementation of an (E)NMPC algorithm that utilizes the value function learned by RL in its optimal control problem formulation to propagate information beyond the prediction horizon.

In order to gain insight in how the two optimal schemes will be combined, it is imperative to understand the differences and similarities of the two algorithms. Key areas such as the approach, optimality, computational effort and prediction horizon is discussed and compared in order to motivate and understand the connection between the two control schemes. This section summarizes [13] works with added literature from [19] and [20].

### 2.4.1. The Optimality

As mentioned in section 2.2 and section 2.3, both control strategies attempt to solve the infinite prediction horizon problem.

The quality of the solution obtained through MPC is subject to the accuracy of the prediction model, which is further simplified to reduce computational burden. However, optimality of the direct optimization methods of the MPC problem is obtained through the Karush–Kuhn–Tucker conditions which are necessary conditions for optimality. Moreover, the local optimal policy obtained may also be sub-optimal due to multiple local optima in the case of non-linear optimization problems.

In contrast, if the state space is countable and the MDP is perfectly known, DP algorithms (which relay on Bellman's principle), offer sufficient conditions for global optimality. However, these algorithms are significantly impacted by the curse of dimensionality. Consequently, approximations are used such as RL. Although RL can only guarantee optimality under specific conditions when solving the Bellman equation ??, the approximated value function contains global optimal information so that the infinite-horizon control policy may be obtained [20]. It is important to note that this is only an approximation. Moreover, RL does not directly impose state and control constraints. While it is possible to indirectly incorporate these constraints through the reward function, such an approach does not ensure that the policy obtained will inherently adhere to these constraints.

### 2.4.2. Computational Effort

The online computational cost of MPC stands out as one of the principal drawbacks of this control strategy, particularly when dealing with complex models featuring numerous variables to optimize. Thus the model is often simplified, resulting in sub-optimal policies. In comparison to DP and RL algorithms, large computational power is expended training the policy, even for simple systems. However, once training is completed, the estimated optimal action may be given by a function evaluation of the policy. The evaluation of the policy, typical through a feed forward pass of a neural network, leads to a limitation in flexibility, especially in continuous control scenarios. Moreover, in obtaining an accurate value function proves to be difficult due to instability, rank loss and overestimation bias of the value function. This is especially prevalent for complex non-linear systems such as a greenhouse.

### 2.4.3. The Prediction Horizon

The most important characteristic of the two algorithms is the prediction horizon, and especially for economic optimization that cover a long time horizon with a system with slow dynamics. As mentioned, MPC employs explicit optimization over a finite prediction horizon to determine the optimal control action. On the other hand, RL explores and interacts with its environment to learn the optimal action, optimizing for both immediate and discounted future rewards. Hence, a shortcoming of MPC is the finite prediction horizon. This limitation becomes even more pronounced when dealing with sparse rewards and slow system dynamics. In such cases, actions taken at the current time step may only yield rewards past the prediction horizon, causing the MPC controller to be myopic. It is possible to counteract this drawback with an extended prediction horizon, however, as discussed, this increases the complexity and computational burden of the controller.

In contrast, RL aims to predict the optimal action to take over an infinite time horizon by incorporating a discount factor on rewards. This discount factor bears similarities to the prediction horizon concept employed in MPC controllers. For RL, it can be shown, through geometric series convergence that

the prediction horizon of the MPC controller is equivalent to  $N_p = 1/(1 - \gamma)$  [13]. It is noted that the prediction horizon over the RL can extend to infinite when  $\gamma = 1$ , however convergence of the total rewards gained is not guaranteed, emphasizing the significance of the discount factor  $\gamma$ . Nonetheless, discounted infinite prediction horizons generally result in improved long-term behaviour. However, as stated in [13], RL makes less efficient use of forecasted information. This inefficiency arises because all future knowledge is condensed and presented to the agent's observation without retaining its time dependency. Consequently, the agent is required to implicitly learn the system's dynamics through interactions with the environment, leading to the difficulty of understanding the time dependency of its actions on future rewards. In comparison, MPC naturally preserves the time dependency since it has the system's dynamics formulated in its problem, however since it only looks  $N$  steps forward, it produces a locally optimal policy [20]. A synergistic approach to combining the two control strategies would be to have a MPC controller optimize a short prediction horizon while propagating global information provided by RL. This integration of the two controllers is further justified in the context of greenhouse dynamics, where actions executed at the current time step may result in rewards that manifest over the long term. Finally, as outlined in ?? within the work of [57], it is imperative, when employing an EMPC, to construct the optimal control problem with an adequate terminal constraint to ensure the performance of the system. This terminal constraint, which must encapsulate information beyond the prediction horizon, underscores the evident synergy with the value function acquired through RL to provide the required information for the desired system performance.

# 3

## Reinforcement Learning Setup

This chapter provides an overview of the process of developing the RL agent that will be used in the development phase of the RL-MPC algorithm. This chapter focuses on the description of the environment on which the RL agent is trained, as well as the performance of the agent in both deterministic and stochastic environments. Finally, the training of a value function for a fixed policy is also investigated.

### 3.1. Environment Description

This section describes the environment for the RL agent to learn an optimal policy. The environment is built on the Greenhouse model as described in section 2.1 and outlines important features to successfully train an RL agent. This includes the observation space available for the agent to make decisions on, the action space available to the agent, the reward function, and finally the weather data that is used for the training period.

**Observation Space** The observation space of the agent must be carefully selected, in order to achieve desirable results. Providing too little information may degrade performance; however, giving the agent too much information about the state of the environment may introduce unwanted noise, making it difficult to infer an optimal policy. Typically, the state of dry weight of the lettuce crop would not be available for an expert grower to make decisions on as it is difficult to measure without disrupting the crop's life cycle. However, various methods exist for predicting the state of the crop dry mass such as a non-linear kalman observer and other machine learning techniques [24]. However it is assumed the dry mass may be measured and is available to the agent. Other states of the greenhouse, such as the temperature, C02 and humidity levels are easily measured and form part of the observation space. The current weather conditions are also made available to the agent in order to make better decisions. As shown in section 2.1, since the control input is dependent on the previous control input (i.e., it may only deviate a maximum of 10% from the previous input), it is important to provide the previous control action to the agent. Lastly, the agent is considered to be time-aware, and so the current time step is also given to the agent. Although not necessary, it enables the agent to learn a non-stationary policy. Considering that the growing period is 40 days (as discussed in subsection 2.1.4), the problem is episodic. By incorporating time awareness, the agent is able to leverage the current time in order to make more optimal decisions. As discussed in subsection 2.1.4 and later in Equation 3.1, the optimization goal includes maximizing the growth difference between time steps, and so knowledge of the previous dry mass state, the growth experienced in the previous time step may be beneficial to learning an optimal policy. However, the 3 following environment state tuples  $s(k)$  at time  $k$  have been separately tested to represent the observation returned to the agent:

$$s(k) = (y_1(k), y_2(k), y_3(k), y_4(k), u(k-1), k, d(k)) \quad (3.1)$$

$$\begin{aligned} s(k) &= (\Delta y_1(k), y_2(k), y_3(k), y_4(k), u(k-1), k, d(k)) \\ \Delta y_1(k) &= y_1(k) - y_1(k-1) \end{aligned} \quad (3.2)$$

$$s(k) = (y_1(k-1), y_1(k), y_2(k), y_3(k), y_4(k), u(k-1), k, d(k)) \quad (3.3)$$

It is noted, that Equation 3.1 is expected to perform better than Equation 3.1 and Equation 3.2 since more information is provided regarding the Markov decision processes of the model and the reward received, thereby allowing the agent to potential infer the system dynamics more accurately. However Equation 3.1 is the simplest and therefore facilitates the learning of a value function and easier integration in the RL-MPC algorithm as discussed in section 3.6 and section 5.1 respectively. It was found that no substantial benefit was gained in providing the previous knowledge of the previous drymass state of the crop, hence for simplicity Equation 3.1 was further used in this thesis.

**Action Space** The continuous action space, denoted as  $A$ , is defined as  $\subseteq [-1, 1]^3$ , where  $a \in A$ . In order to ensure that the current control input,  $u(k)$  satisfies the constraints outlined in Equation 2.24, the agent's action, denoted as  $a(k)$ , is regarded as a modification to the control input. Consequently, the current control input can be determined as follows:

$$u(k) = \text{clip}(u(k-1) + a(k) \cdot \delta u_{\max}, u_{\min}, u_{\max})$$

where  $\delta u_{\max}(k), u_{\min}, u_{\max}$  are defined in subsection 2.1.4

**Initial Conditions** Initial conditions were kept constant for every episode for both the stochastic and deterministic case and shown in Equation 3.4.

$$\begin{aligned} x(0) &= [0 \ 0 \ 0 \ 0]^T \\ y(0) &= g(x(0)) \\ u(0) &= [0 \ 0 \ 50]^T \end{aligned} \quad (3.4)$$

**Reward Function** The reward function is modeled after the optimization goal as defined in subsection 2.1.4 and represents the same optimization goal as defined for the MPC OCP. Although the van Henten model sufficiently describes the dynamics of lettuce growth in a climate-controlled environment, it does not do so over the entire state space. Therefore state constraints are imposed to ensure states are operated within reasonable limits to ensure realistic conditions. As stated in section 2.2, state constraints cannot be directly imposed but can be indirectly incorporated through a penalty function within the reward function. It is common practice to impose a linear penalty function for state violations when learning a policy with RL. As such, the resulting reward function becomes:

$$\begin{aligned} R(k) &= c_{price_3} \cdot (y(k) - y(k-1)) - (c_{price_1} \cdot u_1(k) + c_{price_2} \cdot u_2(k) + 0 \cdot u_3(k)) \\ &\quad - (P_{CO2} \cdot y_2(k) + P_T \cdot y_3(k) + P_H \cdot y_4(k)) \end{aligned} \quad (3.5)$$

where  $c_{price_1}, c_{price_2}, c_{price_3}$  are defined in subsection 2.1.4 and correspond to the pricing of the lettuce and control inputs and the penalty terms  $P_{CO2}, P_T, P_H$  are defined as follows:

$$\begin{aligned} P_{CO2} &= \begin{cases} c_{p_{CO2}} \cdot (y_2(k) - y_2^{\max}) & \text{if } y_2(k) > y_2^{\max}, \\ c_{p_{CO2}} \cdot (y_2^{\min} - y_2(k)) & \text{if } y_2(k) < y_2^{\min}, \\ 0 & \text{otherwise} \end{cases} \\ P_T &= \begin{cases} c_{p_{Tu}} \cdot (y_3(k) - y_3^{\max}) & \text{if } y_3(k) > y_3^{\max}, \\ c_{p_{Tl}} \cdot (y_3^{\min} - y_3(k)) & \text{if } y_3(k) < y_3^{\min}, \\ 0 & \text{otherwise} \end{cases} \\ P_H &= \begin{cases} c_{p_H} \cdot (y_4(k) - y_4^{\max}) & \text{if } y_4(k) > y_4^{\max}, \\ c_{p_H} \cdot (y_4^{\min} - y_4(k)) & \text{if } y_4(k) < y_4^{\min}, \\ 0 & \text{otherwise} \end{cases} \end{aligned} \quad (3.6)$$

The penalty constants  $c_{p_{CO_2}}, c_{p_{T_{ub}}}, c_{p_{T_{lb}}}, c_{p_H}$  were found in empirically in [22] in order to effectively account for deviations from desired states and their impact on the economic benefit. It should be noted that the upper bound of the temperature imposes stricter penalties for violations compared to the lower bounds due to the absence of active cooling in the system. Thus, during periods of increased temperature throughout the day, it is important for the agent to make appropriate decisions. The penalty constants and their respective units are displayed in Table 3.1. The selection of minimum and maximum temperatures was based on the typical operating ranges for lettuce crops and the acceptable levels of CO<sub>2</sub> for human brief operation.

parameter	value	units
$c_{p_{CO_2}}$	$\frac{10^{-3}}{20}$	$\text{€} \cdot (ppm \cdot m^2)^{-1}$
$c_{p_{T_{ub}}}$	$\frac{1}{200}$	$\text{€} \cdot (C^\circ \cdot m^2)^{-1}$
$c_{p_{T_{lb}}}$	$\frac{1}{300}$	$\text{€} \cdot (C^\circ \cdot m^2)^{-1}$
$c_{p_H}$	$\frac{1}{50}$	$\text{€} \cdot (RH\% \cdot m^2)^{-1}$
$y_2^{max}$	1600	ppm
$y_2^{min}$	500	ppm
$y_3^{max}$	20	C°
$y_3^{min}$	10	C°
$y_4^{max}$	100	RH%
$y_4^{min}$	0	RH%

**Table 3.1:** Penalty Constants

## 3.2. Experimental Setup

To facilitate the learning process of RL, the observations returned from the environment were normalized by a running mean and variance. The VecNormalizeWrapper in Stable-Baselines3 is responsible for updating the mean and variance for every observation received from the environment. The observation is normalized as per Equation 3.7 and clipped between [-10, 10].

$$obs_{norm} = \frac{(obs - \mu_{obs})}{\sqrt{\sigma_{obs}^2 + 1 \cdot 10^{-8}}} \quad (3.7)$$

where  $\mu_{obs}$  and  $\sigma_{obs}^2$  represent the running mean and variance, respectively. The value  $1 \cdot 10^{-8}$  is included to prevent division by zero. Although the VecNormalizeWrapper also facilitates this process, it is necessary to replicate this step when incorporating it into the RL-MPC algorithm. Finally, in order to ensure reproducibility, a seed value of 4 was used for the generation of random numbers. This seed value was utilized for both the initialization of neural network weights and the selection of actions for exploration purposes.

**Weather Data** The weather data used in training is obtained from the VenLow Greenhouse in Bleiswijk from the period January 30–March 11, 2014. The weather data was resampled from its original 5-minute interval to a 30-minute interval, in accordance with the timestep of the environment. The weather data remains consistent throughout the episodes, irrespective of whether the training and/or evaluation is conducted under deterministic or stochastic conditions. As such, the validation data is the same as the training data. In practice, it may be necessary to evaluate the agent on unseen weather data, but the thesis aims to develop an RL policy for incorporation with MPC to investigate the resulting controller. Thus, provided that all algorithms/controllers utilize identical weather data, if the agent learns a suitable policy for this specific weather pattern, it can be considered a suitable basis for comparing algorithms.

**Deterministic and Stochastic Case** When learning a policy in both stochastic and deterministic environments, the key distinction lies in the evolution of the state of the greenhouse. In the stochastic case, this evolution follows the principles outlined in Equation 2.21. In the stochastic case, three levels

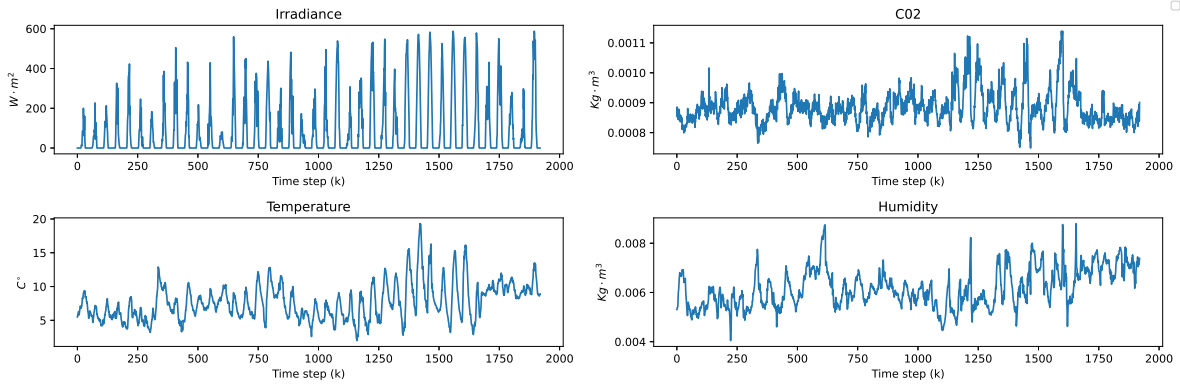


Figure 3.1: Weather Data

of uncertainty were tested, namely  $\delta_p = 5\%$ ,  $\delta_p = 10\%$  and  $\delta_p = 20\%$ . Although these uncertainty levels might be considered extreme, it was desirable to learn a policy for each of these uncertainty levels to compare to MPC and RL-MPC under identical conditions of uncertainty. The optimal configuration(s) that produce the most favorable outcomes in the deterministic scenario will be employed in the stochastic scenario, and there will be no reevaluation of hyperparameters. While the stochastic environment provides a representation of a scenario closer to real-life conditions, the deterministic case offers a nominal measure of the RL agent's performance and the resulting RL-MPC algorithm when combined with MPC.

**Performance Metrics** The primary performance metric used for evaluating RL agents is the final cumulative reward obtained over the 40-day growing period. As demonstrated in Equation 3.5. The performance metric under consideration is conceptually equivalent to the EPI (Equation 2.23) minus the summed temperature, C02 and humidity violations. This is a natural selection of the final performance metric as it directly corresponds to what the agent is optimizing, and subsequently, what the MPC and RL-MPC controllers are optimizing. Other metrics include the EPI, total growth, total C02 usage, total heating, computational time to compute control input, temperature and c02 violations. It is difficult to compare these lesser performance metric across policies, since these are all form part of the reward function (with the exception of the computational time) and are not directly optimized. Therefore, making comparisons would not be meaningful, and only observations can be made. However, the computational time taken to compute the optimal control action is an important metric, particularly when combining RL with MPC. Finally, when comparing the controllers in a stochastic environment, the variance of the final cumulative reward is also examined.

### 3.3. Hyper-parameter Tuning

The process of hyper-parameter tuning is frequently laborious and requires exhaustive exploration to determine the best configuration to maximize the cumulative reward of the agent. Therefore, the final hyper-parameters are posted in Table 3.2 and were found empirically. Refer to **appendix A** for a more comprehensive analysis of the obtained hyper-parameters. The discount factor and activation function are not reported here. The effect of these two hyper-parameters are important to consider when integrating the value function of the learned agent with MPC. The defaults provided by SB3 are used for hyper-parameters that are not reported.

**Activation Function** The importance of the activation function lies in whether the resulting activation allows the output of the neural network to be differentiable with respect to the inputs. For instance, the ReLu activation function is a commonly used activation function due to its simplicity and superior convergence, in contrast to activation functions like tanh and sigmoid, which also encounter the issue of vanishing gradient. Although ReLu is differentiable with respect to the weight of the neural network, it is not differentiable with respect to the inputs of the neural network. This is important to note since it is necessary for the trained value function to be differentiable with respect to its inputs if it is to be

Training Episodes	100
Warm-up episodes	9
Hidden Layers	2
Neurons per Hidden Layer	128
Batch size	1024
Learning Rate	$5 \cdot 10^{-3}$
Buffer size	100000

**Table 3.2:** Hyper-parameters

used as a cost function in the MPC formulation. Hence, the tanh function may be used instead, as it is a frequently used activation function that is differentiable with respect to the inputs.

**Discount Factor** Another consideration is the discount factor, denoted as  $\gamma$ . Since the problem is episodic and therefore the cumulative rewards are bounded, it is possible to have a  $\gamma = 1$ . By setting the discount factor  $\gamma$  to 1, the agent is able to consider the entire prediction horizon when making decisions regarding its actions. Additionally, the value function obtained during training satisfies would contain information pertaining to the entire prediction horizon which is highly desirable especially for optimizing economic benefit. Having  $\gamma < 1$  will shorten the agent's 'prediction horizon' and the resulting value function may not provide significant benefits for the MPC when integrated. However, it may stabilize the learning and therefore yield a better policy as compared to when  $\gamma = 1$ .

Results pertaining to the activation function and discount factor are shown and discussed in subsection 3.4.3

## 3.4. Deterministic Results

The outcomes of modifying the discount factor and the activation function are presented and examined in this section. Finally, a discussion of the chosen policies and the identification of the desirable characteristics that can be integrated with the MPC is performed. While there are several hyperparameters that can impact the performance of the resulting RL policy, this section will focus on the discount factor and activation function. These two hyperparameters are considered necessary aspects of the RL policy, particularly when it is desired to integrate it with MPC.

### 3.4.1. Discount Factor

Typically, the discount factor lies between 0.9 and 0.99. It is desirable for economic optimization to have this discount factor as close to 1 as possible. Therefore 4 discount factors were tested, namely 1, 0.99, 0.95 and 0.9. Going any lower may yield a more stable learning procedure at the cost of a more myopic policy. To note, that the ReLu activation function is used for the following results pertaining to the investigation of the discount factor. The value functions trained on their respective discount factor is denoted  $V_\pi(s|\gamma)$ .

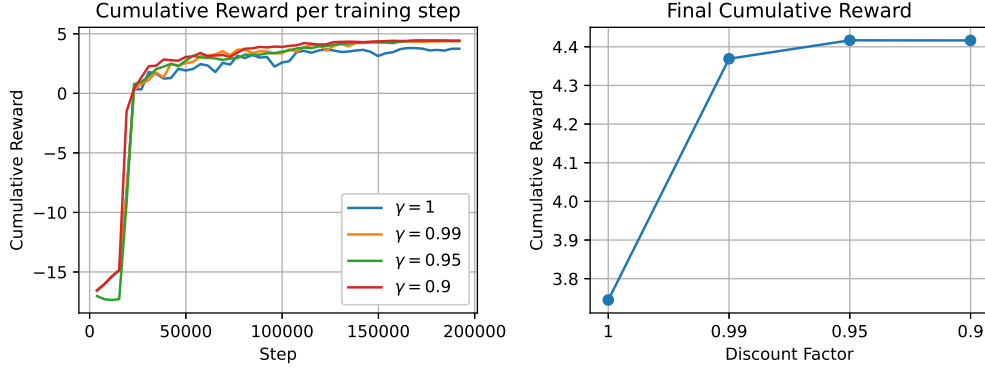


**Figure 3.2:** Cumulative Reward vs Discount factor ( $\gamma$ )

**Performance** The cumulative reward achieved over the training period and the final cumulative reward achieved for each different discount factor are depicted in Figure 3.2. The cumulative reward per training step serves an example of the learning process, while the final cumulative reward depicts the performance of the RL system after training. As can be seen in Figure 3.2, it is clear that  $\gamma = 1$  does not perform as well as lower discount factors. It is noted that the degradation in performance comes from the increase in problem complexity when the discount factor is 1. Hence, it becomes more difficult in finding an optimal policy, requiring a different set of hyper-parameters and potentially a significantly larger number of training episodes. However, the policy generated with this discount factor will provide a value function that holds information across the entire time horizon, which is desirable. Conversely, the learning procedure is much more stable when lower discount values are used and a thus a higher final cumulative reward is achieved. Given the desirability of utilising the value function in the MPC formulation, it is necessary to analyse the value function for each of the tested discount factors.

**Value Function** It is difficult to determine whether the critic has converged. Given that the critic serves as a q-value function approximator in the SAC algorithm, the actor must identify the optimal action for a given state in order to compute the value of that state using the critic. Therefore, convergence of the value function is dependent upon the actor policy as well. Although the training curves indicate that the critic has converged, it has only converged in alignment with the actor's policy. In order to assess whether the critic (and actor) has achieved convergence in predicting the value function, it is necessary to visualize and compare the actual, as computed by Equation 2.28, and the predicted value, as given by the learned value function, of a given visited state during the 40-day simulation. In addition, to compare the accuracy of the learned value function to a value function that encompasses the entire prediction horizon (a non-discounted value function), Equation 3.8 may be used as a visual aid.

$$\begin{aligned}
 V(s_k) &= r_k + V(s_{k+1}) \\
 \therefore V(s_{k-1}) &= r_{k-1} + V(s_k) \\
 \therefore V(s_{k-2}) &= r_{k-2} + r_{k-1} + V(s_k) \\
 \therefore V(s_0) &= \sum_{i=0}^{k-1} r_i + V(s_k)
 \end{aligned} \tag{3.8}$$

During each time step, the computation of the initial state's value is determined by the cumulative rewards received up to that point, as well as the approximation of the current state's value using the value function. If the value function is able to approximate the value of a state (a non-discounted value

function) accurately, then Equation 3.8 should yield the same result for every time step, resulting in a horizontal line,  $y = V_\phi(s_0)$ .

For each discount factor, the predicted value of each state and the cumulative rewards obtained thus far were plotted and evaluated, for the entire 40 day period. It is noted that for the deterministic case, the realizations of state trajectories and rewards received do not differ between simulations, hence the exact value of each state may be calculated. Moreover, it is also noted that a value function trained with a  $\gamma = 1$  is the only value function that would be able to approximate  $y = V_\phi(s_0)$  as given in Equation 3.8, however it serves as an important visual aid to show the accuracy of the trained value functions.

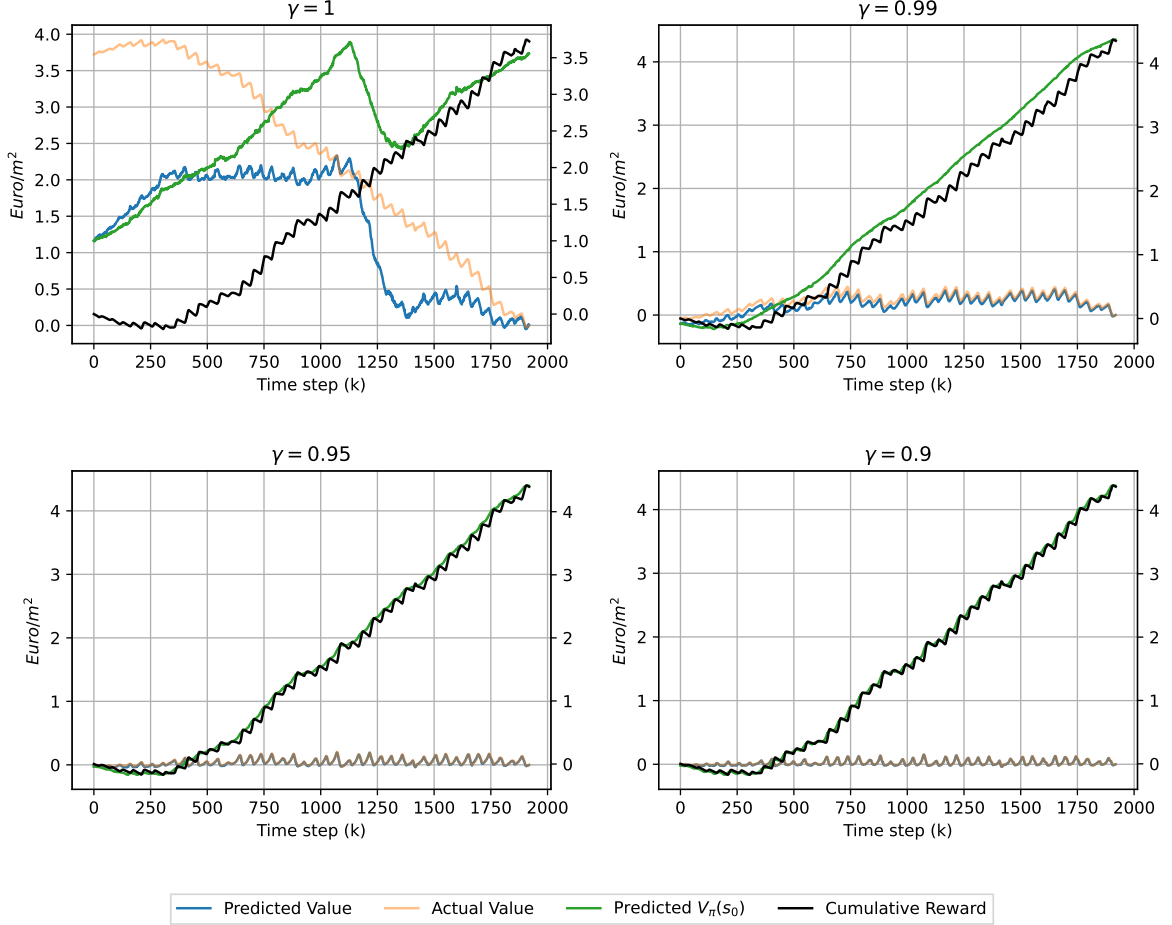


**Figure 3.3:** Predicted value vs actual value vs Discount factor

The figure shown in Figure 3.3 illustrates the comparison between the predicted and actual value of each state for each discount factor. In addition the cumulative reward at each time step is also logged, naturally the cumulative reward differs slightly since the policy generated is also dependent on the obtained value function.

It is acknowledged that the trajectory of the actual value for each state (for  $\gamma = 1$ ) is a horizontally reflected trajectory of the cumulative reward trajectory and can be seen in Figure 3.3. Naturally this is not the case for discount factors lower than one, since the value only embeds knowledge of future rewards to be received over a shorter horizon. This is further seen by the predicted  $V_\pi(s_0)$ , whereby the value functions do not produce a horizontal  $V_\pi(s_0)$  curve, indicating their inadequacy in predicting the true non discounted value function. Not even  $V_\pi(s|\gamma = 1)$  predicts this true value function accurately, shown by the clear non-horizontal predicted  $V_\pi(s_0)$  curve.

It is also noted that the lower the discount factor, the more accurate the predicted value of a state becomes as seen by the overlapping 'Predicted Value' and 'Actual Value' curves. This may be due to the decrease in problem complexity and therefore more accurate approximations. When  $\gamma = 0.9$ , the

critic is capable of accurately predicting the actual value of a state. However, it falls short in accurately representing the true value of a state over the entire time horizon, given its nature of discounting future rewards. The same can be said for all discount factors lower than one. It was important to train an actor and critic with a  $\gamma = 1$  because it was believed that the trained critic, despite having a worse performing policy, could still provide a reasonable estimation of the value of a state throughout the entire simulation. Upon examining Figure 3.3, it becomes evident that this assumption is incorrect. During the investigation into suitable hyper-parameters for the learning agent, it was observed that when  $\gamma = 1$ , the trained critic struggled to accurately estimate the value of a state in all cases. Figure 3.3 is just one such realization.

### 3.4.2. Activation Function

It is also important for the trained critic to utilize a differentiable activation functions to ensure differentiability. This is done so that it may be used within the MPC framework. However, such an activation function, such as the commonly used tanh activation function may or may not yield desirable results in terms of maximizing cumulative reward. This section compares the performance of a learned agent with tanh activation functions against and agents with ReLu activation functions for a  $\gamma = 1$  and  $\gamma = 0.95$  with the ReLu acting as the baseline performance.

Discount Factor	Performance		SpeedUp (%)
	ReLU	tanh	
1	3.72	3.44	-7.53
0.95	4.40	4.17	-6.08

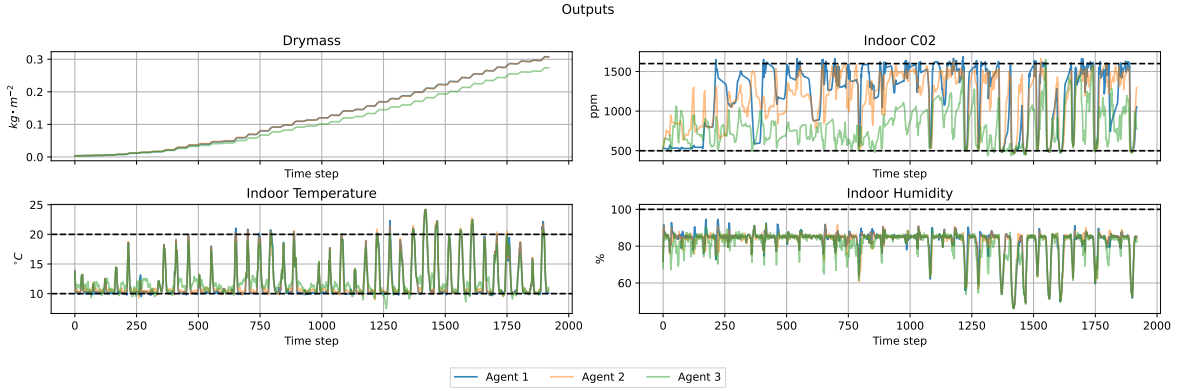
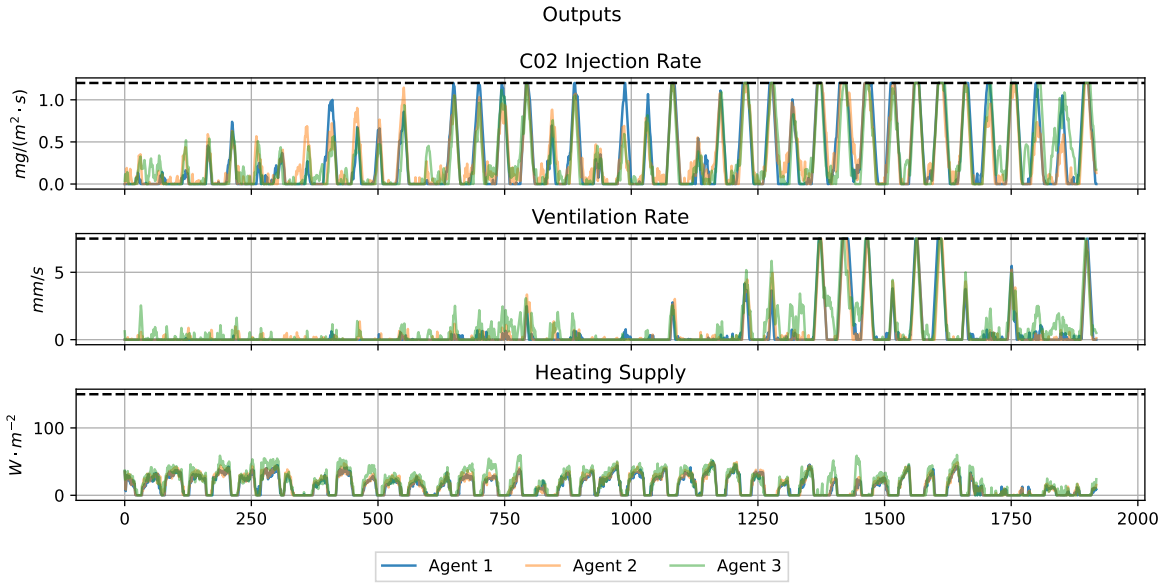
**Table 3.3:** Effect of different activation functions (ReLU and tanh) on performance and speed-up at varying discount factors.

Table 3.3 displays the effect of the tanh activation on the agents final performance. it is clear that ReLu significantly outperforms the tanh activation function in terms of total cumulative reward. This situation presents a dilemma. It is desirable to have an effective reinforcement learning policy in which the critic has differentiability. By incorporating the concept of differentiability into the critic, it seems that there is a decline in performance. While additional investigation into the hyperparameters may be necessary to reject this notion, the focus of this thesis does not lie in the development of the best possible RL generated policy. Rather, chapter 3 aims to create a policy and an accurate critic, that is competitive with MPC so that when merged, produces a potentially better policy. However, these results suggest that special care should be taken when merging RL with MPC.

### 3.4.3. Final Results and Conclusion

From the findings, the best policy produced by RL is with the hyperparameters shown in Table 3.2, with a  $\gamma = 0.95$  and with ReLu activation functions. And while the best performing policy is desired, this configuration does not produce adequate conditions for its critic to be used in the MPC formulation, namely the value function does not hold information across the entire prediction horizon and it is not differentiable. And an agent, learned with a  $\gamma = 1$  and tanh activation function results in a worse performing policy and a critic that struggles to accurately predict the value of states. With that being said, a critic that has undergone training with a discount factor of  $\gamma = 0.95$  is able to accurately predict the value of a state and may still possess sufficient knowledge regarding future rewards to be advantageous for MPC. Additionally, a critic learned with a  $\gamma = 1$ , albeit bad approximations, may also provide enough information. However, the next section delves into how a value function may be trained on a fixed policy, and if an accurate differentiable value function can be trained on the best performing policy, then all other configurations are unnecessary. However a time-series analysis of the state and input trajectories were performed with the agent configuration shown in Table 3.4.

Agent	$\gamma$	Activation Function	Final Performance
1	0.95	ReLU	4.27
2	0.95	Tanh	4.18
3	1	Tanh	3.03

**Table 3.4:** Performance of selected agents with different activation functions and discount factors**Figure 3.4:** Time series of system outputs**Figure 3.5:** Time series of system outputs

The time series plot of the system outputs and inputs across the 40-day period for every agent as selected in Table 3.4 is shown in Figure 3.4. These time series plots are similar to those reported in [9], [22]. Direct comparisons are not possible since [9] does not specify the weather data range used and the reward function differs from what is used in this thesis. Furthermore, [9] include additional constraints on the temperature levels during the day to encourage heating by solar radiation during the day and the heating system by night. These constraints were not included in this paper because the thesis aimed to give RL more independence in optimising EPI while minimising dangerous constraint violations for plant and/or human operation. Furthermore, [22] also reports similar results, however a direct comparison is not possible, since hyper-parameters and reward function differs. However, it is noted that results, time series and cumulative rewards, are similar enough to give confidence in the correct

training of the RL agent.

Metric	Agent 1	Agent 2	Agent 3
EPI	4.964	4.807	3.727
Total Growth	0.304	0.303	0.270
Total C02 Usage	1.057	1.0318	1.029
Total Heating	12.5462	13.661	16.381
Computational Time	0.000216	0.00024	0.00023
Temp Violations	110.007	119.2	138.93
C02 Violations	3311.43	1046.47	1972.61
Final Performance	4.27	4.173	3.031

Table 3.5: Performance Metrics of agents

Other performance metrics are reported for completeness in Table 3.5. The computational time needed to compute the optimal control action is noted to take  $\approx 0.2ms$ . This is expected since a simple inference of the actor network is required to calculate the optimal action. Other metrics as reported in Table 3.5 may be useful metrics in designing a controller specifically for greenhouse control, however the RL-MPC controller developed in this thesis focuses on economic optimization of a system and is tested on a greenhouse.

### 3.5. Stochastic Results

In training the stochastic RL agent the same hyper-parameter configuration was used that produced the best nominal agent, namely the same configuration as Agent 1 (Table 3.4). Although this produces a critic that is problematic for the integration with MPC, this is solved in section 3.6. Three stochastic agents were trained, each trained on a different level of uncertainty as specified in section 3.1 with the uncertainty model according to Equation 2.21. Performance metrics are reported and a comparison is made with the nominal model (Agent 1 from Table 3.4). Performance metrics are evaluated by repeating the 40-day simulation period 30 times and taking the average and variance of the cumulative rewards over the complete time horizon. Each agent is assigned a name based on the degree of uncertainty on which they received training. For example, an agent that has undergone training in a stochastic environment with a  $\delta_p = 20\%$  is referred to as 'Agent 0.2'. The agent named 'Agent 1' will be referred to as the 'Nominal Agent'. Each Agent is compared to the other stochastic Agents in an environment with every level of uncertainty.

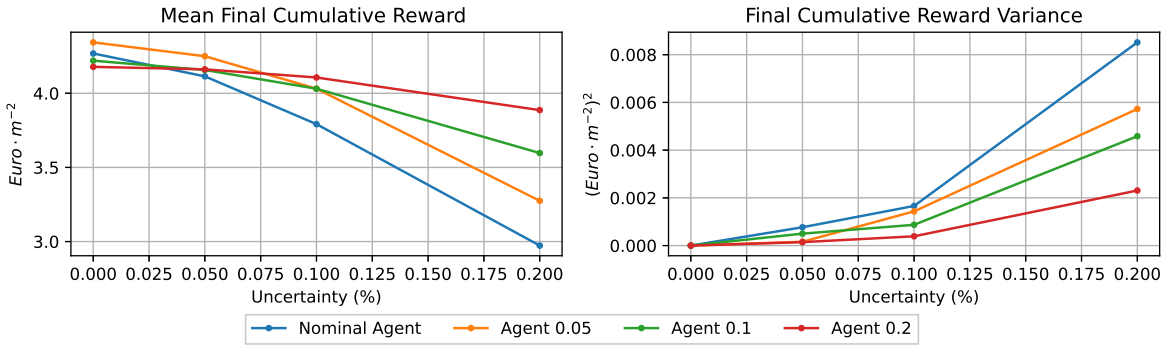


Figure 3.6: Stochastic RL policy performances

The final mean cumulative reward and variance of each agent under different uncertainty levels are presented in 3.6. As expected, as more uncertainty is injected into the environment, mean cumulative reward decreases and the variance increases. There is a noticeable trend where agents trained with higher levels of uncertainty tend to have a slower decline in performance as uncertainty increases, although they may not perform as well at lower levels of uncertainty compared to agents trained with lower levels of uncertainty. Similarly, agents trained on higher uncertainty levels maintain a lower

variance in their final cumulative reward as uncertainty increases, compared to agents trained on data with lower uncertainty. Although in practice, the uncertainty is not known however if a more reliable policy is desired, training a reinforcement learning agent on a higher level of uncertainty than expected may achieve the desired outcomes. Also in general, th

Results also suggest that an agent trained on a level of uncertainty does not necessarily produce the best policy for that level of uncertainty. It seems that in the nominal case ( $\sigma = 0\%$ ), the agent trained on a 5% uncertainty level (Agent 0.05) outperforms the nominal agent. Moreover, Agent 0.2 seems to achieve a higher average cumulative reward than Agent 0.1 when tested on a 10% uncertain model. It is anticipated that agents who are trained and tested based on their respective uncertainty would exhibit superior performance. However, this disparity in performance can be attributed to the agent's increased exploration as a result of the added noise.

### 3.5.1. Conclusion

It is widely recognized that RL has the capability to address uncertainty through appropriate training methods, as evidenced by the findings presented in Figure 3.6. The incorporation of these stochastic policies into the MPC framework will be examined to determine whether a RL policy learned from stochastic data can transfer its characteristics to the RL-MPC framework. Finally, each agent, specifically the Nominal agent, Agent0.05, Agent0.1, and Agent0.2, is employed in its corresponding stochastic environment. Although Agent0.05 may outperform the Nominal Agent under nominal conditions, for the purpose of this thesis, its corresponding agent would be used. Moreover, the value function as trained by the RL algorithm is clearly problematic as the selection of the activation function and prediction horizon play a significant role in accuracy and the performance of the learned value function and policy respectively.

## 3.6. Trained Value Function

Although training an agent using SAC produces an actor and a critic network, it was shown in subsection 3.4.3 that the produced critic had undesirable characteristics. This critic was trained based on a changing policy that was dependent on the critic itself, therefore it is not surprising that the approximation to the value function was sub-optimal. However this section aims at training a value function approximator with a fixed policy<sup>1</sup>. Therefore, a value function may be trained on the best policy obtained in subsection 3.4.3, namely Agent 1 (Table 3.4). Additionally, there is more freedom in choosing the architecture of the value function since it is now trained independently of the policy. Therefore, simpler models may be made to approximate the value function. Specifically, upon inspection of Figure 3.4 and Figure 3.3, it is noticed that the cumulative reward at each time step is mostly dependent on the state of the crop's dry mass at time  $k$ , due to the similarity in the two curves. Therefore it may be possible to learn a value approximator solely based on the crop's dry mass and current time. It is noted that this value function is only accurate under the policy it was trained on. Lastly the tanh activation functions must be used to ensure differentiability.

Two methods were employed to learn various value function approximators, namely the temporal difference learning method and expected return method, each with their respective advantages.

### 3.6.1. Temporal Difference Learning

This method uses a similar method by which SAC, DDPG and TD3 update their critic. Most similar to DDPG. Two neural networks are used to represent the value function, a current and target network. The mean squared bellman error is minimized between the target values (from the target network) and the current values (from the current network) as shown in eq XXX. Moreover, a polyak averaging is used to update the target networks. This method is very sample-efficient compared to the Expected Return learning. As a result, it will be easier to cover a wide range of states in the sampled state space. Consequently, the method is effective in learning a value function that can effectively generalise across the entire state space. This sample efficiency allows one to generate data from an MPC policy, as done in [20], however the RL policy was used because of its significant speed.

<sup>1</sup>This fixed policy may come from any control lay, however the RL policy is used due to its computational efficiency in determining control actions, enabling large amounts of data points and/or trajectories to be obtained

**Obtaining Data** The nominal Agent (Agent 1 from Table 3.4) was used to acquire the data. A similar methodology for data acquisition as described in [20] was employed. Along the nominal trajectory,  $q$  ( $q \in \mathbb{N}_{>0}$ ) internal states,  $x$  and inputs  $u$ , were uniformly sampled from  $\hat{\mathbb{X}}^4$  (Equation 3.9) and  $\mathbb{U}^3$  at time  $k$  respectively. So that at time  $k$ , a set denoted as  $\hat{S}_k = \{\hat{s}_{k_1}, \hat{s}_{k_2}, \dots, \hat{s}_{k_q}\}$ , where  $\hat{s}_{k_i}$  is constructed using Equation 3.1 from the sampled states and inputs. Each element in  $\hat{S}_k$ , denoted  $\hat{s}_{k_i}$ , is taken separately as an initial state and evolved one step in time with the RL agent, receiving a reward  $\hat{r}_{k_i}$  and a boolean  $d$  indicating whether a terminal state has been reached.  $\hat{s}_{k_i}$  and  $\hat{s}_{k+1_i}$  are both normalized as per Equation 3.7 and stored in a transition tuple along with the received reward and  $d$ , denoted as  $(\hat{s}_{k_i}, \hat{s}_{k+1_i}, \hat{s}_{k_i}, d)$ . The environment is then set back to the actual state  $s_k$  and evolved for one time step, and the process repeats itself, until the 40 day period is over. The transition tuple of the actual system is also stored. To ensure a value function approximator generalizes well across the state space, the quality of sampled internal states and inputs is important. From the time series plot Figure 3.4 and Figure 3.5 it can be seen that not the entire state space needs to be sampled, especially for the dry mass state,  $x_1$ . The control actions were sampled across the entire set  $\mathbb{U}^3$  as shown in Equation 2.24. States  $x_2, x_3, x_4$  were sampled with a range slightly larger than their respective minimum and maximum constraints (Equation 2.25) range. This decision was made as it was deemed unnecessary to sample states that significantly violate constraints. Finally,  $x_1$  was sampled around the nominal  $x_1$  trajectory such that the sampled state space  $\hat{\mathbb{X}}^4$  is defined as:

$$\begin{aligned} \hat{\mathbb{X}}^4 = \{(x_1, x_2, x_3, x_4) &| x_1 \in [\hat{x}_{1\min}(x_{1_k}), \hat{x}_{1\max}(x_{1_k})], \\ &x_2 \in [\hat{x}_{2\min}, \hat{x}_{2\max}], \\ &x_3 \in [\hat{x}_{3\min}, \hat{x}_{3\max}], \\ &x_4 \in [\hat{x}_{4\min}, \hat{x}_{4\max}]\} \end{aligned} \quad (3.9)$$

where the bounds are specified in Table 3.6 and were found empirically.

Parameter	value	unit
$\hat{x}_{1\min}(x_{1_k})$	$x_{1_k} \cdot (1 - 0.8) - 0.01$	$kg \cdot m^{-2}$
$\hat{x}_{1\max}(x_{1_k})$	$x_{1_k} \cdot (1 + 0.7) + 0.01$	$kg \cdot m^{-2}$
$\hat{x}_{2\min}$	$g_2^{-1}(x_{3_k}, 400)$	$ppm$
$\hat{x}_{2\max}$	$g_2^{-1}(x_{3_k}, 1800)$	$ppm$
$\hat{x}_{3\min}$	7	$C^\circ$
$\hat{x}_{3\max}$	30	$C^\circ$
$\hat{x}_{4\min}$	$g_3^{-1}(x_{3_k}, 50)$	$RH\%$
$\hat{x}_{4\max}$	$g_3^{-1}(x_{3_k}, 100)$	$RH\%$

**Table 3.6:** Sample State Space bounds

With only 10 additional samples every time step ( $q = 10$ ), the desired state space can be adequately covered.

**Figure 3.7:** Sampled States for Temporal Difference

**Figure 3.8:** Sampled Inputs for Temporal Difference

Figure 3.7 and Figure 3.8 display the states and inputs that were sampled during a 40-day period respectively, with an additional 10 samples taken at each time step, resulting in a total of 21120 data points, or transition tuples.

**Training** Once data is generated, it is split into a validation and training dataset with a 20% and 80% split respectively to ensure that the function approximator does not over fit to the seen data. Transition tuples are sampled from the training set and the following loss function is minimized:

$$\mathcal{L}(\phi, \mathcal{D}) = V_\phi(s_k) - (r_k + (1 - d)V_{\phi_{targ}}(s_{k+1})) \quad (3.10)$$

where  $\phi$  and  $\phi_{targ}$  are the current and target weights of the respective function approximators and  $\mathcal{D}$  is the training data set. The Adam optimizer is used to minimize Equation 3.10 over a batch size  $\mathcal{B}$ . The target weight  $\phi_{targ}$  are updated every learning iteration by Polyak averaging  $\phi$  by:

$$\phi_{targ} \leftarrow (1 - \rho)\phi_{targ} + \rho\phi \quad (3.11)$$

where  $\rho$  represents the Polyak coefficient, which is a hyperparameter that needs to be tuned. Despite its widespread usage, it was discovered that the learning of the value function was consistently unstable regardless of the chosen hyperparameters. It failed to learn an appropriate value function, but further research can be conducted to make it functional. However, stable learning was not attained in this thesis.

### 3.6.2. Expected Return Learning

This method includes obtaining the expected return of each state visited, from a simulated trajectory under a fixed policy, and using them as targets for that state. In comparison to the temporal difference

learning method, this approach offers the benefit of training that is considerably more stable. Unlike the TD method, the targets remain unchanged while the weights of the function approximator are updated. However, this method of learning is much less sample efficient, requiring significant more data to generalize across the state space. Many trajectories are simulated until termination, and the return must be calculated for each state visited. More importantly, only starting states of the trajectory are sampled, which makes it harder to obtain the same data spread as the TD-method.

**Obtaining Data** A greater number of starting points must be sampled in order to obtain a spread that is comparable to the TD-Method; however, because the trajectory must be run through to the end of the simulation, a significantly larger amount of data is needed. However, targets are calculated not only for the initial state, but also for each state encountered along the trajectory by using Equation 2.28. Given the inferior sample efficiency of this method, it is important to carefully choose the initial points to ensure that the learned value function can effectively generalise across the state space that the agent is likely to encounter during its simulation. A similar approach to subsection 3.6.1 was used, however, all states and inputs were uniformly sampled around a region of the nominal trajectory at time  $k$  and not only the dry mass,  $y_1$ . Therefore, initial states and inputs were sampled from  $\hat{\mathbb{X}}^4$  and  $\hat{\mathbb{U}}^3$  and time  $k$  is uniformly sampled across the entire time horizon as shown in Equation 3.12.

$$\begin{aligned}\hat{\mathbb{X}}^4 &= \{(\hat{x}_1, \hat{x}_2, \hat{x}_3, \hat{x}_4) \mid \hat{x}_1 \in [\hat{x}_{1\min}(x_{1_k}), \hat{x}_{1\max}(x_{1_k})], \\ &\quad \hat{x}_2 \in [\hat{x}_{2\min}(x_{2_k}), \hat{x}_{2\max}(x_{2_k})], \\ &\quad \hat{x}_3 \in [\hat{x}_{3\min}(x_{3_k}), \hat{x}_{3\max}(x_{3_k})], \\ &\quad \hat{x}_4 \in [\hat{x}_{4\min}(x_{4_k}), \hat{x}_{4\max}(x_{4_k})]\} \\ \hat{\mathbb{U}}^3 &= \{(\hat{u}_1, \hat{u}_2, \hat{u}_3) \mid \hat{u}_1 \in [\hat{u}_{1\min}(u_{1_k}), \hat{u}_{1\max}(u_{1_k})], \\ &\quad \hat{u}_2 \in [\hat{u}_{2\min}(u_{2_k}), \hat{u}_{2\max}(u_{2_k})], \\ &\quad \hat{u}_3 \in [\hat{u}_{3\min}(u_{3_k}), \hat{u}_{3\max}(u_{3_k})]\} \\ k &\sim U(0, 1919)\end{aligned}\tag{3.12}$$

where the minimum and maximum limits are calculated as per Equation 3.13

$$\begin{aligned}\hat{z}_{\min} &= z_k \cdot (1 - \sigma) \\ \hat{z}_{\max} &= z_k \cdot (1 + \sigma)\end{aligned}\tag{3.13}$$

which represent the minimum and maximum range of the sample state space for a specific state and input where  $z_k$  represents the nominal trajectory.  $\sigma$  denotes the desired spread of sampled initial states, which is expressed as a percentage. In doing this, initial states maybe uniformly sampled around/near the nominal trajectory. As can be seen from Figure 3.5 and Figure 3.4, it can be observed that the performance of policies can vary significantly with minimal changes in the state and input trajectories. Thus, it can be expected that sampling the trajectories in this manner covers enough of the state space to represent the optimal trajectory. Because these methods require a significant amount of sampled data, it is not practical to use an MPC controller. Therefore, Agent 1 (or the nominal Agent) was employed to implement the fixed policy. Given that the computation of a control action requires a time of  $0.2ms$ , it is possible to sample a large number of trajectories in order to achieve appropriate coverage of both state and input spaces. In the case of stochastic conditions, the same state may yield a different return, therefore if a state has been visited more than once, then the mean of the return is used as training data.

**Training** Once trajectories is sampled, for each state observed/visited, the total return is calculated, and the tuple  $(s_k, TR)$  stored in a dataset. The dataset is then divided into an 80:20 ratio, with 80% of the data used for training and 20% used for validation. A neural network as a function approximator is now trained with inputs as the state,  $s_k$ , and labels as the total return,  $TR$  and the loss function in Equation 3.14 is minimized with the Adam optimizer.

$$\mathcal{L}(\phi, \mathcal{D}) = \mathbb{E}[(V_\phi(s_k) - TR)^2]\tag{3.14}$$

where  $V_\phi$  is the function approximator with weights  $\phi$  and  $TR$  is the total return of state  $s_k$ . Hyperparameters include the structure of the neural network, learning rate, and batch size.

**Experimental Setup** To investigate the effect of the value function in the MPC framework, it was decided to train four value functions that were based on different architects and/or states used as inputs. These models are listed in Table 3.7 along with their distinctive network architecture. All models were trained on 200 epochs with a learning rate of  $1 \cdot 10^{-3}$  and batch size of 1024.

Name	Observation Space	Hidden Layers	Neurons per Layer
$V_{\phi_1}$	Equation 3.1	2	128
$V_{\phi_2}$	Equation 3.1	2	32
$V_{\phi_3}$	Equation 3.1	1	128
$V_{\phi_4}$	$(y_1(k), k)$	2	128

Table 3.7: Value Functions

Each value function was trained on the nominal agent, Agent 1. Additionally,  $V_{\phi_4}$  was trained on each stochastic policy, namely 'Agent 0.05', 'Agent 0.1', and 'Agent 0.2'. 1000 trajectories were simulated and sampled from these agents, resulting in nearly one million data points consisting of states and their corresponding total return. Finally, the initial state and inputs were sampled with a spread of  $\sigma = 0.5$  to ensure adequate coverage of the state and inputs spaces. The architects are chosen based on the principle that each subsequent architecture model becomes less complex, with  $V_{\phi_1}$  serving as the initial baseline architecture. This is done to investigate the effect of these value functions in the RL-MPC framework.

Performance metrics include the squared error between the predicted total return and the actual total return as shown in Equation 3.14. Moreover, the accuracy of the resulting value function across the simulation period will be visualized by using Equation 3.8.

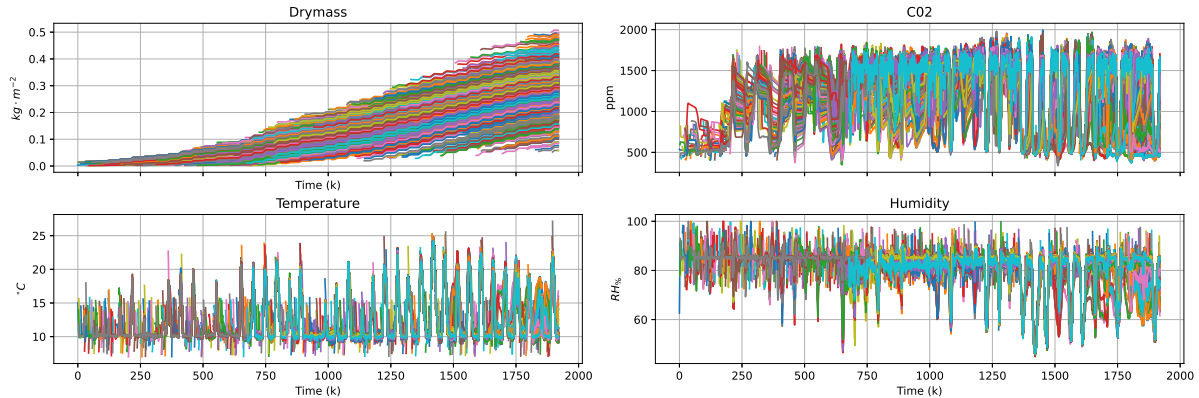
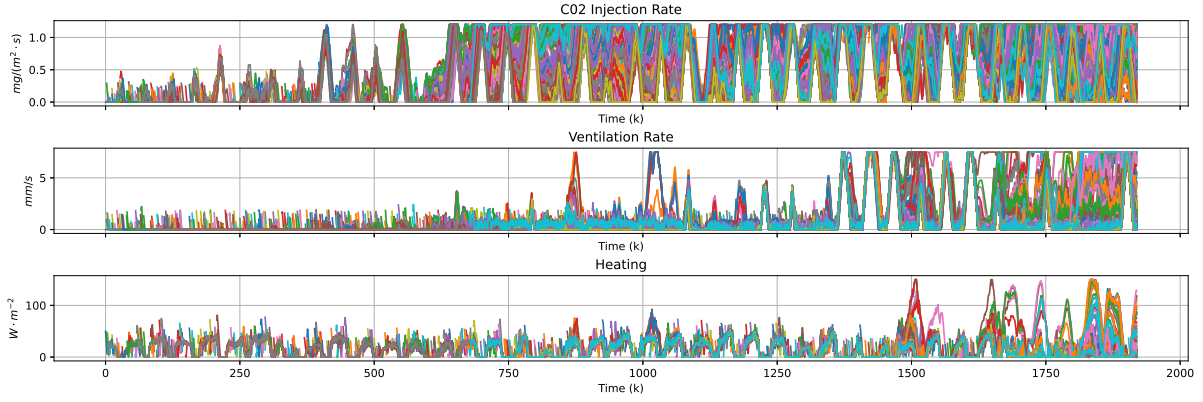


Figure 3.9: Sampled States



**Figure 3.10:** Sampled Inputs from Nominal conditions

Figure 3.9 and Figure 3.10 are the results of all the 1000 trajectories sampled from the nominal agent. The figures reveal that the sampled trajectories exhibit a lesser extent of coverage of the state and input spaces as compared to the temporal difference learning, Figure 3.7 and Figure 3.8. Nevertheless, a sufficient level of coverage is achieved. Following the completion of training and validation, a small number of additional trajectories will be sampled in order to verify the accuracy of the prediction model.

### 3.6.3. Results

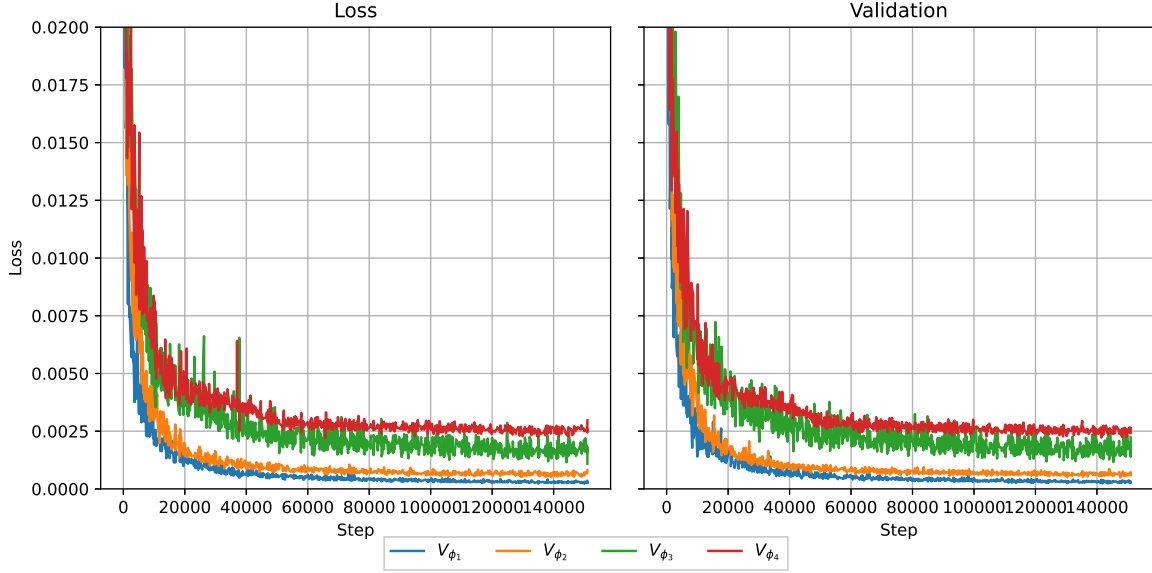


**Figure 3.11:** Performance Curves, trained on the nominal Agent

Figure 3.11 displays the loss curves of all four models trained on data generated by the nominal agent. As expected, the baseline model ( $V_{\phi_1}$ ) is able to achieve the highest accuracy compared to the simpler models. This can be attributed to its more complex structure and using the full observation returned by the agent, with each subsequent simpler model exhibiting lower accuracy. Nevertheless, when utilizing the reduced observation space model, denoted as  $V_{\phi_4}$ , the model demonstrates a high level of accuracy, as evidenced by a mean squared error of less than 0.5% between the actual and predicted values. The high level of accuracy indicates that the value of a state is primarily influenced by the current time and the condition of the crop's dry mass. In addition, when incorporating these value functions into the RL-MPC framework, the optimizer would only need to optimise over 2 variables for  $V_{\phi_4}$ , as opposed to 11 variables for the other value functions.

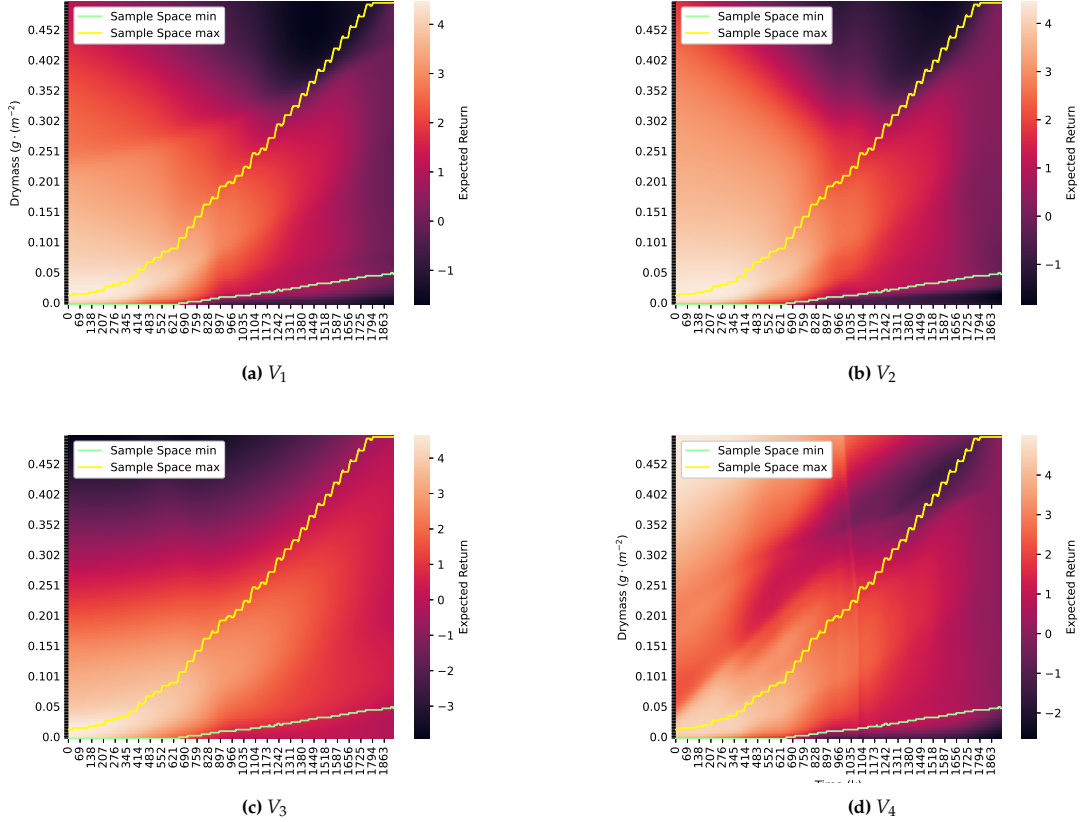


Figure 3.12: Value vs Drymass vs time

Figure 3.12 gives a visual representation of the value of a state given the dry mass and time. It is noted that although  $V_{\phi_1}$ ,  $V_{\phi_2}$  and  $V_{\phi_3}$  require an observation space as given in Equation 3.1 to determine its value, since the value is highly dependent on the dry mass state and time, the other states in the observation space were averaged.  $V_{\phi_4}$  naturally has an observation space of only time and the dry mass state. The lower and upper limits in Figure 3.12 are displayed to indicate the range within which the value function approximator can be deemed reliable. This range corresponds to the portion of the sample space from which the dry mass was sampled for training.

The intuitiveness of Figure 3.12 stems from the fact that the highest return is observed at the beginning of the growing period, which can be attributed to the longer duration of the growing period. Moreover, having a higher dry mass at any specific time leads to greater rewards, this behavior is seen across all four models within the training bounds. It is important to note that the greenhouse model limits the dry mass to a maximum of  $400 \text{ g} \cdot \text{m}^{-2}$ , therefore for dry masses close to this value, very little reward can be expected, hence the lower returns in Figure 3.12. While it is reasonable to anticipate that a higher dry mass would result in a greater return, the reward function is actually determined by the difference in growth. Consequently, the return is calculated based on the difference in growth starting from the initial state. It is also noted that Figure 3.12 suggests that the value function is smooth with respect to the drymass and time.

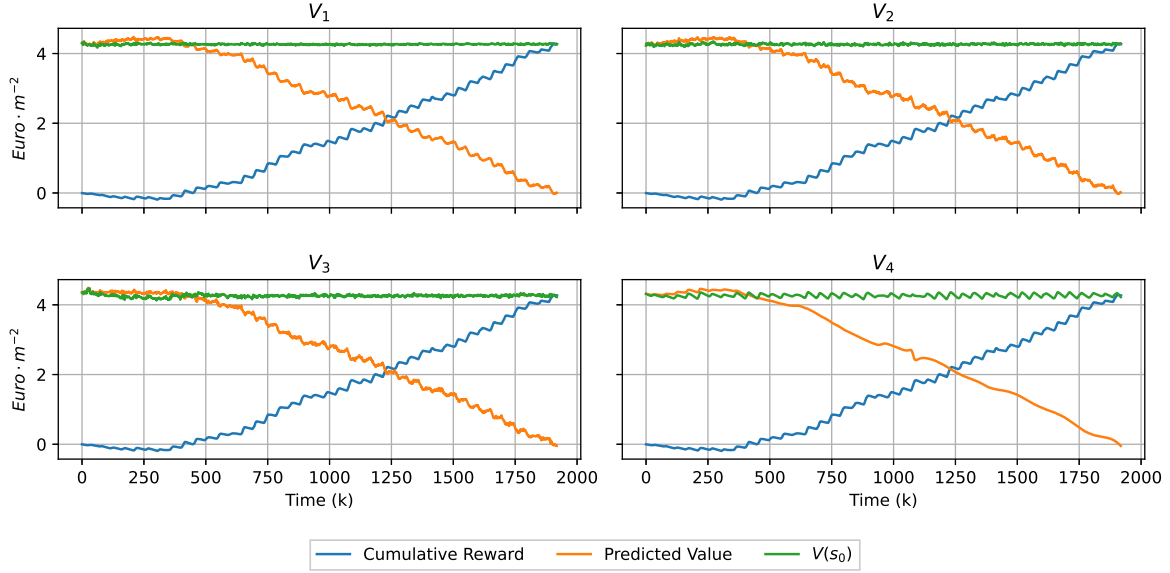


Figure 3.13: Value predictions - Entire Time Horizon

Figure 3.13 displays a time series plot of the cumulative rewards plotted against the predicted value at each time step over the entire simulation period. This plot is similar to what is shown in Figure 3.3. Additionally, it includes the calculated  $V_\pi(s_0)$  at each time step using Equation 3.8 as a visual indicator of the accuracy of the value function. As demonstrated in Figure 3.13 in conjunction with Figure 3.11, the predicted values show a high level of accuracy. This is evident from the nearly perfect horizontal line at  $V_\phi(s_0)$  that spans across the prediction horizon and substantially outperforms the prediction accuracy of the trained value functions in Figure 3.3. However, what is interesting and that cannot be seen in Figure 3.12 but in Figure 3.13 is the level of noise present in each prediction. Naturally,  $V_{\phi_4}$  is not able to make a precise prediction of the value since it only gets the time and dry mass as inputs, however its prediction is a lot smoother than all the others. While  $V_{\phi_1}, V_{\phi_2}, V_{\phi_3}$  may be more accurate, more noise is present. This observation again suggests that the primary factors determining the value of a state are its drymass and time, while the minor fluctuations in rewards and expected return are influenced by other factors that have minimal impact over the entire time period.

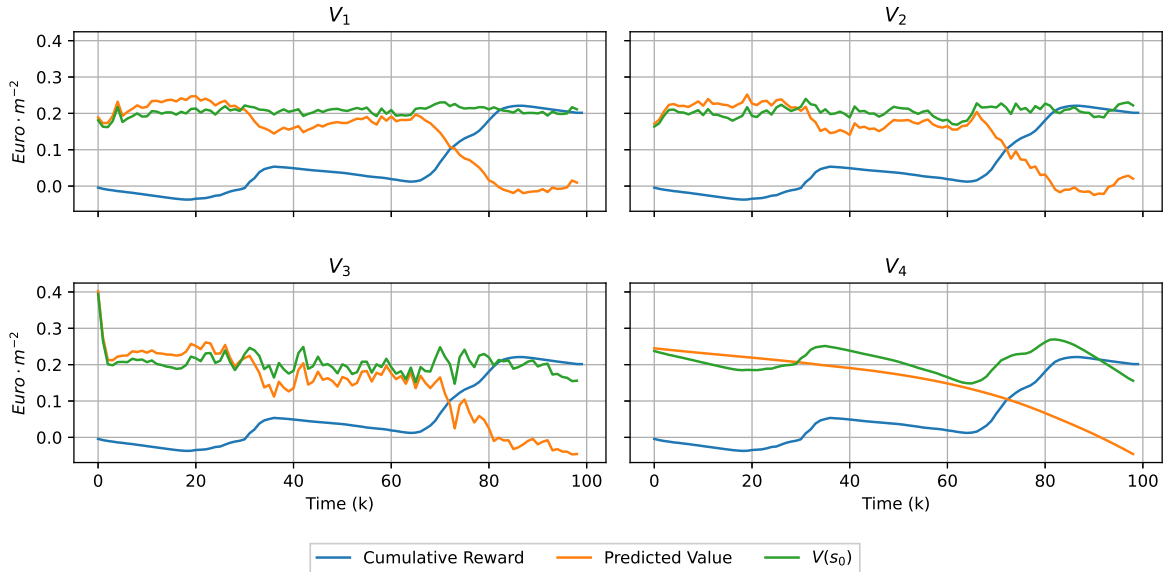


Figure 3.14: Value predictions - 2 Days

Figure 3.14 shows a time series of the cumulative reward and predicted values over a two day span.

**Remark 1** It is evident that while  $V_{\phi_1}, V_{\phi_2}, V_{\phi_3}$  can produce more precise estimations (as demonstrated by the proximity of their prediction line  $V_{s_0}$  to the actual value),  $V_{\phi_4}$  remains significantly smoother. Moreover,  $V_3$  is not as smooth as it may have seemed in Figure 3.12 and displays the highest level of noise across the four models trained. Although this is one realization of a trajectory, this behavior was observed in all simulated trajectories. This behaviour should be noted since it is important for integrating it with MPC

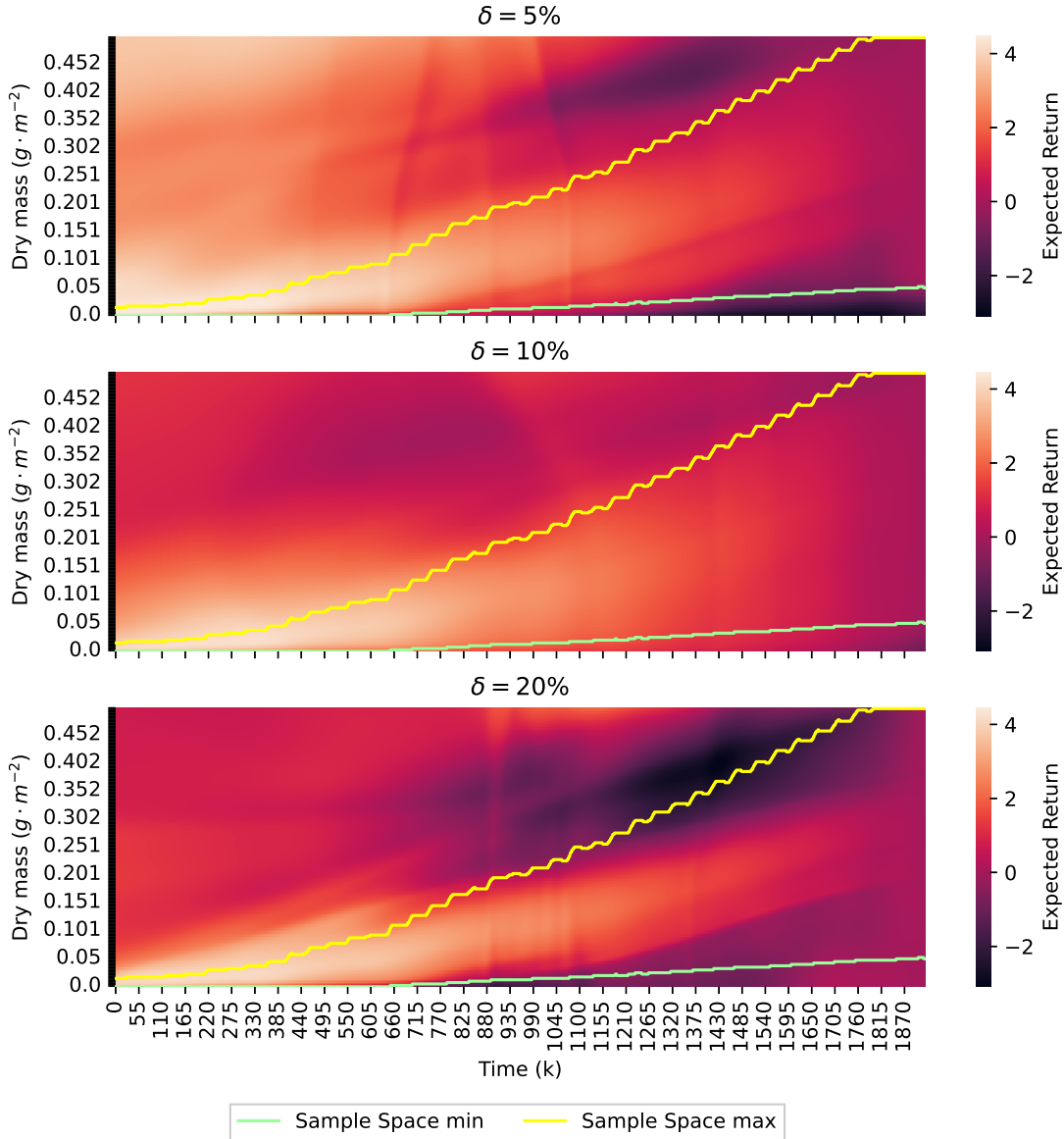


Figure 3.15: Drymass vs Time vs Value - Stochastic

Finally, for each level of uncertainty in the environment, a value function was trained with its corresponding agent. Figure 3.15 displays the same heatmap as Figure 3.12, yielding similar behaviour as compared to the nominal conditions. However, it appears to be more coarse, particularly beyond the range of the training data. Specifically, it seems that for high uncertainties (i.e. 20%), it seems that the trained value function exhibits a higher degree on non-linearity as compared to the others trained on lower levels of uncertainty. This may indicate that more sample trajectories are required for further training, however it seems to still generalize well in the region of the nominal trajectory.

### 3.7. Conclusion

The objective of this chapter was to develop a policy that is competitive with MPC and a value function that can accurately approximate the expected return given the state of the environment, both for the nominal and stochastic environment.

It was discovered that a policy trained with a discount factor of 1 resulted in a critic that provides inaccurate value estimations and a policy that performs worse than an agent trained with lower discount factors. While reducing the discount factor leads to improved policies and a more precise critic, the critics fail to provide information about the entire growth period. Furthermore, in order to integrate the critic with MPC, it is necessary for the critic to be differentiable. This requires the use of the tanh activation function. However, using this activation function leads to a policy that is not as effective as when using a non-differentiable activation function like ReLu.

Given these obstacles, it became evident that additional measures were necessary. It was decided to train a separate critic/value-function on the best rl policy obtained. Therefore lower discount factors and non-differentiable activation functions may be used in the training of the policy. The best policy found and trained on the nominal data was denoted as Agent 1 with parameters shown in Table 3.4. Using the same hyper parameters as Agent 1, 3 different agents were learned based on each level of uncertainty in the greenhouse model, namely 'Agent 0.05', 'Agent 0.1' and 'Agent 0.2'.

Empirical evidence demonstrated that the stochastic agents were more robust to noise than the nominal agent. Agents trained with greater levels of uncertainty exhibited policies with reduced variance across different levels of uncertainty. While the overall performance decreased as uncertainty levels increased in the environment, the decline becomes more gradual when trained on higher levels of uncertainty. After generating sufficient policies for both the nominal and stochastic environment, it was necessary to train an appropriate critic/value function approximator. Four different model architectures were used to train the critics, where each model architecture becomes progressively less complex. Every agent, whether in the nominal or stochastic case, had a critic that was trained to evaluate its policy under its particular level of uncertainty.

Results showed that accurate value function approximators could be trained, provided enough data was sampled. However, although they were accurate, the predictions were very noisy, which could be problematic later on when integrating the function appropriators into the RL-MPC framework. However, the simplest model architecture, trained on only the dry mass state and time, provided very smooth predictions, albeit not as accurate as the more complex models. It was this model architecture that was used to train value function approximators for the stochastic agents.

These agents and corresponding value function establishes the foundation for incorporating RL with MPC into the RL-MPC framework.

# 4

## Model Predictive Control Setup

This chapter presents the setup and creation of the MPC controller, and investigates the performance of the resulting controller on the greenhouse environment. Moreover, the effect of the prediction horizon is investigated on both nominal and stochastic conditions. The works in this chapter is similar to what is presented in [36] and [9]. However, direct comparisons are not possible. [36] develops to create a robust sample based controller, while this chapter will focus on constructing a conventional MPC. This is done to examine the effects of uncertainty on this controller and later asses whether the integration of RL can mitigate these effects. In [9], such an MPC controller is developed. However, it does not provide specific weather data. Finally the optimization goal used in this thesis differs from that in both papers. However, a qualitative comparison may be done.

### 4.1. Greenhouse MPC problem formulation

In order to directly compare to RL and to the RL-MPC controller, it is important that the optimization goal is equivalent. As discussed in subsection 2.1.4, it is desired to optimize the economic benefit of the greenhouse environment. Similarly to section 3.1, the optimization goal of the MPC is done to ensure that the sum of stage costs are equal to the actual economic benefit of the system. As such the following optimization goal is solved at every time step:

$$\min_{u(k), x(k)} \sum_{k=k_0}^{k_0+N_p-1} l(u(k), y(k)) \quad (4.1a)$$

$$\text{s.t. } x(k+1) = f(x(k), u(k), d(k), p), \quad (4.1b)$$

$$y(k) = g(x(k+1), p), \quad (4.1c)$$

$$-\delta u_{max} \leq u(k) - u(k-1) \leq \delta u_{max}, \quad (4.1d)$$

$$u_{\min} \leq u(k) \leq u_{\max}, \quad (4.1e)$$

$$x(k_0) = x_{k_0}. \quad (4.1f)$$

To ensure that the optimization goal is exactly the same as the RL reward function (section 3.1), the cost function  $V(u(k), y(k))$  becomes:

$$\begin{aligned}
l(u(k), y(k)) &= -\kappa_1(y(k) - y(k-1)) + \sum_{j=2}^4 \kappa_j u_{j-1} + \sum_{i=1}^4 s_i(k) \\
\text{where } s_i(k) &\geq 0, \\
s_1(k) &\geq c_{p_{C02}} \cdot (y_2^{min} - y_2(k)), \\
s_2(k) &\geq c_{p_{C02}} \cdot (y_2(k) + y_2^{max}), \\
s_3(k) &\geq c_{p_{T_{lb}}} \cdot (y_3^{min} - y_3(k)), \\
s_4(k) &\geq c_{p_{T_{ub}}} \cdot (y_3(k) + y_3^{max}), \\
s_5(k) &\geq c_{p_H} \cdot (y_4^{min} - y_4(k)), \\
s_6(k) &\geq c_{p_H} \cdot (y_4(k) + y_4^{max}),
\end{aligned} \tag{4.2}$$

where the slack variables are introduced in order to accommodate the output constraint in equation Equation 4.1, resulting in an optimization problem equivalent to that of RL. The penalty constants  $c_{p_{C02}}, c_{p_{T_{lb}}}, c_{p_{T_{ub}}}, c_{p_H}$  are the same as what is used in the RL problem formulation and given in Table 3.1.

**Experimental Setup** Furthermore, the experimental setup is identical to what is used in section 3.2 with the exception of normalizing observations. The performance metrics are the sum of the stage costs during the simulation period, which is equivalent to the EPI minus the sum of the state violations. For the stochastic environment, the performance metric is calculated by taking the average of the sum of stage costs over 30 simulation periods, as well as considering the variance of the resulting stage costs. In the case of stochasticity, the MPC algorithm still solves the optimization problem defined by equation Equation 4.1 using the nominal system parameters. However, it is only during the system evolution that the uncertainty in parameters is taken into account.

Finally, to increase the computational time and feasibility of the MPC solver, the solver is warm-started with the previous solution to reduce the number of iterations required to reach the optimal solution <sup>1</sup>. The computational time of computing the optimal control actions will also be examined for each prediction horizon. These performance metrics are given for all prediction horizons. Finally, The MPC framework is built using the open source software Casadi [ref XXX](#) and the non-linear solver IPOPT [ref xxx](#) in python.

## 4.2. Deterministic Results

Simulations are conducted for every prediction horizon  $N_p$ . The prediction horizons to be tested will include time intervals of 1 hour, 2 hours, 3 hours, 4 hours, 5 hours, and 6 hours. Results include the final cumulative reward and the average time required to solve Equation 4.1 for each prediction horizon.

---

<sup>1</sup>The solution to the OCP is heavily reliant on initial guesses due to the non-linearity nature of the problem, lagrangian multipliers from the previous solutions were also reused to mitigate instability in the solver. These instabilities are especially prevalent in longer prediction horizons

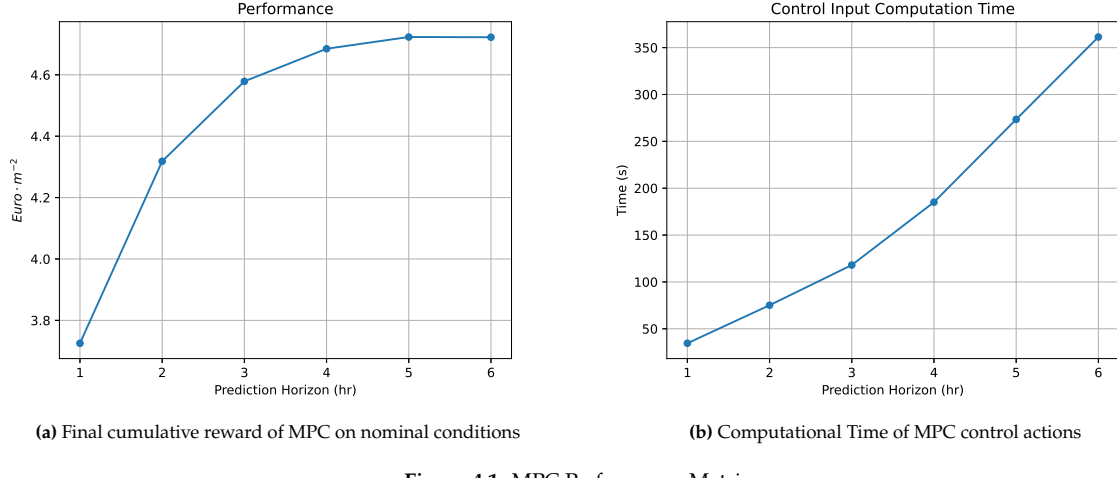


Figure 4.1: MPC Performance Metrics

Figure 4.1a and Figure 4.1b exhibit the performance and the computational time of the MPC for each prediction horizon respectively. It can be seen that performance increases with an increase in prediction horizon up until 6 hrs. This increase in performance however is not guaranteed for an economic model predictive controller as stated in [57] and [59], without a sufficiently long time horizon or an appropriate terminal cost function or constraints. Although not entirely clear in Figure 4.1a, a prediction horizon of 6hr, actually produces a slightly lower performing policy than with a prediction horizon of 5 hours.

This is also clear in Figure 4.1a that increasing the MPC's time horizon past 6hrs to 12 and 24 hrs produces a less optimal policy. As expected though, the computational time in computing the control action seems to increase with an increase in complexity. It is noted that while RL can compute the optimal control action in  $\sim 0.2ms$ , whereas even the fastest MPC controller (1hr prediction horizon) takes  $\sim 35ms$ . It is nearly 175x slower. While this outcome is not surprising, it effectively demonstrates the computational demand of MPC, specifically for a highly non-linear model.

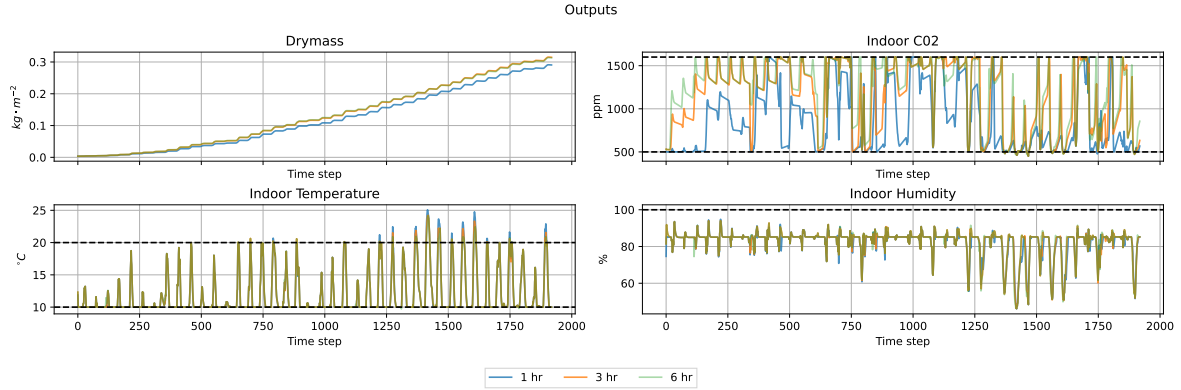
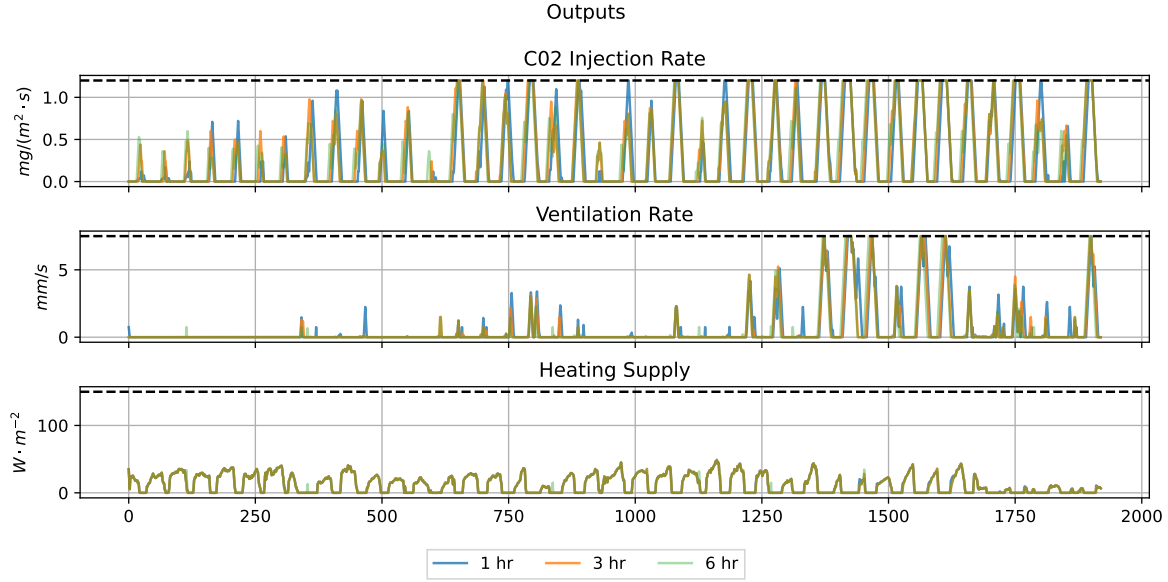


Figure 4.2: MPC 1hr and 5hr Time series of greenhouse outputs



**Figure 4.3:** MPC 1hr and 5hr time series of controller inputs

Figure 4.2 and Figure 4.3 displays the trajectories of the states and inputs of the best performing MPC controller (5hr prediction horizon) and the worst performing (1 hr). These bear similarities to those of the RL agents Figure 3.4 and Figure 3.5 respectively. It is noted that in both cases (RL and MPC), the better performing policies rapidly raises the indoor CO<sub>2</sub> levels at the beginning of the growing period by reducing ventilation and increasing CO<sub>2</sub> injection. However, the trajectories of other states and inputs, particularly the indoor temperature, humidity and heating, appear to be unchanged. Either the temperature does not play a vital role in plant growth or the prediction horizon is not long enough to see the effect of temperature at initial growth stages. However, it is clear that the MPC controller uses heating at night and the irradiance during the day to ensure that temperature constraints are met. These results are very similar to [9] and [36] although difficult to compare quantitatively due to the difference in the optimization goal and MPC problem formulation.

### 4.3. Stochastic Results

For each stochastic level,  $\delta = 5\%$ ,  $\delta = 10\%$ ,  $\delta = 20\%$ , was analyzed with prediction horizons of 1, 3, and 5 hours. Additional prediction horizons were not considered due to limitations in simulation time.

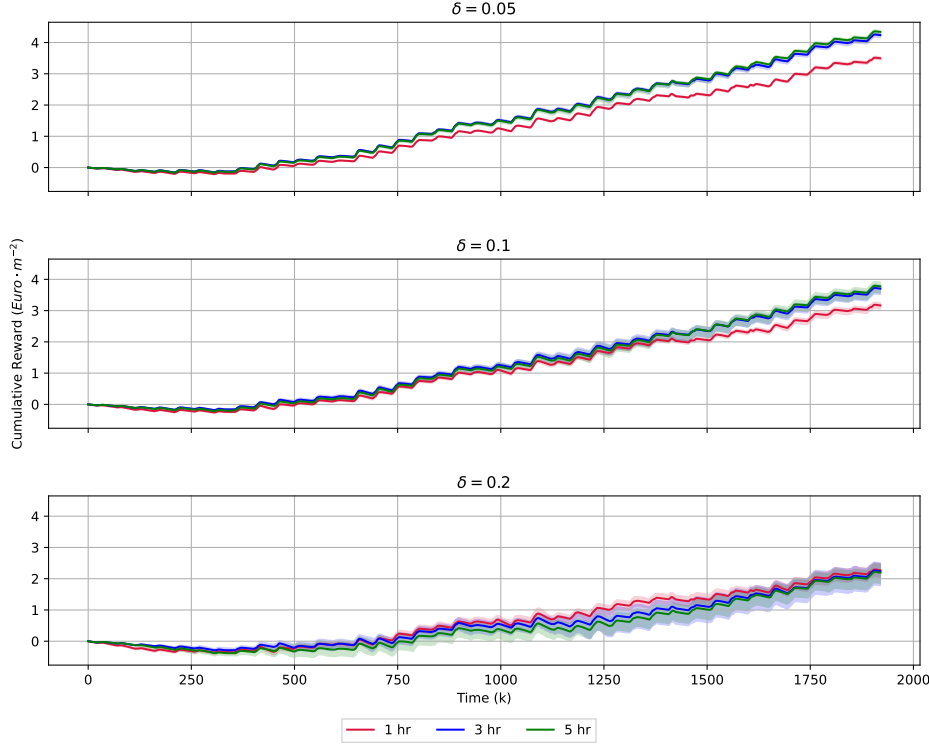


**Figure 4.4:** Time evolution of cumulative Rewards. Displays the evolution of the cumulative reward over the growing period, for each level of stochastic and prediction horizon. Solid lines represent the mean cumulative reward trajectory with a range indicating the minimum and maximum trajectory recorded in the 30 runs.

Figure 4.4 shows the impact of introducing uncertainty and its effect on the cumulative reward obtained by the MPC controller at each time step. While a  $\delta = 0.05$  does not impact performance noticeable, there is significant performance degradation for  $\delta = 0.2$ . Also to note, is that a longer prediction still results in a higher mean cumulative reward, however for high uncertainties, specifically  $\delta = 0.2$ , it seems that a longer prediction horizon results in worse performance.

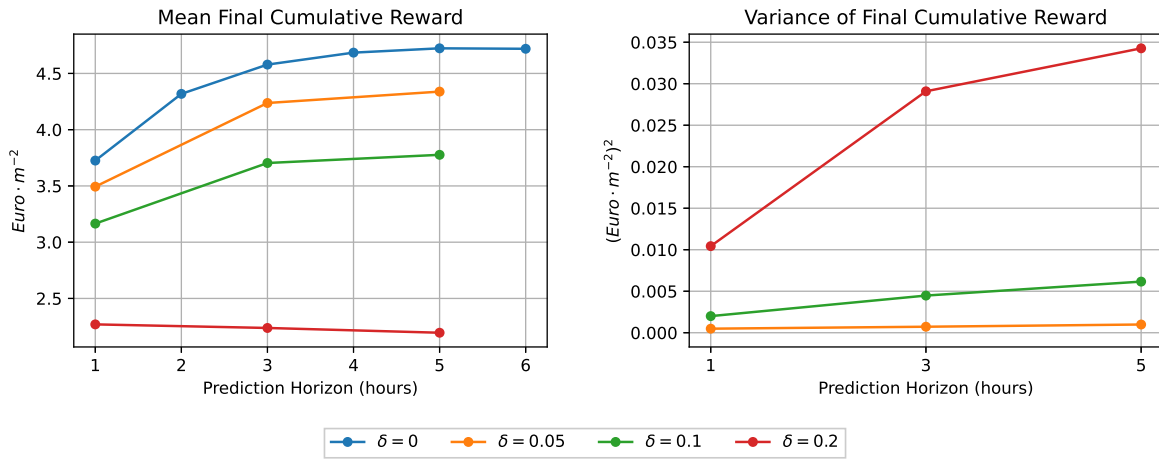


**Figure 4.5:** MPC performance in stochastic conditions

Figure 4.5 depicts the final mean and variance values of the cumulative reward for each prediction horizon and uncertainty level, including nominal conditions. Figure 4.5 may provide a better representation of how stochasticity affects performance. Longer prediction horizons appear to have a greater negative

impact on the system beyond a certain level of uncertainty. Moreover, there is a clear adverse affect on variance as prediction horizon is increased for all uncertainty levels. This can be attributed to the fact that longer prediction horizons become progressively less accurate due to the increasing uncertainty of the model parameters. It is widely acknowledged that MPC is not adept at handling uncertainty, and these results are confirmation of this. Although it is possible to formulate a robust MPC, such as in [36], it introduces a heavy computational burden on the controller. As previously mentioned, RL's decrease in performance due to uncertainty is not as drastic as MPC's. Thus, it is worth exploring whether the RL agent can assist the MPC in mitigating the adverse impacts of parametric uncertainty.

## 4.4. Conclusion

MPC is a highly beneficial and efficient control strategy that has shown remarkable achievements in diverse fields. The formulation of the EMPC OCP was formulated and aimed to maximize the economic advantage of the greenhouse by aligning its optimization goal with that of the RL agent. This was done to facilitate direct comparisons between the two control schemes. Minimal adjustments were necessary to attain the level of performance showcased in this chapter. While the performance of the MPC is satisfactory, as anticipated for an EMPC, increasing the prediction horizon may not yield an increase in performance without an adequate terminal constraint or region. Moreover, the computational time required to calculate a control input is costly. The scalability of the computational time is considerably inferior to that of the RL agent. Therefore in more complex systems, the model is typically linearized or simplified, leading to a suboptimal policy. Furthermore, the performance of the MPC is significantly affected by the presence of parametric uncertainty, and increasing the prediction to address only exacerbates this.

EMPC has clearly shown to have advantages over its RL counterpart however clear downfalls exist. Lastly, to guarantee performance for an EMPC, appropriate additions to its formulation must be made.

# 5

## Deterministic RL-MPC

This chapter aims to construct the RL-MPC framework and examines various implementations to determine their effectiveness. The resulting controllers are evaluated by comparing it with the MPC and RL controllers developed in previous sections. In addition, this chapter will analyze the nominal case in which the model is precisely known.

The smoothness of the value function curve is crucial because, when optimized, it can lead to the generation of numerous local optima, which can disrupt the controller's performance.

### 5.1. Implementation

While there are numerous implementations of RL-MPC, there is limited research focused on maximizing economic benefit specifically for continuous state and action spaces while training RL separately from MPC. As stated in [57] and [59], an EMPC without a terminal constraint and/or terminal cost function does not provide performance and stability guarantees. Specifically [57] states that a terminal constraint is required to ensure closed-loop performance, while [59] extends this concept by proving that applying a terminal region constraint with an appropriate terminal cost function is required to guarantee closed-loop performance. [59] further claims that the terminal cost function with a terminal region is superior to the terminal constraint because it increases the size of the feasible set of initial conditions and may possibly improve the closed-loop performance. However finding such suitable terminal constraints and cost functions prove to be very difficult. It is the objective of this thesis is to ascertain whether the RL agent is capable of providing this.

The integration of RL into MPC will increasingly involve more complex implementations to analyze the impact at each stage. Firstly, initial guesses from the actor will be examined. Subsequently, a terminal constraint will be established by the RL agent. Following this, a terminal constraint region will be defined, also determined by the RL agent. The various value functions trained by the nominal agent will then be used at the terminal cost function, with and without the terminal region constraint. Lastly, a parallel problem will be presented in order to explore an slightly alternative application of the value function.

#### 5.1.1. RL-MPC problem formulations

**Implementation 1** Implementation 1 is the same as Equation 4.1, with the addition of initial guesses. Two sets of initial guesses will be tested and compared with one another. Given that the solution to the OCP in Equation 4.1 at time  $k_0$  denoted as:

$$\begin{aligned}\mathbf{x}^{k_0} &= [x_{k_0}, x_{k_0+1}, x_{k_0+2}, \dots, x_{k_0+N_p}] \\ \mathbf{u}^{k_0} &= [u_{k_0}, u_{k_0+1}, \dots, u_{k_0+N_p-1}]\end{aligned}\tag{5.1}$$

then the two sets of initial guesses at the next time,  $k_1$  step can be denoted as:

$$\begin{aligned}\tilde{\mathbf{x}}^{k_1} &= [x_{k_0+1}, \dots, x_{k_0+N_p}, f(x_{k_0+N_p}, \pi(x_{k_0+N_p}), d_{k_0+N_p}, p)]^T \\ \tilde{\mathbf{u}}^{k_1} &= [u_{k_0+1}, \dots, u_{k_0+N_p-1}, \pi(x_{k_0+N_p})]^T\end{aligned}\quad (5.2)$$

$$\begin{aligned}\tilde{\mathbf{x}}^{k_1} &= [x_{k_1}, f(x_{k_1}, \pi(x_{k_1}), d_{k_1}, p), \dots, f(x_{k_1+N_p-1}, \pi(x_{k_1+N_p-1}), d_{k_1+N_p-1}, p)]^T \\ \tilde{\mathbf{u}}^{k_1} &= [\pi(x_{k_1}, \pi(x_{k_1+1}), \dots, \pi(x_{k_1+N_p-1}))]^T\end{aligned}\quad (5.3)$$

The first initial guess (Equation 5.2) takes the previous time steps solution, shifts it and uses the policy  $\pi(\cdot)$ , as provided by the actor, to calculate the optimal action and resulting state to take at the last time step. Essentially the actor is unrolled once from the last time step of the previous solution to Equation 4.1. The second initial guess, Equation 5.3, involves unrolling the actor  $N_p$  steps from the current state, and using the resulting actions and states as initial guesses.

**Implementation 2** The second implementation incorporates a terminal constraint. The asymptotic average performance of the EMPC can be guaranteed to be no worse than the performance of a optimal reference trajectory under certain assumptions. From [59], these assumptions are:

**Assumption 1** (Properties of constraint sets) The set  $\mathbb{Z}$  is compact, where  $\mathbb{Z} \subseteq \mathbb{X} \times \mathbb{U}$

**Assumption 2** (Continuity of cost and system) The functions  $l(\cdot), f(\cdot)$  are continuous on  $\mathbb{Z}$ . The terminal cost function  $V_f(\cdot)$  is continuous on  $\mathbb{X}_f$

**Assumption 3** (Stability assumption) There exist a compact terminal region  $\mathbb{X}_f \subseteq \mathbb{X}$ , containing the point  $x_s$  in its interior, and control law  $\kappa_f : \mathbb{X}_f \rightarrow \mathbb{U}$ , such that the following holds

$$V_f(f(x, \kappa_f(x))) \leq V_f(x) - l(x, \kappa_f(x)) + l(x_s, u_s) \quad \forall x \in \mathbb{X}_f \quad (5.4)$$

Assumptions 1 and 2 holds since all states and inputs are bounded and the stage cost, as defined in Equation 4.2 is continuous. For this implementation,  $V_f(\cdot) \equiv 0$ , therefore, assumption 3 clearly holds since  $x, \kappa_f(x)$  is constrained to  $x_s, u_s$ . [60], [59] proves that to ensure this for a time-varying system a reference trajectory  $(\tilde{\mathbf{x}}, \tilde{\mathbf{u}})$  that serves as a bases for a meaningful economic performance for the system must be provided. The terminal constraint should be imposed to keep the system close to this reference trajectory. Since the RL policy can be used as the optimal reference policy, it can be guaranteed that the resulting policy will be at least as good as the RL policy. In order to keep the EMPC close to RL's reference trajectory, initial guesses as given in Equation 5.2 with a terminal constraint equal to the last initial guess such that:

$$\begin{aligned}x_{N_p}^{k_0} &= \mathbf{e}_{N_p}^T \tilde{\mathbf{x}}^{k_0} \\ u_{N_p-1}^{k_0} &= \mathbf{e}_{N_p-1}^T \tilde{\mathbf{u}}^{k_0}\end{aligned}\quad (5.5)$$

where  $\mathbf{e}_{N_p+1}$  and  $\mathbf{e}_{N_p}$  represents the  $i$ th standard basis vector in  $\mathbb{R}^{N_p+1}$  and  $\mathbb{R}^{N_p}$  respectively. i.e.,  $e_i$  provides a selection vector to extract the last state and input from the initial guess, to be used as a terminal constraint. Both the last control input and the state must be constrained since the current control action depends on the previous control action (Equation 4.1d).

**Implementation 3** Implementation 3 builds upon implementation 2, in that instead of providing a terminal constraint, a terminal region as provided by the actor will be used. The terminal region is defined as:

$$\begin{aligned}(1 - \delta_T) \mathbf{e}_{N_p}^T \tilde{\mathbf{x}}^{k_0} &\leq x_{N_p}^{k_0} \leq (1 + \delta_T) \mathbf{e}_{N_p}^T \tilde{\mathbf{x}}^{k_0} \\ (1 - \delta_T) \mathbf{e}_{N_p-1}^T \tilde{\mathbf{u}}^{k_0} &\leq u_{N_p-1}^{k_0} \leq (1 + \delta_T) \mathbf{e}_{N_p-1}^T \tilde{\mathbf{u}}^{k_0}\end{aligned}\quad (5.6)$$

[59] suggests that this has the same performance guarantees as Implementation 2 under the same assumptions. However introducing a terminal region for the terminal state makes it difficult to meet assumption 3 as shown in Equation 5.4. However, [59] suggest that providing a terminal region may be more beneficial than a terminal constraint. Finally, a terminal constraint and initial guesses will also be provided by Equation 5.3 to investigate performance. However, since the action of unrolling from the current state does not result in following a fixed trajectory, no performance guarantee can be made.

**Implementation 4** Implementation 4 consists of only including the value function as learned in section 3.6, and initial guesses as given in Equation 5.2. This implementation examines the effect of the value function on the performance of the resulting controller. The value function can be incorporated into Equation 4.1 by defining a cost function:

$$\min_{u(k), x(k)} \sum_{k=k_0}^{k_0+N_p-1} l(u(k), y(k)) - \tilde{V}(s'(k_0 + N_p)) \quad (5.7)$$

where  $\tilde{V}$  represents the learned value function and  $s'(k_0 + N_p)$  is the normalization of  $s(k_0 + N_p)$ . For  $\tilde{V}^1, \tilde{V}^2, \tilde{V}^3$ , the unnormalized input is Equation 3.1, where as in  $\tilde{V}^4$ , this is  $(y_{k_0+N_p}, k_0 + N_p)$  as discussed in section 3.6. Normalization of the state observation is performed with Equation 3.7. This implementation aims to evaluate the impact of different neural network architectures, including a deep neural network ( $\tilde{V}^1$ ), a smaller deep neural network ( $\tilde{V}^2$ ), a shallow neural network ( $\tilde{V}^3$ ), and a deep neural network trained to learn the value function on only two system states. This can be considered a naive implementation of RL-MPC, and would essentially equate to the rolling out the value function. According to approximate dynamic programming as stated in [18], this policy could be better than the policy that generated the value function. The performance is heavily dependent on the quality of the value function. If the approximate value function is inaccurate and the errors are significant and systematic then unrolling this value function could lead to a worse policy. This implementation may be conceptually viewed as either unrolling the value function, or providing the MPC knowledge of the future, essentially extending its prediction horizon. Note that the value function is maximized by minimizing the negative of it, since the learned value function represents total return and not cost.

**Implementation 5** Implementation 5 essentially combines Implementation 3 and Implementation 4. [59] states that finding an appropriate terminal cost function and corresponding terminal region proves to be non-trivial in order to satisfy assumption 3. This implementation is also claimed to be superior to the terminal constraint of implementation 2 ([59]) under necessary conditions. Therefore the resulting RL-MPC OCP is defined as:

$$\min_{u(k), x(k)} \sum_{k=k_0}^{k_0+N_p-1} l(u(k), y(k)) - \tilde{V}(s(k_0 + N_p)) \quad (5.8a)$$

$$\text{s.t. } x(k+1) = f(x(k), u(k), d(k), p), \quad (5.8b)$$

$$y(k) = g(x(k+1), p), \quad (5.8c)$$

$$-\delta u \leq u(k) - u(k-1) \leq \delta u, \quad (5.8d)$$

$$u_{\min} \leq u(k) \leq u_{\max}, \quad (5.8e)$$

$$x(k_0) = x_{k_0}. \quad (5.8f)$$

$$\tilde{\mathbf{x}}^{k_0} = [x_{k-1+1}, \dots, x_{k-1+N_p}, f(x_{k-1+N_p}, \pi(x_{k-1+N_p}), d_{k-1+N_p}, p)]^T \quad (5.8g)$$

$$\tilde{\mathbf{u}}^{k_0} = [u_{k-1+1}, \dots, u_{k-1+N_p-1}, \pi(x_{k-1+N_p})]^T \quad (5.8h)$$

$$(1 - \delta_T) \mathbf{e}_{N_p}^T \tilde{\mathbf{x}}^{k_0} \leq x_{N_p}^{k_0} \leq (1 + \delta_T) \mathbf{e}_{N_p}^T \tilde{\mathbf{x}}^{k_0} \quad (5.8i)$$

$$(1 - \delta_T) \mathbf{e}_{N_p-1}^T \tilde{\mathbf{u}}^{k_0} \leq u_{N_p-1}^{k_0} \leq (1 + \delta_T) \mathbf{e}_{N_p-1}^T \tilde{\mathbf{u}}^{k_0} \quad (5.8j)$$

$$(5.8k)$$

This implementation was investigated to determine whether RL might provide both an adequate terminal region and cost function to improve the MPC's performance.

**Implementation 6** Implementation 6 serves an alternative method of incorporating the value function. This implementation involves solving implementation 3 however with Equation 5.2 and Equation 5.3 separately. Once solved, the terminal state of the two solution trajectories are compared by evaluating them with the value function. The solution trajectory with the terminal state that yields the most favourable outcome (as given from the value function) is selected as the final solution and the first control input of this solution is taken. It essentially selects the best policy. Although only 2 policies are compared, this method may warrant further research whereby multiple generated policies could be compared. The policies generated could originate from multiple RL agents, each providing their initial estimations along with corresponding terminal constraints. Although each problem could be solved in parallel to speed up computational speed, it was implemented sequentially in this thesis.

### 5.1.2. Initial RL and MPC performance

A review of the RL and MPC policies will be evaluated for the nominal conditions.

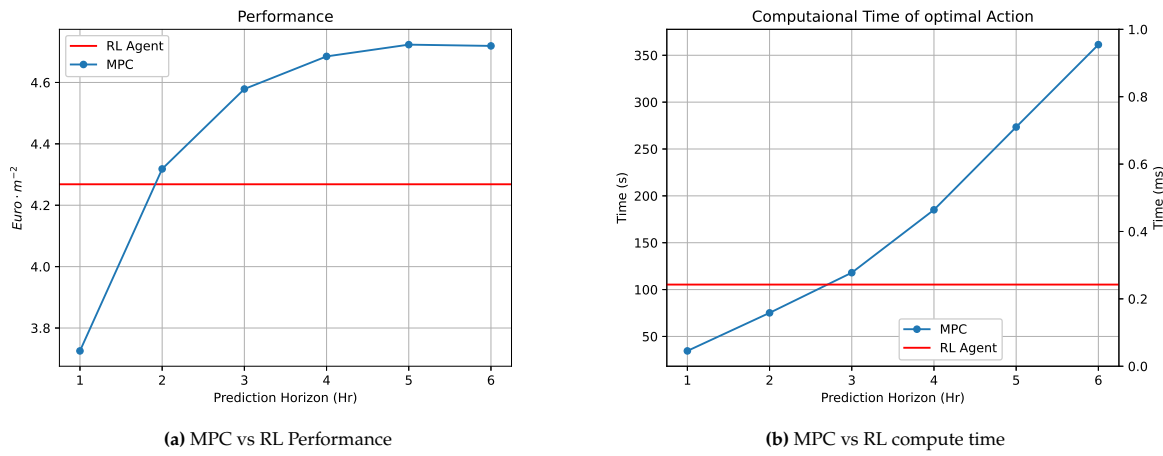


Figure 5.1: MPC vs RL

Figure 5.1 demonstrated the performance of the MPC and RL agent in the nominal setting. Although MPC does perform better for all prediction horizons (except 1 hour) as shown in Figure 5.1a, it does not imply that this is the best RL policy obtainable. A more extensive hyper parameter tuning may have to be forgone in order to achieve a policy that outperforms MPC. However the RL agent is clearly competitive and as seen in Figure 5.1b, can compute actions significantly faster. It is evident that the RL agent can be utilized to generate a reference trajectory for MPC with minimal increase in computational time. The performance of the resulting RL-MPC and its potential superiority will be analyzed in following sections and compared to the baseline performances, as depicted in Figure 5.1.

## 5.2. Results - Implementations 1

This implementation consists of passing in initial guesses for the MPC solver by unrolling the agent. Initial guess 1 refers to Equation 5.2 and Initial guess 2 refers to Equation 5.3.

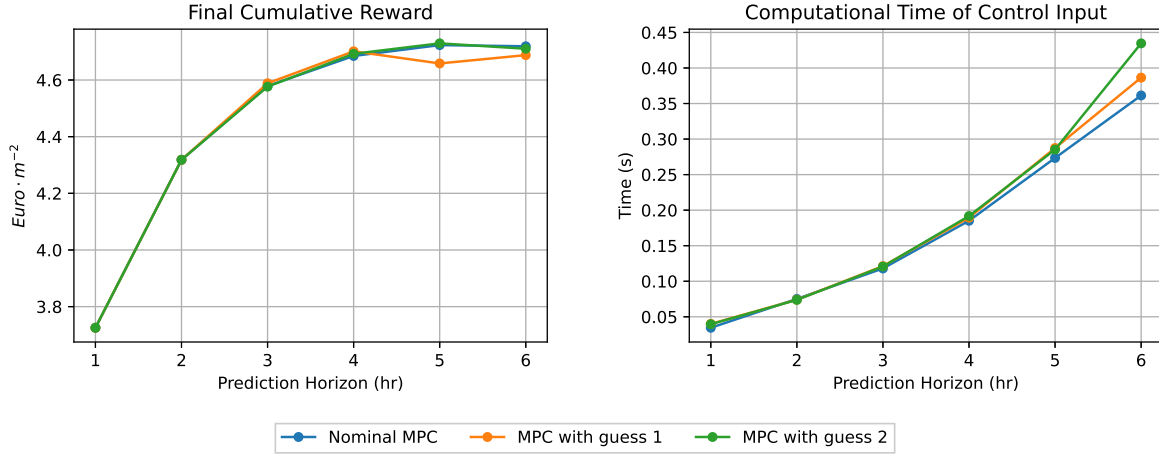


Figure 5.2: MPC vs MPC with initial guesses

Figure 5.2 presents the results of passing in initial guesses from the actor. Unrolling the actor from the current state and using the resulting state and control inputs as initial guesses (Equation 5.3) seems to have very little impact on the final cumulative reward, however it noticeable increases the computational time of the control input. This could be because the initial guesses are derived from a less than optimal policy. Moreover, initial guesses by extending the prediction horizon from Equation 5.2 also has minimal impact on the final cumulative reward for shorter prediction horizons, and seems to be slightly beneficial for a 3 and 4 hour prediction horizon. However performance degrades significantly for a prediction horizon of 5 and 6 hours as compared to the nominal MPC. Additionally, computational also time increases. It would be expected that computational time decreases for both initial guesses. A reason for the sub-optimal performance may be due the initial guesses of the Lagrangian multipliers (the found Lagrangian multipliers from the previous solution). The actor's initial guesses may differ significantly from the previous solution, rendering the Lagrangian multipliers' guesses nonsensical. While the actor may offer initial guesses, they are insufficient for improving or assisting the MPC, and simply using the previous solution as an initial guess may be more beneficial. However, the importance of having optimal initial guesses becomes more significant as the prediction horizon is extended, as the problem complexity increases. Therefore, if a superior policy to the Nominal MPC were to provide initial guesses instead of a suboptimal policy at a longer prediction horizon, it could result in a more favourable outcome.

### 5.3. Results - Implementations 2

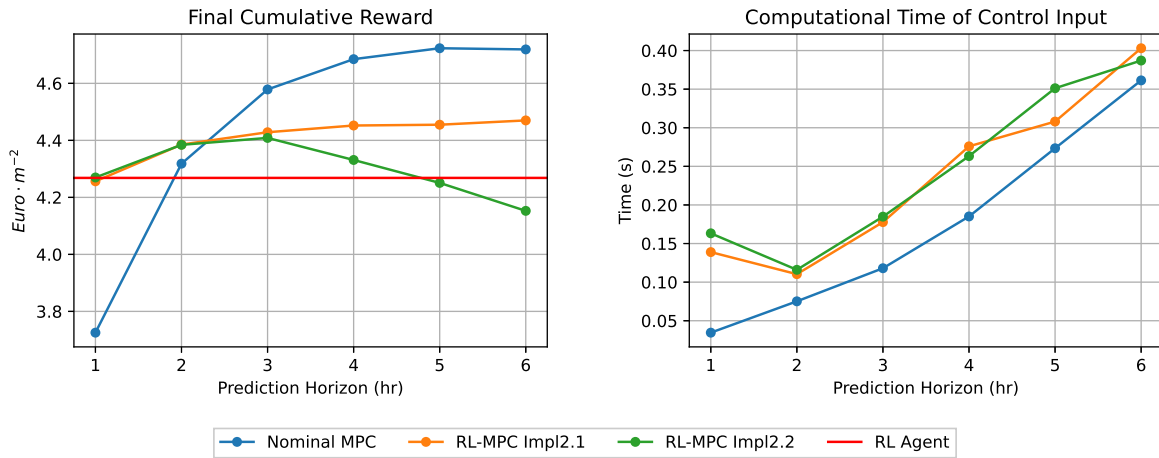


Figure 5.3: MPC with terminal constraints from agent

In order to guarantee that the RL-MPC policy achieves a performance level that is equal to or better than the RL policy, the approach described in Implementation 2 was used. The performance of the resulting policies is illustrated in Figure 5.3. It is evident that for a terminal constraint and initial guesses as given by Equation 5.2, that the resulting policy is at least as good as the RL's, even at lower prediction horizons where RL performs better than MPC. Nevertheless, the RL-MPC policy exhibits notably inferior performance compared to the MPC policy when the prediction horizon exceeds 3 hours. Beyond the 3-hour mark, the MPC policy consistently outperforms the RL policy and RL-MPC policy. While the implementation of RL-MPC may enhance the RL policy, it does not guarantee that the resulting policy will surpass the policy generated purely by MPC. If the RL policy is more competitive and surpasses the performance of the MPC, then implementing this RL-MPC implementation would be advantageous, as is the case for a prediction horizon of 1 and 2 hours. This marks a very important design choice. One can choose to either impose a terminal constraint to guarantee a certain level of performance or instead opt to extend the prediction horizon of the MPC. Again, by extending the horizon for the MPC controller is not guaranteed to perform better under economic optimization, therefore a safer choice may be to implement the terminal constraint as provided by the RL agent.

The lack of performance guarantees for the terminal constraint and initial guesses, as indicated by equation Equation 5.3, is evident in the decrease in performance, which is even worse than that of reinforcement learning, when longer prediction horizons are considered.

The computational time for the control input significantly increases when the prediction horizon is set to 5 or 6 hours. The terminal constraint may excessively limit the MPC due to the presence of a sub-optimal terminal constraint, particularly when dealing with longer prediction horizons.

## 5.4. Results - Implementation 3

This implementation aims to move away from the terminal constraint and allow the MPC more freedom by providing it with a terminal region constraint as outlined in Equation 5.6, with a chosen  $\delta = 5\%$ , allowing for a 10\$ deviation in the terminal state. As claimed in [59], this could prove to be more beneficial than the terminal constraint, provided that an appropriate cost function is supplied. For this implementation, the cost function supplied is effectively  $V(s) \equiv 0$ .

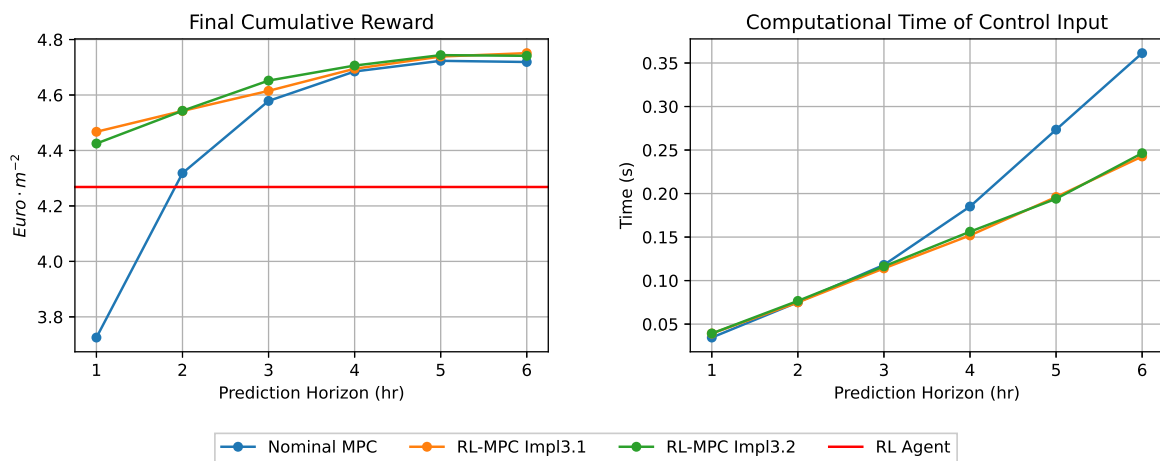


Figure 5.4: MPC with terminal region

The results from the implementation are depicted in Figure 5.4. Shortening the prediction time horizons results in a substantial increase in the overall cumulative reward compared to both the stand-alone MPC and RL policies. Furthermore, the RL-MPC obtains a marginally superior final cumulative reward in comparison to the MPC even at longer prediction horizons. Lastly, it appears that this performance is increasing monotonically with an increase in prediction horizon, unlike for MPC. This could indicate that an appropriate cost function and terminal region has been found to guarantee performance and stability. However, longer prediction horizons would be required to provide conclusive evidence of this.

Additionally, this terminal region also allowed for a lower computation time of the control inputs, with a more noticeable faster compute time at longer prediction horizons. This is likely because the terminal region is less limiting than the terminal constraint, while also providing guidance to the MPC, resulting in reduced computational times.

It is noted that the resulting performance (increase in total cumulative reward and decrease in computational time) of the RL-MPC policy outperforms both standalone policies, even when the terminal region and initial guesses are supplied by a policy that performs substantially worse than the MPC controller. This underscores the necessity of giving certain future-oriented information to the EMPC in order to attain optimal economic advantage, performance, and stability.

## 5.5. Results - Implementation 4

This implementation investigates the effect of supplying the MPC with a cost function, specifically an approximate value function represented by a neural network.

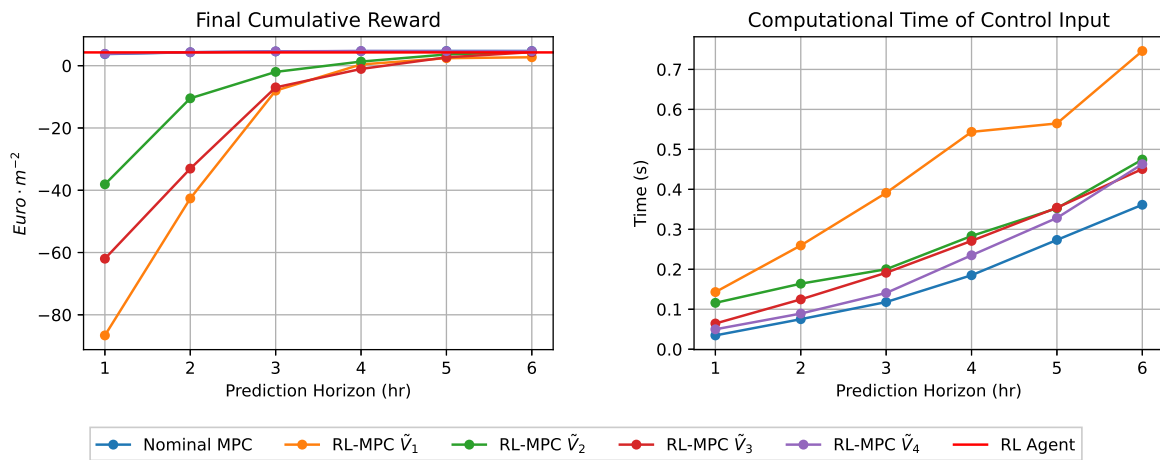


Figure 5.5: MPC with terminal cost function

Figure 5.5 is a naive implementation of merging RL and MPC. However, the outcomes are unsatisfactory in terms of both the overall cumulative reward and the computational time required for generating control inputs. Caution must be exercised when employing a neural network in an optimizer, as they possess a profoundly non-linear nature. As illustrated in Figure 5.5, the performance deteriorates as the neural network becomes more intricate. The neural networks exhibit highly non-convex behaviour that may cause the MPC optimizer to become easily trapped in local optima. The only value function that seems to not destabilize the optimizer is  $\tilde{V}_4$  which is also the only value function that exhibits a smooth behaviour, see remark 1. The MPC's optimisation task is solely focused on maximising the drymass in this particular value function, with time being a constant parameter. However, for the other value functions, the MPC needs to optimise across all possible model states and inputs. Although this leads to more accurate inference for the value of the specific environmental state, it also introduces additional dimensions and consequently a greater number of possibilities for becoming stuck in local optima that may not be meaningful.

It is natural to observe an increase in computational time in Figure 5.5. Once again, the extremely non-convex nature of the behaviour can disrupt the MPC optimizer and lead to unpredictable computational times. However, it is worth noting that  $\tilde{V}_4$  consistently exhibits a predictable computational time, highlighting the significance of obtaining a high-quality value function.

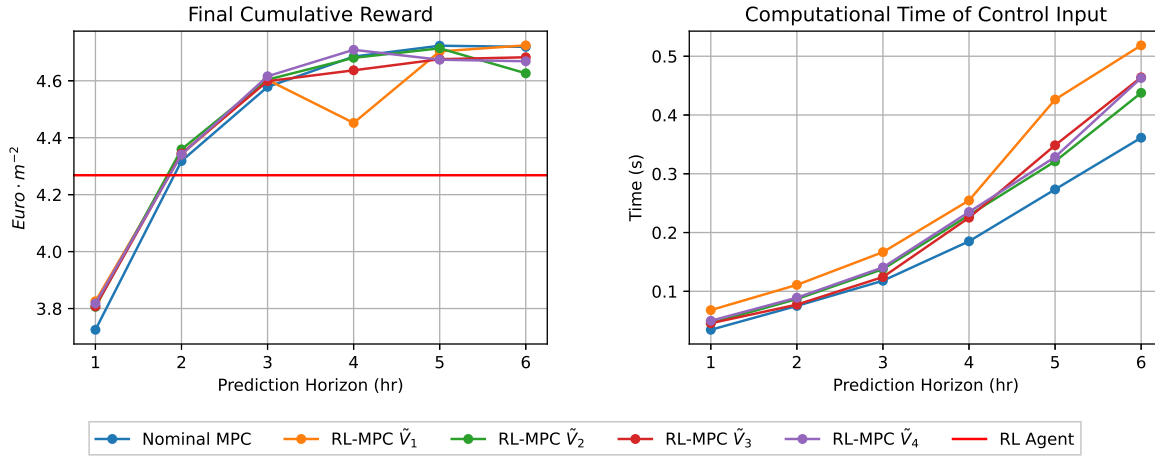


Figure 5.6: MPC with terminal cost function

To minimise the non-linearity of the value functions, the decision variables, except for the drymass, were kept fixed at their initial guesses. This was done because it is evident that the value of a state can be estimated based solely on the current time and the state of the drymass. Thus, the optimisation process was exclusively focused on optimising the dry mass, as was done with  $\tilde{V}_4$ . The performance of the resulting RL-MPC policy is demonstrated in Figure 5.6. The addition of the value functions improves the final cumulative reward over MPC at shorter prediction horizons but degrades performance for longer prediction horizons (5 and 6hr). Although the value functions have been simplified, increasing the prediction horizon allows the MPC's optimization process to get trapped in local optima, this could be the reason for the observed performance degradation in Figure 5.6. Moreover, the simplification of the value function also resulted in more consistent times, with very little increase as compared to the nominal MPC.

$\tilde{V}_4$  was used for further testing, since it exhibits the greatest performance increase (final cumulative reward) over the nominal MPC (1-4hrs) as compared to the other simplified value functions. The performance of  $\tilde{V}_4$  is expected to be superior to the others because it was trained exclusively on the drymass state and time, enabling it to make more accurate predictions of the value of a specific state using only these two inputs. These results suggests that a value function can increase performance over nominal MPC, but necessarily over the RL policy that it was derived from. In addition, in order for the value function to be effective, it should have a minimal number of local optima while maintaining accuracy. Furthermore, it should be smooth and capable of generalising effectively across the state space to ensure reliable performance. Lastly, it is important to balance the performance gains with the increased computational time, and as shown in Table 5.1, the increase in computational time, far outweighs the marginal performance increase for shorter prediction horizons.

	1hr	2hr	3hr	4hr	5hr	6hr
Final Cumulative Reward Increase(%)	2.484	0.525	0.814	0.512	-1.041	-1.069
Computational Time Increase (%)	50.888	40.358	30.859	29.062	14.243	23.013

Table 5.1: RL-MPC  $\tilde{V}_4$  performance comparison compared to MPC

## 5.6. Results - Implementation 5 and 6

Implementation 5 aims to incorporate both a terminal region constraint as well as a terminal cost function.  $\tilde{V}_4$  is used as a cost function with a terminal region generated by initial guesses as in Equation 5.2, with a  $\delta_T = 5\%$ . Implementation 6 solves two problems, each with its own initial guesses and terminal region (Equation 5.2 and Equation 5.3 respectively). It determines the optimal policy by evaluating the terminal state in each solution using the value function.

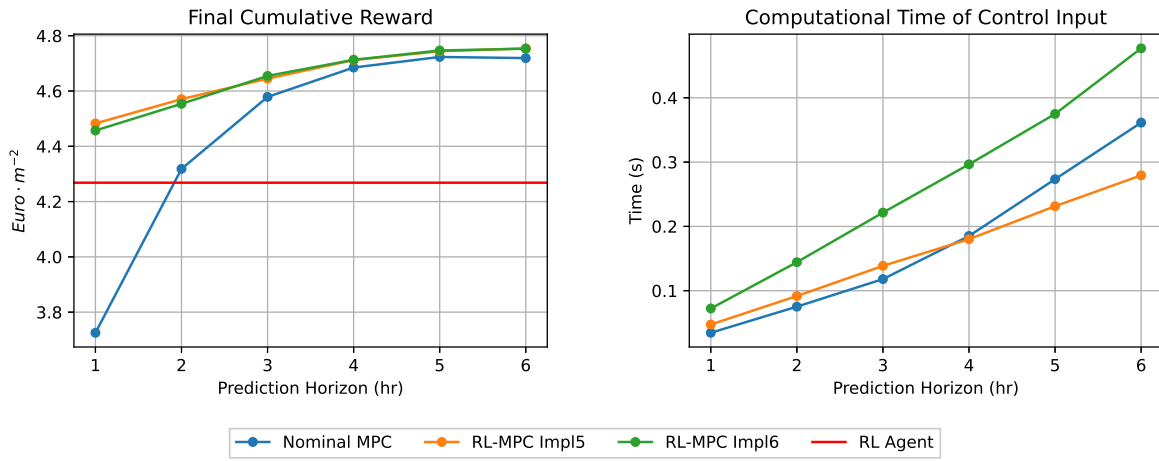


**Figure 5.7:** MPC vs RL-MPC with terminal region and cost function vs RL-MPC solving two separate problems and evaluating best policy with value function

As demonstrated in Figure 5.7, both implementations outperform the standalone MPC and RL policies across all MPC prediction horizons. The computational time of implementation 6 is notably higher because it solves two optimisation problems instead of just one. Nevertheless, it is possible to solve the 2 problems in parallel, effectively reducing the computational time by half. Although the performance gains are substantial as compared to the standalone MPC, it is noted that majority of this performance increase is due to the terminal region constraint. In addition, this constraint on the terminal region also seems to make the performance increase monotonically, even with the addition of the value function. Furthermore, despite the inclusion of a neural network in the optimisation problem (Implementation 5), the computational time is reduced to a similar level as the standalone MPC when a terminal region constraint is present.

However , whether a value function is necessary when the terminal region

## 5.7. Final Result and Conclusion

The three best implementations are compared, namely Implementation 3 (with guesses and terminal region provided by Equation 5.2), Implementation 5 and 6.

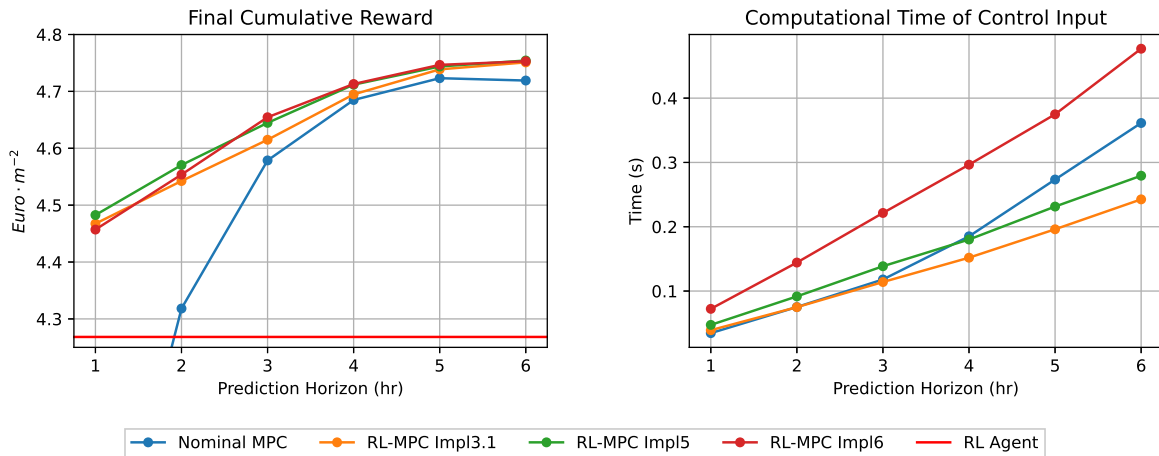


**Figure 5.8:** MPC final

The final results of the mentioned implementations are shown in Figure 5.8. While the inclusion of a terminal region is the primary factor in improving performance, the incorporation of the value function

can additionally enhance performance, albeit with the drawback of increased computational time. This suggests that the value function and terminal region provided by RL satisfy the necessary assumptions to ensure performance of an EMPC. However, a formal proof would be needed to confirm this conclusively. Moreover, the increase in computational time is not that drastic when a neural network is implemented, especially with the addition of a terminal region to aid the MPC in finding solutions faster. While the computational time increase may appear insignificant, this system is relatively uncomplicated compared to others. If this approach is used in highly complex systems, this increase in computational time could result in destabilizing the system. Therefore any methods in reducing the computational time is highly beneficial. Moreover, it seems that there is very little benefit to adding a cost function when the advantages of adding a terminal constraint is already so beneficial.

**Table 5.2:** RL-MPC 3 and 5 vs MPC and RL

	1hr		2hr		3 hr		4 hr		5 hr		6 hr		RL @ 1 hr Perf
	Perf	Time	Perf	Time	Perf	Time	Perf	Time	Perf	Time	Perf	Time	
RL-MPC 3 (%)	19.91	10.91	5.191	2.38	0.79	-5.38	0.21	-8.47	0.328	-16.2	0.67	-18.95	4.67
RL-MPC 5 (%)	20.32	24.26	5.84	18.26	1.44	44.37	0.57	3.68	0.435	2.71	0.746	-7.86	5.02

Table 5.2 displays the performance increase of RL-MPC 3 and RL-MPC 5 against the nominal MPC and a comparison with RL at a 1hr prediction horizon. Incorporating both a terminal region and value function appears to offer minimal advantages compared to only using a terminal region, as the marginal improvement in performance results in a significantly larger increase in computational time. This reiterates the importance of reducing the computational cost of the neural network in the optimization problem. As seen in Figure 5.8, RL-MPC 6 offers promising results as an alternative method to using the value function, and could yield even more benefits when more than two initial trajectories and terminal regions are provided by various agents and methods. The computational time of RL-MPC 6 can be theoretically halved by solving the problems in parallel, resulting in a compute cost similar to RL-MPC 3 and a similar performance to RL-MPC 5. Further research should be conducted on this implementation in the future.

While the combination of RL and MPC shows promising results, it is important to note that the simulations remain deterministic. These results primarily indicate which implementations are worth testing further in a stochastic environment, to create a more accurate depiction of reality. Moreover, it may be tempting to use RL-MPC 2 (with terminal constraint) to guarantee performance as good as RL. However, in a stochastic environment, this may not be practically achievable and there are no equivalent performance guarantees available. It may not be feasible because the terminal constraint, as determined by the generated reference trajectory, may not be attainable due to the random nature of the state evolution. Consequently, allowing a terminal region relaxes this constraint and makes the problem computational tractable. Finally, a value function derived from a policy that inherently considers uncertainty can provide the MPC with valuable insights regarding the impact of uncertainty on its calculated control actions. Therefore, RL-MPC 3 and RL-MPC 5 are suitable choices for testing in a stochastic environment.

# 6

## Stochastic RL-MPC

This chapter outlines the performance gains of various RL-MPC implementations as selected from chapter 5 in a stochastic environment. The initial performances of the standalone RL agents and MPC in various levels of uncertainty will be investigated followed by comparisons with the RL-MPC implementations. This chapter seeks to demonstrate the effectiveness of RL-MPC controllers in a realistic setting, providing insight into the controller's potential performance in real-world applications.

### 6.1. Initial RL and MPC Performance

The uncertainty present in the environment, as mentioned in section 3.2, is characterised as parametric uncertainty. Nevertheless, this uncertainty affects the parameters utilised in the computation of the system's outputs (output noise). Consequently, it is customary to utilise a state estimator to mitigate this noise. An approach that is both common and effective for MPC is to utilise the Moving Horizon Estimation (MHE) technique, which can be naturally integrated into the MPC framework. However, this thesis does not incorporate such an estimator in order to clearly observe the impact of combining RL with MPC in a stochastic environment. Moreover, RL was trained on a stochastic environment and the learned policy inherently takes the uncertainty into account. Finally, it is also important to note that for each level of uncertainty a new agent was trained (see section 3.5). Unless specified otherwise, it can be assumed that the corresponding agent is used for each uncertainty level, both in pure RL and RL-MPC. Performance metrics include the mean and variance of the final cumulative reward achieved (averaged across 30 simulations). The computational time required to calculate a control action is not considered, as the presence of uncertainty does not affect it.

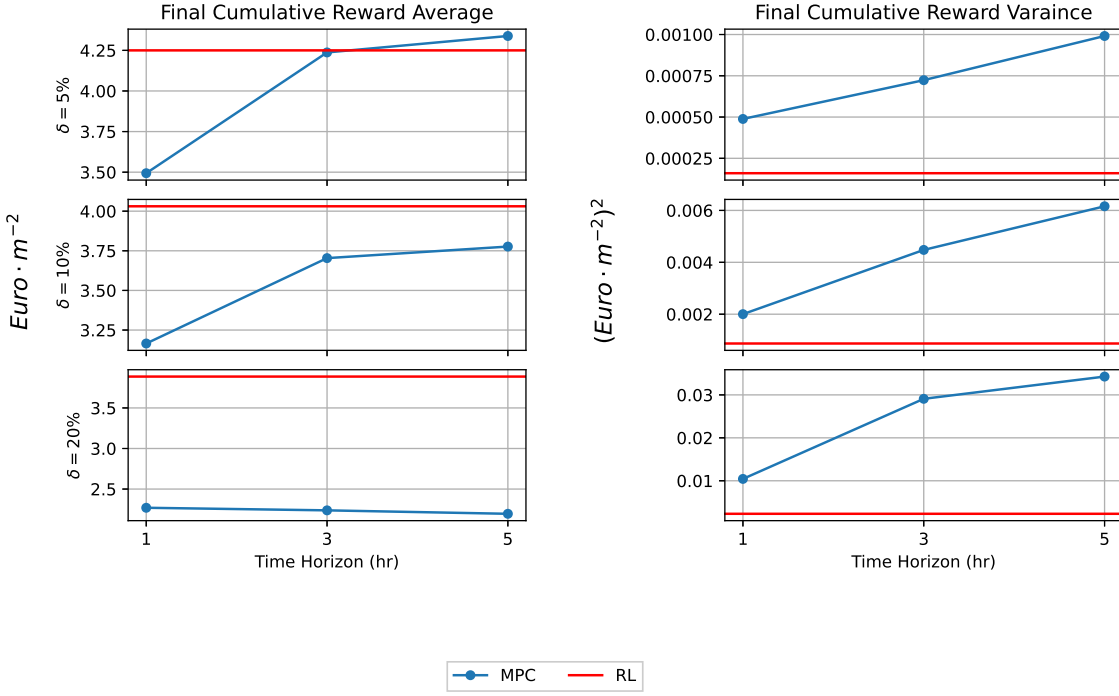


Figure 6.1: RL vs MPC in stochastic conditions

Figure 6.1 demonstrates the performance of RL and MPC for each prediction horizon and uncertainty level. Contrary to the nominal case shown in 5.1, RL consistently outperforms MPC for all prediction horizons and demonstrates superior performance particularly when faced with higher levels of uncertainty. The variance obtained through RL is significantly lower than that of MPC, indicating even greater performance superiority. While it is not surprising given that RL was trained on stochastic data, the findings from Figure 6.1 indicate that as uncertainty levels increase, the effect of increasing the prediction horizon on performance improvement diminishes and may even hinder the performance of MPC in extreme cases of uncertainty. Furthermore, it is worth noting that while both MPC and RL demonstrate comparable performance under conditions of low uncertainty, the final cumulative reward of MPC exhibits significantly higher variance compared to RL. This highlights the robustness of the RL policy. As stated in section 5.7, RL-MPC 3 (which includes a terminal region constraint) and RL-MPC 5 (which includes both a terminal region constraint and a value function as a terminal cost function) are evaluated at different levels of uncertainty. The performance of these implementations is then compared to that of the standalone RL and MPC controllers. The reference trajectory is generated by the RL agent and is based on deterministic predictions.

## 6.2. Results - VF and Terminal Region

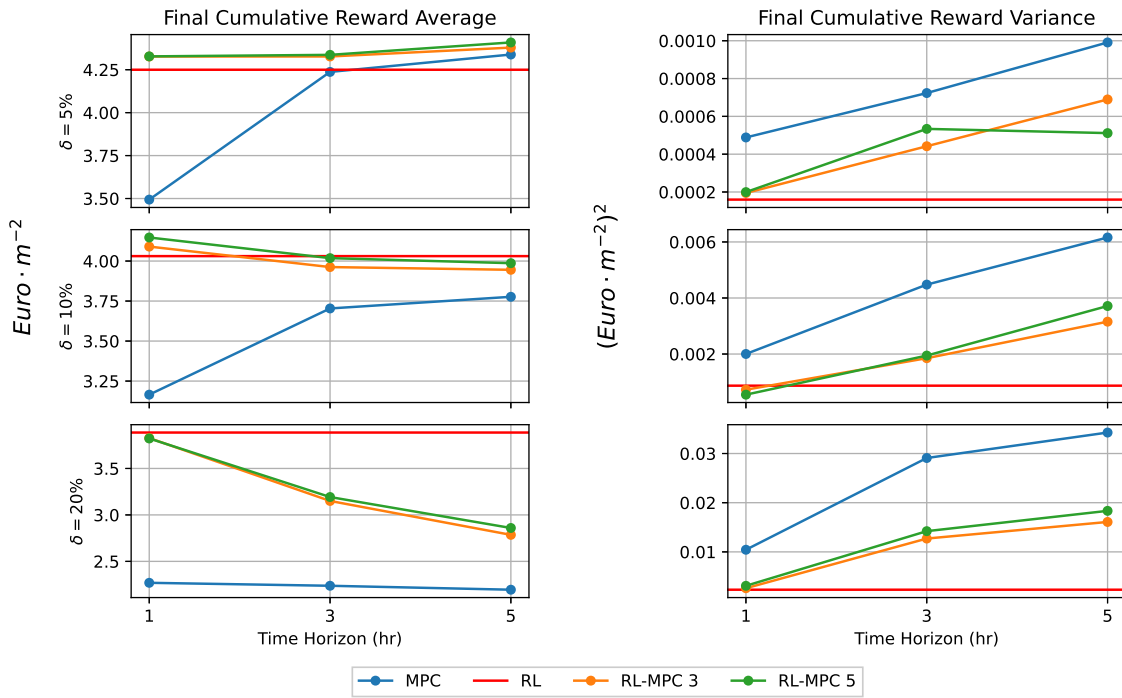
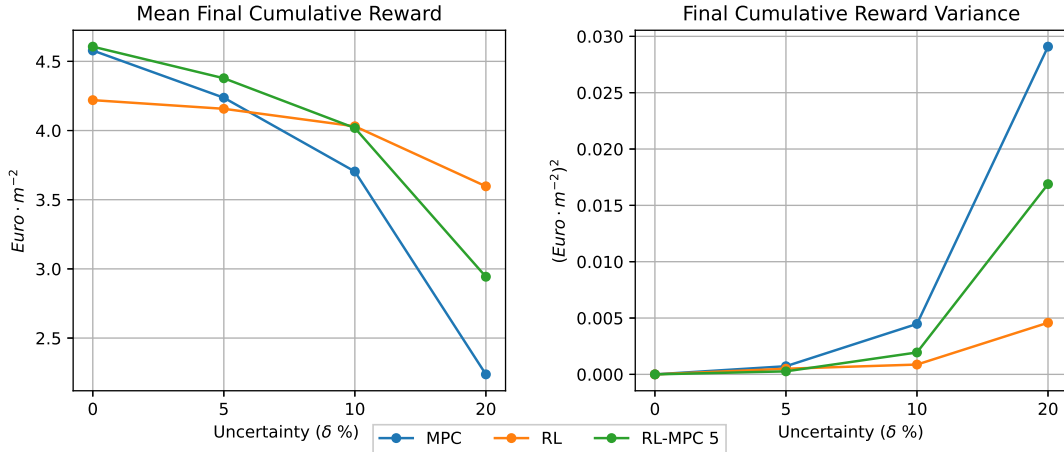


Figure 6.2: MPC vs stochastic RL vs stochastic RL-MPC 3 and RL-MPC 5

The performance comparison between RL-MPC 3 and RL-MPC 5 in a stochastic environment, as well as their comparison with standalone RL and MPC controllers, is shown in Figure 6.2. Similarly to the nominal case, it is evident that when uncertainty is low ( $\delta = 5\%$ ), the RL-MPC controllers outperform both RL and MPC in terms of the mean final cumulative reward. However, it appears that the variance of the resulting RL-MPC controllers is notably greater than that of RL controllers, but notably lower than that of MPC controllers, with the exception of a 1 hr prediction horizon. However, the behaviour of the RL-MPC controllers becomes intriguing when faced with higher levels of uncertainty. It seems that when there is a high degree of uncertainty, the performance of the RL-MPC controller is significantly impacted due to the poor performance of MPC in such highly stochastic environments. The same can be seen for the variance. While the performance of RL-MPC in a stochastic environment with a  $\delta = 10\%$  is comparable to that of RL, it is evident that increasing the prediction horizon significantly affects performance, since it brings the RL-MPC's performance closer to that of MPC. For an uncertainty level of  $\delta = 20\%$  the RL-MPC performance is drastically impacted by an increase in prediction horizon, however still outperforming MPC. As the prediction horizon increases, the RL-MPC controller becomes more similar to the MPC controller. Conversely, with shorter prediction horizons, it becomes more similar to the RL policy. Due to the performance superiority of RL, for higher levels of uncertainty, it is desirable to keep the RL-MPC prediction horizon as short as possible in order to achieve performance, in terms of both the mean and variance of the final cumulative reward, similar to that of RL. Furthermore, it is clear that the inclusion of a value function as a terminal cost function, in conjunction with a terminal region, has improved performance when compared to using only a terminal region (RL-MPC 3 vs RL-MPC 5). This behaviour is similar to what is observed in the nominal case.

In practice, the exact uncertainty of a model is not known, so a conservative estimate of uncertainty is assumed during the development of a controller. A parametric uncertainty of  $\delta = 20\%$  may be considered too conservative, and if the model is indeed highly accurate, it could have a detrimental effect on performance to design a controller on such a high level of uncertainty. Similarly for when developing a controller assuming a low parametric uncertainty. Therefore a controller is usually developed assuming a middle ground uncertainty level. Thus, it was determined to examine the effectiveness of the RL-MPC controller when designed with an uncertainty level of  $\delta = 10\%$  and evaluated under different uncertainty

levels. This evaluation was compared to an RL agent that was also trained with an uncertainty level of  $\delta = 10\%$  and a nominal MPC. Moreover, it can be seen in Figure 6.2, that careful consideration must be taken when selecting a predication horizon for both RL-MPC and MPC since a longer prediction horizon may lead to substantially worse performance due to the accumulation of uncertainty across the prediction horizon. Thus, a prediction horizon of 3 hours was chosen for both the MPC and RL-MPC, which was considered to be a suitable compromise for this study.



**Figure 6.3:** MPC vs RL vs RL-MPC 5 using an RL agent trained on  $\delta = 10\%$  uncertainty and prediction horizon of 3 hours for both MPC and RL-MPC

The performance of the RL-MPC controller under various levels of parametric uncertainty is shown in Figure 6.3. Both the the RL-MPC controller and the RL agent are designed on an RL agent trained on a  $\delta = 10\%$ . The superiority of the RL-MPC controller over both the MPC and RL controllers under normal conditions is once again demonstrated in Figure 6.3 in terms of mean final cumulative reward. This trend persists until the uncertainty reaches a threshold where the MPC framework is unable to handle it, resulting in a significant decline in performance. Nevertheless, the RL-MPC consistently outperforms the MPC in terms of mean final cumulative reward, and the decrease in performance is not as severe when compared to MPC. The RL-MPC controller also outperforms the MPC controller in terms of variance in the final cumulative reward. The RL agent continues to demonstrate superior performance in terms of variance under conditions of increased uncertainty. However, it is evident that RL's capacity to handle uncertainty has been successfully transferred to RL-MPC. It is mentioned again that no state estimator is employed in the MPC's framework. By implementing this approach, the performance of the MPC is likely to significantly enhance under conditions of high uncertainty. As a result, the performance of the RL-MPC is also expected to improve, and potentially outperforming RL even at high levels of uncertainty.

### 6.3. Conclusion

This chapter has demonstrated the performance gains of the RL-MPC controller in a stochastic environment, which builds upon the deterministic evaluations performed in chapter 5. These results highlights the effectiveness of the RL-MPC controller as well as its robustness in varying levels of uncertainties.

The initial experiments conducted a comparison between standalone RL agents (trained on the stochastic data) and an MPC controller. The results consistently showed that RL outperformed MPC in terms of performance across all prediction horizons and uncertainty levels, except for cases with very low uncertainty and a long prediction horizon. Furthermore, RL's capacity to manage uncertainty was further demonstrated by the significantly reduced variance in the final cumulative reward, in comparison to MPC. This level of robustness is essential for practical applications in which uncertainty is a common problem.

Further analysis evaluated RL-MPC controllers, specifically RL-MPC 3 and RL-MPC 5, under different uncertainty levels. The findings indicate that RL-MPC controllers consistently outperform the MPC

controller and the RL controller when uncertainty is low. However, as uncertainty increases, the performance of RL-MPC approaches that of MPC, especially with longer prediction horizons. This trend suggests that shorter prediction horizons are preferable for maintaining the superior performance of RL policies within the RL-MPC framework. Moreover, incorporating a value function as a terminal cost function, as in RL-MPC 5, consistently enhances performance over using only a terminal region.

In real-world scenarios, exact uncertainty levels are often unknown, necessitating conservative estimates during controller development. The performed study with a conservative uncertainty level of  $\delta = 10\%$  shows that the RL-MPC controller, with a balanced prediction horizon, can effectively manage varying uncertainty levels, outperforming both RL and MPC at low uncertainty levels with a more gradual drop in performance at higher uncertainty levels as compared to MPC. The MPC framework may be adapted in order to accommodate for uncertainty, specifically a state estimator for output uncertainty and a sample-based approach for model parametric uncertainty as developed in [36]. By implementing this approach, the performance of the MPC can be expected to improve in a stochastic environment. Furthermore, if these methodologies are also applied to the RL-MPC framework, even greater performance improvements can be anticipated.

In conclusion, this chapter has demonstrated that the RL-MPC controller is a highly efficient controller, even in a stochastic environment. While RL still performs better than the RL-MPC controller under high levels of uncertainty, significant performance enhancements can be achieved at low uncertainty levels when the model is well known.

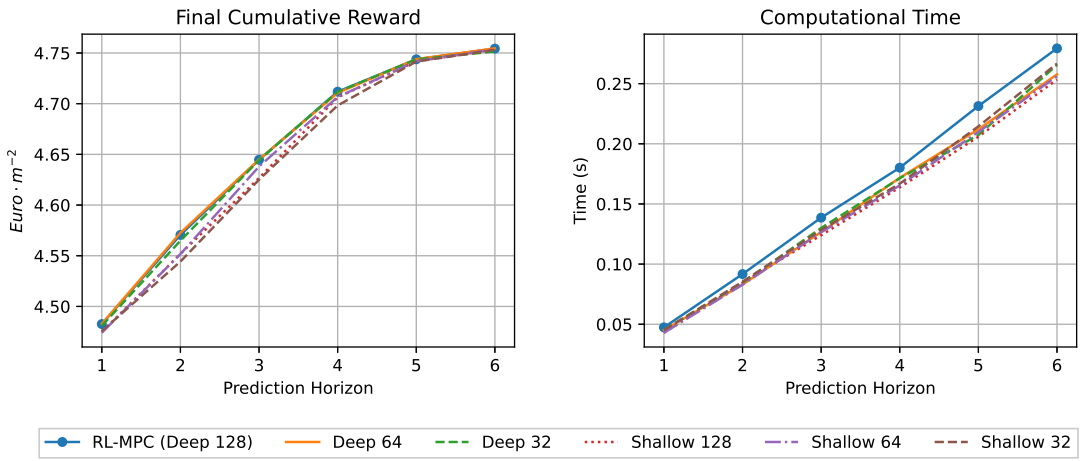
# 7

## Computational Speed Up of RL-MPC

The purpose of this chapter is to provide an overview of the application of making the best performing RL-MPC (RL-MPC 5) algorithm more computationally efficient. While the controller has demonstrated on marginal increase in computational time as compared to nominal MPC, incorporating a neural network as a cost function in larger and more intricate systems may introduce excessive delays and hinder performance. 2 Experiments were conducted in order to achieve speedup and the resulting performance and computational time was investigated. Given that the longer computation time is caused by the inclusion of the value function in the formulation of the MPC algorithm, it is logical to focus on optimising this aspect to improve speed. Three approaches were devised to accelerate the algorithm, with the initial one involving the training of a less intricate surrogate value function instead of employing the complete complex neural network for the terminal cost function. The aforementioned procedure has previously been performed, and the resulting outcomes were documented in chapter 5. It was determined that  $\tilde{V}_4$  can be regarded as a surrogate value function for  $\tilde{V}_1$ . The surrogate value function exhibited greater stability and computational efficiency compared to the full order model. Consequently, it was employed in all subsequent experiments due to its stability. The following experiments are designed to accelerate the algorithm by implementing further simplifications to the neural network. It is important to note that the following experiments were performed on the nominal environment with zero parametric uncertainty.

### 7.1. Reducing Neurons and Hidden Layers

A simple, and yet an effective approach was to reduce the size of the neural network representing the value function. The policy on which the value function was trained on remained fixed. All trained neural networks were trained with the same hyper parameters as outlined in section 3.6. An investigation was conducted on multiple network architects. The initial architecture, on which previous results have been established on and will be considered the baseline performance, comprised of a deep neural network with 2 hidden layers, each containing 128 neurons. To create the smaller neural networks, it was decided to create 3 deep and 3 shallow neural networks. For both the deep and shallow networks, there 128, 64 and 32 neurons in each hidden layer respectively. By doing this, it effectively generates neural networks that become simpler as the number of neurons and hidden layers decreases. Thus makes it possible to examine the impact of the complexity of the neural network on the RL-MPC's performance and computational time. It is important to note that for the deep neural networks, both hidden layers use the same number of neurons.

**Figure 7.1:** Fast RL-MPC with Reduced Neurons

The performance gains, in terms of final cumulative reward, and the computational time of the RL-MPC controller with different neural network architectures vs prediction horizon are shown in Figure Figure 7.1. It is evident that the simpler models reduce computational time, but also at the expense of a decrease in performance. To be more precise, it appears that all simpler neural networks have comparable computational times. However, shallow neural networks have a much more pronounced negative effect on performance compared to deep neural networks, which have a minimal impact on performance.

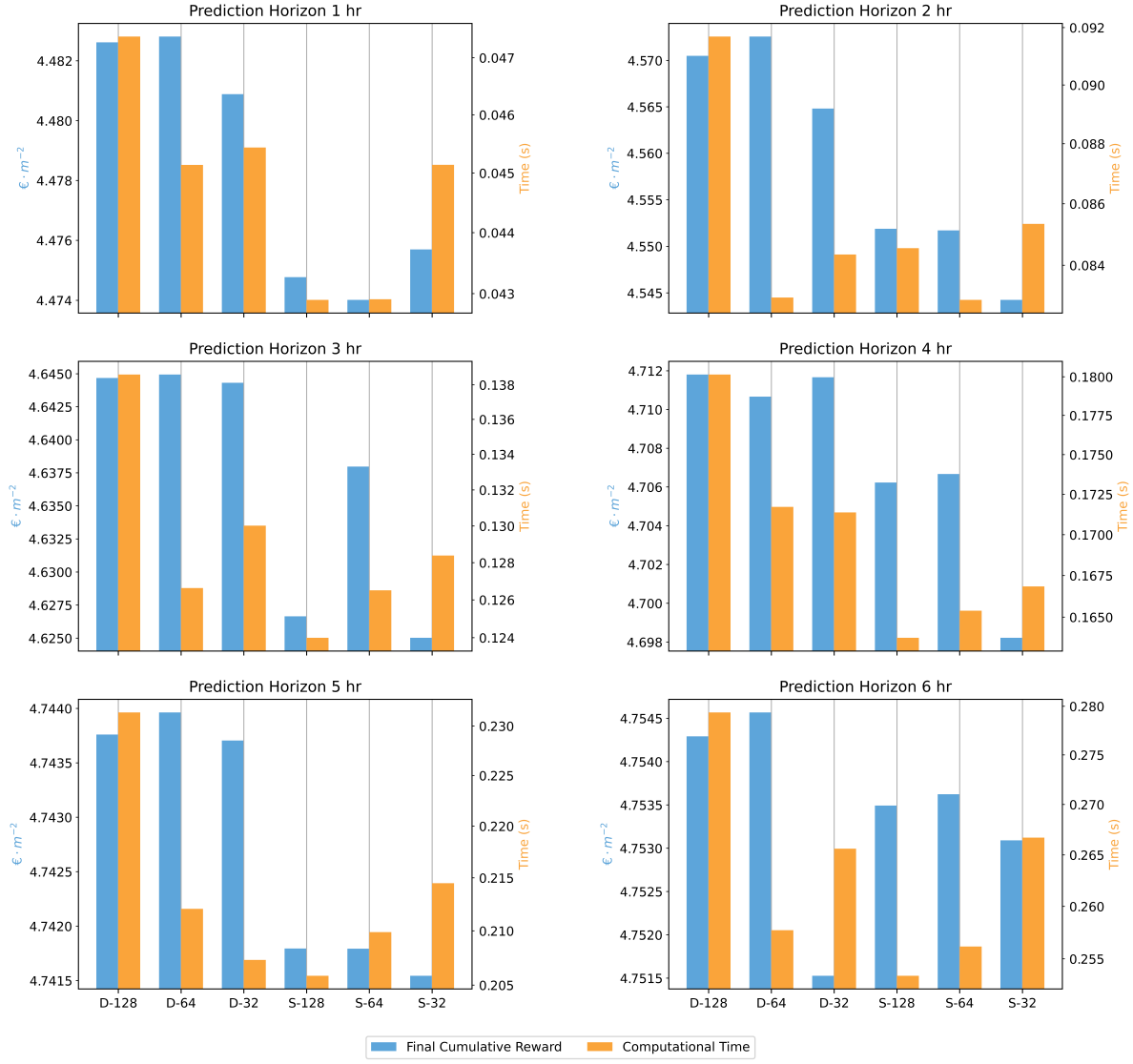


**Figure 7.2:** RL-MPC with reduced neural network complexity for its terminal cost function. where D-128 would stand for "Deep neural network of 128 Neurons per hidden layer".

Figure 7.2 displays a more in depth analysis into the performance gains and computational times of each of the tested neural networks vs prediction horizon. From Figure 7.2, There is no observable correlation between the complexity of the neural network and the improvements in performance and computational time. Contrary to expectations, decreasing complexity does not necessarily result in a decrease in performance time. Although it does suggest the a simpler network can most definitely result in lower computational times albeit at the cost of performance. Furthermore, Figure 7.2 does suggest that the shallow networks offer less benefit, due to their substantial decrease in performance as compared to the simpler deep neural networks. The most effective neural network architecture appears to be a deep neural network with 64 neurons per hidden layer. This architecture achieves performance that is very similar to the original deep neural network with 128 neurons per layer, but with a noticeable reduction in computational time for all prediction horizons. This can both be seen in Figure 7.1 and Figure 7.2. Thus, these findings indicate that while reducing network complexity can speed up the algorithm with minimal to no performance degradation, thorough testing of the neural network architecture is necessary to achieve this.

## 7.2. Taylor Approximation

Perhaps a more intuitive approach would be to use a taylor expansion around a point to locally approximate the neural network in order to achieve speedup. The taylor expansion provides a first order (linear approximation) or a second order (quadratic approximation) of the neural network's outputs with respect to its inputs. While the calculation of the Jacobian of a neural network, which is required for the first-order Taylor approximation, is generally considered to be straightforward. However, determining the Hessian, used in the second order taylor approximation, of a neural network is considerably more difficult and computationally intensive. Nevertheless, employing a second order Taylor approximation would result in more precise approximations around the chosen point, potentially leading to better value function approximations and therefore increase in performance. Fortunately, since the structure of the neural network does not change over the course of the control period, both the Jacobian and Hessian only needs to be calculated once.

The taylor expansion of the neural network was accomplished using Casadi and L4Casadi. The first and second order Taylor expansions were both conducted around the terminal point, which is determined by the initial guess (Equation 5.2) for every time step. The performance and computational time of these approximations were then compared to that of the original neural network when used in the RL-MPC 5 implementation.

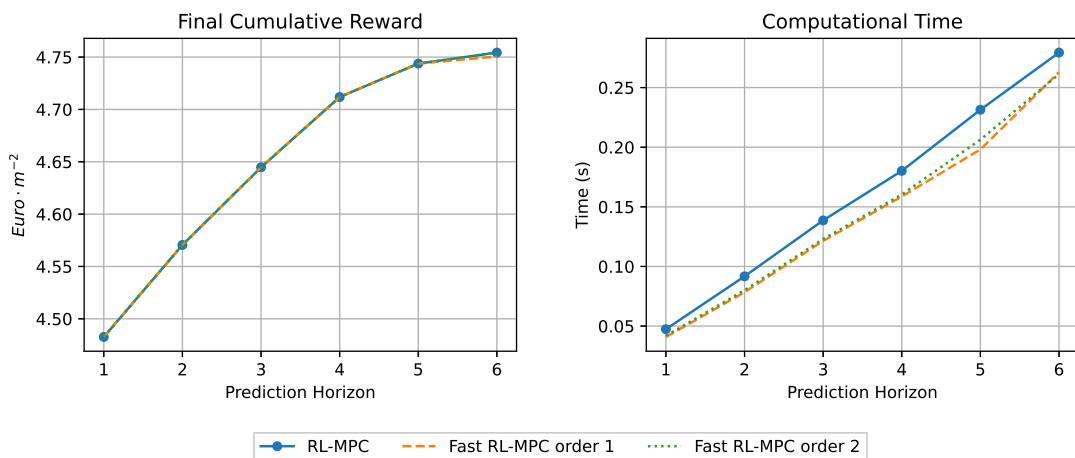


Figure 7.3: Fast RL-MPC with Taylor Expansion

The impact of a linear and quadratic approximation of the neural network around the terminal guess was illustrated in Figure 7.3. Locally approximating the neural network has evident advantages, as both first and second order approximations result in a substantial reduction in computational time without any noticeable decline in performance. It appears that a second order approximation is unnecessary and a first order approximation may be preferable due to its lower computational time without sacrificing performance.

## 7.3. Combined

The following study investigated the combined effects of the two speedup techniques on the RL-MPC algorithm. The experiment includes combining the best results from the previous two experiments.

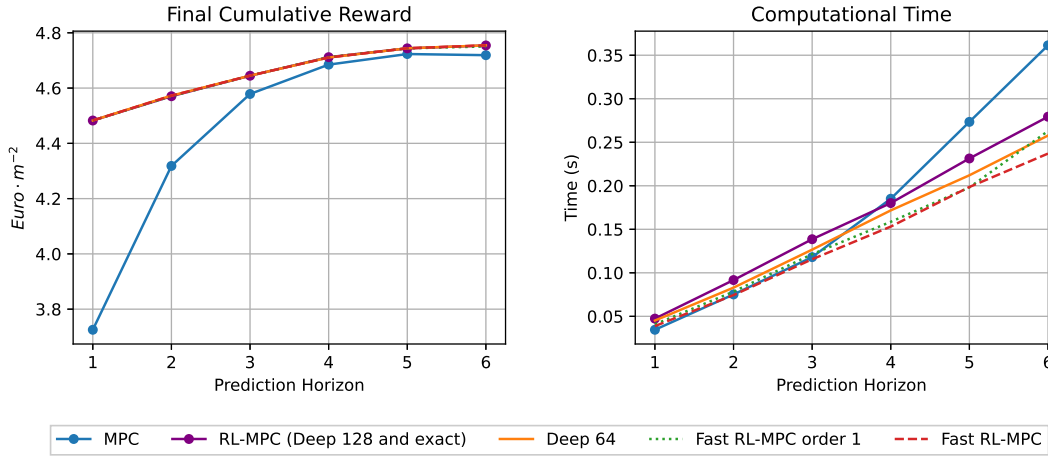


Figure 7.4: Fast RL-MPC

The results of utilising a deep neural network with 64 neurons per hidden layer, along with a first order Taylor approximation around the terminal guess, are presented in Figure 7.4. These findings are compared to the individual speedup techniques used, the original RL-MPC and the nominal MPC. Similar to previous results, Figure 7.1 and Figure 7.3, the combination of the two have zero or little impact on the performance. Although utilising a first-order Taylor expansion reduces computational time more compared to using a smaller deep neural network, the combination of both methods further decreases computational time. The final reduction is significant enough that the computational cost becomes equivalent to or less than that of MPC, even at shorter prediction horizons of 1, 2, and 3 hours. These results are significant because they demonstrate the successful implementation of methods that achieve speedup without compromising performance. These findings could have even greater implications for more complex (greenhouse) systems, where achieving real-time control or minimizing delay is crucial for system performance.

## 7.4. Discussion and Conclusion

Based on the findings of this chapter, it is evident that speedup of the RL-MPC can be achieved. This speedup can be achieved by focusing on strategic adjustments to the neural network used in the terminal cost function. The aim of the experiments detailed in this chapter was to reduce computational time with little to no performance impact.

Initially, efforts focused on making the neural network smaller by reducing neurons and hidden layers. This approach showed that changing the number of neurons and hidden layers has a noticeable impact on both performance and computational time. However, there was no discernible relationship between simpler models and faster computational time or performance improvements. Nevertheless, the results indicated that shallow neural networks generally have a higher trade-off between performance improvements and computational time compared to deep neural networks. It was found that a deep neural network with 64 neurons per hidden layer reduced computational time with no performance losses as compared to the original deep neural network with 128 neurons per hidden layer. Thus it is necessary to do a thorough search of the design space to achieve the desirable reduction in computational time.

Moreover, applying Taylor approximations, both linear and quadratic, around the terminal guess provided further insights to reducing computational time. For both linear and quadratic approximations, the speedup in computational time was noticeable while having no impact on the performance, particularly the first order approximation. In addition, the Jacobian of a neural network is substantially easier to compute than the Hessian. Consequently, opting for a linear approximation may be a more attractive option.

Combining these two approaches yielded the most promising results. Using a smaller deep neural network of 64 neurons per hidden layer with a first-order Taylor approximation achieved computational speeds comparable to or faster than the nominal MPC for every prediction horizon tested. Not only was

the amount of time required for computation decreased, but there was also no noticeable decline in performance.

In conclusion, these findings underscore the feasibility of enhancing RL-MPC's computational efficiency through thoughtful adjustments in neural network complexity and approximation techniques. Such optimizations are crucial for scaling RL-MPC applications to more intricate systems, potentially facilitating real-time control and minimizing delays, consequently enhancing overall system performance. Future research may explore further refinements to the structure of the cost function, potentially using alternative, more intuitive non-linear function approximators instead of neural networks.

# 8

## Discussion and Conclusion

*A conclusion...*

**8.1. Discussion**

**8.2. Conclusion**

**8.3. Recommendations & Future Work**

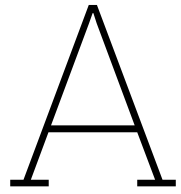
# References

- [1] V. Blazhevska, *Growing at a slower pace, world population is expected to reach 9.7 billion in 2050 and could peak at nearly 11 billion around 2100: UN Report*, Jun. 2019. (visited on 12/01/2023).
- [2] FAO, *The Future of Food and Agriculture: Trends and Challenges*. Rome: Food and Agriculture Organization of the United Nations, 2017, ISBN: 978-92-5-109551-5.
- [3] M. van Dijk, T. Morley, M. L. Rau, and Y. Saghai, "A meta-analysis of projected global food demand and population at risk of hunger for the period 2010–2050," *Nature Food*, vol. 2, no. 7, pp. 494–501, Jul. 2021, ISSN: 2662-1355. doi: [10.1038/s43016-021-00322-9](https://doi.org/10.1038/s43016-021-00322-9). (visited on 12/01/2023).
- [4] Nishat, *The "Green Deal" Greenhouse: A promise for sustainable food supply*, Sep. 2020. (visited on 12/01/2023).
- [5] K. Winkler, R. Fuchs, M. Rounsevell, and M. Herold, "Global land use changes are four times greater than previously estimated," *Nature Communications*, vol. 12, no. 1, p. 2501, May 2021, ISSN: 2041-1723. doi: [10.1038/s41467-021-22702-2](https://doi.org/10.1038/s41467-021-22702-2). (visited on 12/01/2023).
- [6] P. Muñoz, A. Antón, M. Nuñez, et al., "Comparing the environmental impacts of greenhouse versus open-field tomato production in the Mediterranean region," *Acta Horticulae*, vol. 801, pp. 1591–1596, Nov. 2008. doi: [10.17660/ActaHortic.2008.801.197](https://doi.org/10.17660/ActaHortic.2008.801.197).
- [7] C. F. Alvarez and G. Molnar, *What is behind soaring energy prices and what happens next? – Analysis*, <https://www.iea.org/commentaries/what-is-behind-soaring-energy-prices-and-what-happens-next>, Oct. 2021. (visited on 12/01/2023).
- [8] A. Breukers, O. Hietbrink, and M. N. A. Ruijs, "The power of Dutch greenhouse vegetable horticulture : An analysis of the private sector and its institutional framework,"
- [9] B. Morcego, W. Yin, S. Boersma, E. van Henten, V. Puig, and C. Sun, *Reinforcement Learning Versus Model Predictive Control on Greenhouse Climate Control*, Mar. 2023. arXiv: [2303.06110](https://arxiv.org/abs/2303.06110) [math]. (visited on 12/01/2023).
- [10] DevOps, *Greenhouse Climate Control – How to Improve Plant Growth - DryGair*, Aug. 2021. (visited on 12/01/2023).
- [11] P. Rusnak, *What Is the Current State of Labor in the Greenhouse Industry?* Nov. 2018. (visited on 12/01/2023).
- [12] S. Zhang, Y. Guo, H. Zhao, Y. Wang, D. Chow, and Y. Fang, "Methodologies of control strategies for improving energy efficiency in agricultural greenhouses," *Journal of Cleaner Production*, vol. 274, p. 122 695, Nov. 2020, ISSN: 09596526. doi: [10.1016/j.jclepro.2020.122695](https://doi.org/10.1016/j.jclepro.2020.122695). (visited on 12/01/2023).
- [13] J. Arroyo, C. Manna, F. Spiessens, and L. Helsen, "Reinforced model predictive control (RL-MPC) for building energy management," *Applied Energy*, vol. 309, p. 118 346, Mar. 2022, ISSN: 0306-2619. doi: [10.1016/j.apenergy.2021.118346](https://doi.org/10.1016/j.apenergy.2021.118346). (visited on 12/01/2023).
- [14] L. Beckenbach, P. Osinenko, and S. Streif, "Addressing infinite-horizon optimization in MPC via Q-learning," *IFAC-PapersOnLine*, 6th IFAC Conference on Nonlinear Model Predictive Control NMPC 2018, vol. 51, no. 20, pp. 60–65, Jan. 2018, ISSN: 2405-8963. doi: [10.1016/j.ifacol.2018.10.175](https://doi.org/10.1016/j.ifacol.2018.10.175). (visited on 12/13/2023).
- [15] J. Lubars, H. Gupta, S. Chinchali, et al., *Combining Reinforcement Learning with Model Predictive Control for On-Ramp Merging*, Sep. 2021. arXiv: [2011.08484](https://arxiv.org/abs/2011.08484) [cs]. (visited on 12/24/2023).
- [16] S. Lubbers, "Autonomous greenhouse climate control with Q-learning using ENMPC as a function approximator," 2023. (visited on 12/01/2023).
- [17] H. Sikchi, W. Zhou, and D. Held, *Learning Off-Policy with Online Planning*, Oct. 2021. arXiv: [2008.10066](https://arxiv.org/abs/2008.10066) [cs]. (visited on 01/10/2024).

- [18] D. P. Bertsekas, "Lessons from AlphaZero for Optimal, Model Predictive, and Adaptive Control,"
- [19] D. Bertsekas, "Newton's method for reinforcement learning and model predictive control," *Results in Control and Optimization*, vol. 7, p. 100121, Jun. 2022, issn: 2666-7207. doi: [10.1016/j.rico.2022.100121](https://doi.org/10.1016/j.rico.2022.100121). (visited on 12/01/2023).
- [20] M. Lin, Z. Sun, Y. Xia, and J. Zhang, "Reinforcement Learning-Based Model Predictive Control for Discrete-Time Systems," *IEEE Transactions on Neural Networks and Learning Systems*, pp. 1–13, 2023, issn: 2162-2388. doi: [10.1109/TNNLS.2023.3273590](https://doi.org/10.1109/TNNLS.2023.3273590). (visited on 12/01/2023).
- [21] G. De la Torre-Gea, D. Soto-Zarazúa, I. Lopez-Cruz, I. Pacheco, and E. Rico-García, "Computational fluid dynamics in greenhouses: A review," *AFRICAN JOURNAL OF BIOTECHNOLOGY*, vol. 10, pp. 17651–17662, Dec. 2011. doi: [10.5897/AJB10.2488](https://doi.org/10.5897/AJB10.2488).
- [22] Y. Jansen, "Optimal Control of Lettuce Greenhouse Horticulture using Model-Free Reinforcement Learning," M.S. thesis, 2023. (visited on 12/01/2023).
- [23] I. Lopez-Cruz, E. Fitz-Rodríguez, S. Raquel, A. Rojano-Aguilar, and M. Kacira, "Development and analysis of dynamical mathematical models of greenhouse climate: A review," *European Journal of Horticultural Science*, vol. 83, pp. 269–279, Nov. 2018. doi: [10.17660/eJHS.2018/83.5.1](https://doi.org/10.17660/eJHS.2018/83.5.1).
- [24] L. Gong, M. Yu, S. Jiang, V. Cutsuridis, and S. Pearson, "Deep Learning Based Prediction on Greenhouse Crop Yield Combined TCN and RNN," *Sensors*, vol. 21, no. 13, p. 4537, Jan. 2021, issn: 1424-8220. doi: [10.3390/s21134537](https://doi.org/10.3390/s21134537). (visited on 12/05/2023).
- [25] B. Maestrini, G. Mimić, P. A. Van Oort, et al., "Mixing process-based and data-driven approaches in yield prediction," *European Journal of Agronomy*, vol. 139, p. 126569, Sep. 2022, issn: 11610301. doi: [10.1016/j.eja.2022.126569](https://doi.org/10.1016/j.eja.2022.126569). (visited on 01/15/2024).
- [26] J. C. Roy, T. Boulard, C. Kittas, and S. Wang, "PA—Precision Agriculture: Convective and Ventilation Transfers in Greenhouses, Part 1: The Greenhouse considered as a Perfectly Stirred Tank," *Biosystems Engineering*, vol. 83, no. 1, pp. 1–20, Sep. 2002, issn: 1537-5110. doi: [10.1006/bioe.2002.0107](https://doi.org/10.1006/bioe.2002.0107). (visited on 01/16/2024).
- [27] W. J. P. Kuijpers, M. J. G. van de Molengraft, S. van Mourik, A. van 't Ooster, S. Hemming, and E. J. van Henten, "Model selection with a common structure: Tomato crop growth models," *Biosystems Engineering*, vol. 187, pp. 247–257, Nov. 2019, issn: 1537-5110. doi: [10.1016/j.biosystemseng.2019.09.010](https://doi.org/10.1016/j.biosystemseng.2019.09.010). (visited on 01/16/2024).
- [28] M. Ławryńczuk, "MPC Algorithms," in *Computationally Efficient Model Predictive Control Algorithms: A Neural Network Approach*, ser. Studies in Systems, Decision and Control, M. Ławryńczuk, Ed., Cham: Springer International Publishing, 2014, pp. 1–30, isbn: 978-3-319-04229-9. doi: [10.1007/978-3-319-04229-9\\_1](https://doi.org/10.1007/978-3-319-04229-9_1). (visited on 12/19/2023).
- [29] G. Dulac-Arnold, D. Mankowitz, and T. Hester, *Challenges of Real-World Reinforcement Learning*, Apr. 2019. arXiv: [1904.12901 \[cs, stat\]](https://arxiv.org/abs/1904.12901). (visited on 01/16/2024).
- [30] W. J. Knibbe, L. Afman, S. Boersma, et al., "Digital twins in the green life sciences," *NJAS: Impact in Agricultural and Life Sciences*, vol. 94, no. 1, pp. 249–279, Dec. 2022, issn: 2768-5241. doi: [10.1080/27685241.2022.2150571](https://doi.org/10.1080/27685241.2022.2150571). (visited on 01/16/2024).
- [31] E. J. van Henten, *Greenhouse climate management: an optical control approach*. 1994, isbn: 978-90-5485-321-3.
- [32] E. J. Van Henten, "Validation of a dynamic lettuce growth model for greenhouse climate control," *Agricultural Systems*, vol. 45, no. 1, pp. 55–72, Jan. 1994, issn: 0308-521X. doi: [10.1016/S0308-521X\(94\)90280-1](https://doi.org/10.1016/S0308-521X(94)90280-1). (visited on 01/16/2024).
- [33] G. Van Straten and E. J. V. Henten, "Optimal Greenhouse Cultivation Control: Survey and Perspectives," *IFAC Proceedings Volumes*, vol. 43, no. 26, pp. 18–33, 2010, issn: 14746670. doi: [10.3182/20101206-3-JP-3009.00004](https://doi.org/10.3182/20101206-3-JP-3009.00004). (visited on 12/14/2023).
- [34] M. Ghoumari, H.-J. Tantau, and J. Serrano, "Non-linear constrained MPC: Real-time implementation of greenhouse air temperature control," *Computers and Electronics in Agriculture - COMPUT ELECTRON AGRIC*, vol. 49, pp. 345–356, Dec. 2005. doi: [10.1016/j.compag.2005.08.005](https://doi.org/10.1016/j.compag.2005.08.005).

- [35] G van Straten, H Challa, and F Buwalda, "Towards user accepted optimal control of greenhouse climate," *Computers and Electronics in Agriculture*, vol. 26, no. 3, pp. 221–238, May 2000, issn: 0168-1699. doi: [10.1016/S0168-1699\(00\)00077-6](https://doi.org/10.1016/S0168-1699(00)00077-6). (visited on 06/25/2024).
- [36] S. Boersma, C. Sun, and S. van Mourik, "Robust sample-based model predictive control of a greenhouse system with parametric uncertainty," *IFAC-PapersOnLine*, 7th IFAC Conference on Sensing, Control and Automation Technologies for Agriculture AGRICONTROL 2022, vol. 55, no. 32, pp. 177–182, Jan. 2022, issn: 2405-8963. doi: [10.1016/j.ifacol.2022.11.135](https://doi.org/10.1016/j.ifacol.2022.11.135). (visited on 12/05/2023).
- [37] W. van den Bemd, "Robust Deep Reinforcement Learning for Greenhouse Control and Crop Yield Optimization," Ph.D. dissertation. (visited on 12/01/2023).
- [38] S. Hemming, F. de Zwart, A. Elings, A. Petropoulou, and I. Righini, "Cherry Tomato Production in Intelligent Greenhouses—Sensors and AI for Control of Climate, Irrigation, Crop Yield, and Quality," *Sensors*, vol. 20, no. 22, p. 6430, Jan. 2020, issn: 1424-8220. doi: [10.3390/s20226430](https://doi.org/10.3390/s20226430). (visited on 12/01/2023).
- [39] Bonsai, *Why Reinforcement Learning Might Be the Best AI Technique for Complex Industrial Systems*, Nov. 2017. (visited on 12/06/2023).
- [40] K. Daaboul, *Uncertainty and Prediction in Model-based Reinforcement Learning*, Oct. 2020. (visited on 12/06/2023).
- [41] A. Ajagekar and F. You, "Deep Reinforcement Learning Based Automatic Control in Semi-Closed Greenhouse Systems," *IFAC-PapersOnLine*, vol. 55, no. 7, pp. 406–411, 2022, issn: 24058963. doi: [10.1016/j.ifacol.2022.07.477](https://doi.org/10.1016/j.ifacol.2022.07.477). (visited on 12/01/2023).
- [42] L. Wang, X. He, and D. Luo, "Deep Reinforcement Learning for Greenhouse Climate Control," in *2020 IEEE International Conference on Knowledge Graph (ICKG)*, Nanjing, China: IEEE, Aug. 2020, pp. 474–480, isbn: 978-1-72818-156-1. doi: [10.1109/ICBK50248.2020.00073](https://doi.org/10.1109/ICBK50248.2020.00073). (visited on 12/01/2023).
- [43] A. Ajagekar, N. S. Mattson, and F. You, "Energy-efficient AI-based Control of Semi-closed Greenhouses Leveraging Robust Optimization in Deep Reinforcement Learning," *Advances in Applied Energy*, vol. 9, p. 100119, Feb. 2023, issn: 2666-7924. doi: [10.1016/j.adapen.2022.100119](https://doi.org/10.1016/j.adapen.2022.100119). (visited on 12/05/2023).
- [44] Decardi-Nelson Benjamin and You Fengqi, "Improving Resource Use Efficiency in Plant Factories Using Deep Reinforcement Learning for Sustainable Food Production," *Chemical Engineering Transactions*, vol. 103, pp. 79–84, Oct. 2023. doi: [10.3303/CET23103014](https://doi.org/10.3303/CET23103014). (visited on 12/05/2023).
- [45] W. Zhang, X. Cao, Y. Yao, Z. An, X. Xiao, and D. Luo, *Robust Model-based Reinforcement Learning for Autonomous Greenhouse Control*, Oct. 2021. doi: [10.48550/arXiv.2108.11645](https://doi.org/10.48550/arXiv.2108.11645). arXiv: [2108.11645 \[cs\]](https://arxiv.org/abs/2108.11645). (visited on 12/01/2023).
- [46] S. van Mourik, B. van't Ooster, and M. Vellekoop, *Plant Performance in Precision Horticulture: Optimal climate control under stochastic uncertainty*, Jul. 2023. doi: [10.48550/arXiv.2303.14678](https://doi.org/10.48550/arXiv.2303.14678). arXiv: [2303.14678 \[cs, eess, math\]](https://arxiv.org/abs/2303.14678). (visited on 12/01/2023).
- [47] R. S. Sutton and A. Barto, *Reinforcement Learning: An Introduction* (Adaptive Computation and Machine Learning), Nachdruck. Cambridge, Massachusetts: The MIT Press, 2014, isbn: 978-0-262-19398-6.
- [48] R. Bellman, "Dynamic programming," *Science (New York, N.Y.)*, vol. 153, no. 3731, pp. 34–37, Jul. 1966, issn: 0036-8075. doi: [10.1126/science.153.3731.34](https://doi.org/10.1126/science.153.3731.34).
- [49] A. Rao, "OPTIMAL POLICY FROM OPTIMAL VALUE FUNCTION,"
- [50] H. Dave, *Understanding the Bellman Optimality Equation in Reinforcement Learning*, Feb. 2021. (visited on 12/11/2023).
- [51] V. Mnih, K. Kavukcuoglu, D. Silver, et al., *Playing Atari with Deep Reinforcement Learning*, Dec. 2013. arXiv: [1312.5602 \[cs\]](https://arxiv.org/abs/1312.5602). (visited on 12/11/2023).
- [52] L. Dai, Y. Xia, M. Fu, et al., "Discrete-Time Model Predictive Control," in *Advances in Discrete Time Systems*, IntechOpen, Dec. 2012, isbn: 978-953-51-0875-7. doi: [10.5772/51122](https://doi.org/10.5772/51122). (visited on 12/05/2023).

- [53] J. K. Gruber, J. L. Guzmán, F. Rodríguez, C. Bordons, M. Berenguel, and J. A. Sánchez, "Non-linear MPC based on a Volterra series model for greenhouse temperature control using natural ventilation," *Control Engineering Practice*, vol. 4, no. 19, pp. 354–366, 2011, issn: 0967-0661. doi: [10.1016/j.conengprac.2010.12.004](https://doi.org/10.1016/j.conengprac.2010.12.004). (visited on 12/13/2023).
- [54] A. Montoya, J. Guzmán, F. Rodriguez, and J. Sánchez-Molina, "A hybrid-controlled approach for maintaining nocturnal greenhouse temperature: Simulation study," *Computers and Electronics in Agriculture*, vol. 123, pp. 116–124, Apr. 2016. doi: [10.1016/j.compag.2016.02.014](https://doi.org/10.1016/j.compag.2016.02.014).
- [55] C. Bersani, A. Ouammi, R. Sacile, and E. Zero, "Model Predictive Control of Smart Greenhouses as the Path towards Near Zero Energy Consumption," *Energies*, vol. 13, no. 14, p. 3647, Jan. 2020, issn: 1996-1073. doi: [10.3390/en13143647](https://doi.org/10.3390/en13143647). (visited on 12/01/2023).
- [56] J. B. Rawlings, D. Q. Mayne, and M. Diehl, *Model Predictive Control: Theory, Computation, and Design*, 2nd edition. Madison, Wisconsin: Nob Hill Publishing, 2017, isbn: 978-0-9759377-3-0.
- [57] M. Ellis, H. Durand, and P. D. Christofides, "A tutorial review of economic model predictive control methods," *Journal of Process Control, Economic Nonlinear Model Predictive Control*, vol. 24, no. 8, pp. 1156–1178, Aug. 2014, issn: 0959-1524. doi: [10.1016/j.jprocont.2014.03.010](https://doi.org/10.1016/j.jprocont.2014.03.010). (visited on 12/05/2023).
- [58] J. B. Rawlings, D. Angeli, and C. N. Bates, "Fundamentals of economic model predictive control," in *2012 IEEE 51st IEEE Conference on Decision and Control (CDC)*, Dec. 2012, pp. 3851–3861. doi: [10.1109/CDC.2012.6425822](https://doi.org/10.1109/CDC.2012.6425822). (visited on 12/01/2023).
- [59] R. Amrit, J. B. Rawlings, and D. Angeli, "Economic optimization using model predictive control with a terminal cost," *Annual Reviews in Control*, vol. 2, no. 35, pp. 178–186, 2011, issn: 1367-5788. doi: [10.1016/j.arcontrol.2011.10.011](https://doi.org/10.1016/j.arcontrol.2011.10.011). (visited on 12/05/2023).
- [60] M. J. Risbeck and J. B. Rawlings, "Economic Model Predictive Control for Time-Varying Cost and Peak Demand Charge Optimization," *IEEE TRANSACTIONS ON AUTOMATIC CONTROL*, vol. 65, no. 7, 2020.
- [61] S. Hemming, F. de Zwart, A. Elings, I. Righini, and A. Petropoulou, "Remote Control of Greenhouse Vegetable Production with Artificial Intelligence—Greenhouse Climate, Irrigation, and Crop Production," *Sensors*, vol. 19, no. 8, p. 1807, Jan. 2019, issn: 1424-8220. doi: [10.3390/s19081807](https://doi.org/10.3390/s19081807). (visited on 12/01/2023).
- [62] D. Silver, T. Hubert, J. Schrittwieser, et al., "A general reinforcement learning algorithm that masters chess, shogi, and Go through self-play," *Science (New York, N.Y.)*, vol. 362, no. 6419, pp. 1140–1144, Dec. 2018, issn: 1095-9203. doi: [10.1126/science.aar6404](https://doi.org/10.1126/science.aar6404).
- [63] M Jonker, "Model-based Reinforcement Learning: A Survey,"
- [64] V. Mnih, A. P. Badia, M. Mirza, et al., *Asynchronous Methods for Deep Reinforcement Learning*, Jun. 2016. doi: [10.48550/arXiv.1602.01783](https://doi.org/10.48550/arXiv.1602.01783). arXiv: 1602.01783 [cs]. (visited on 12/11/2023).
- [65] D. Silver, G. Lever, N. Heess, T. Degris, D. Wierstra, and M. Riedmiller, "Deterministic Policy Gradient Algorithms,"
- [66] T. P. Lillicrap, J. J. Hunt, A. Pritzel, et al., *Continuous control with deep reinforcement learning*, Jul. 2019. doi: [10.48550/arXiv.1509.02971](https://doi.org/10.48550/arXiv.1509.02971). arXiv: 1509.02971 [cs, stat]. (visited on 12/11/2023).
- [67] J. Schulman, S. Levine, P. Moritz, M. I. Jordan, and P. Abbeel, *Trust Region Policy Optimization*, Apr. 2017. doi: [10.48550/arXiv.1502.05477](https://doi.org/10.48550/arXiv.1502.05477). arXiv: 1502.05477 [cs]. (visited on 12/11/2023).
- [68] C. Yoon, *Understanding Actor Critic Methods*, <https://towardsdatascience.com/understanding-actor-critic-methods-931b97b6df3f>, Jul. 2019. (visited on 12/13/2023).
- [69] J. Schulman, F. Wolski, P. Dhariwal, A. Radford, and O. Klimov, *Proximal Policy Optimization Algorithms*, Aug. 2017. doi: [10.48550/arXiv.1707.06347](https://doi.org/10.48550/arXiv.1707.06347). arXiv: 1707.06347 [cs]. (visited on 12/11/2023).
- [70] S. Fujimoto, H. Hoof, and D. Meger, "Addressing Function Approximation Error in Actor-Critic Methods," in *Proceedings of the 35th International Conference on Machine Learning*, PMLR, Jul. 2018, pp. 1587–1596. (visited on 12/13/2023).
- [71] T. Haarnoja, A. Zhou, P. Abbeel, and S. Levine, *Soft Actor-Critic: Off-Policy Maximum Entropy Deep Reinforcement Learning with a Stochastic Actor*, Aug. 2018. doi: [10.48550/arXiv.1801.01290](https://doi.org/10.48550/arXiv.1801.01290). arXiv: 1801.01290 [cs, stat]. (visited on 12/11/2023).



# RL & RL Training

## A.1. Overview of RL Algorithms

Various RL algorithms exist to solve the MDP problem as discussed above (??). There are two main categories which exist in RL, model-based and model-free. Where model free reinforcement learning solely learns from the interactions between the agent and the environment, without any knowledge of the underlying dynamics. Both have been successfully applied in the greenhouse control problem with model-based RL being used in [45] and model-free in [22], [37], [41], [61]. Both offer their respective advantages and disadvantages. Most commonly, since model-based reinforcement learning encodes the dynamics of the environment, it offers efficient sampling and faster learning since it allows the agent to plan its action ahead of time, whereas model-free has shown to have better asymptotic performance in complex environments. An interesting model-based algorithm as used in Alpha-Zero [62], utilizes a known model, where the policy is planned over the known model and horizon but uses learning for the global solution.[63]. Alpha-Zero was considered the best chess engine upon its release and continues to be recognized as one of the top contenders [62]. However the ground-truth model of the environment is usually not available, and therefore only the simplified dynamics is used in model-based RL. However, model-free is able to learn the model only from experience.

Additionally, model-free algorithms may be classified into two further categories: Policy Gradient methods (Policy Optimization) and Q-learning. Actor-Critic algorithms are an amalgamation of the two. Figure A.1 displays an overview of the non-exhaustive taxonomy of RL algorithms. These RL algorithms (Figure A.1) are used to learn a various aspects (or a combination) of the MDP. These aspects encompass policies (both stochastic and deterministic), Q-functions, value functions, and/or environment models.

This thesis will explore a model-based method of RL. It is imperative to understand both Q-learning and Policy Optimization (and actor-critic methods), although the developed algorithm may be classified as model-based, model-free RL techniques are used to gain an estimation of the value function.

## A.2. Selection of RL Algorithm

In order to select an RL algorithm, it must first be determined what is needed from the respective algorithm. Since the objective of the thesis is to combine RL with MPC with RL as the initial approximate solution to the MPC problem, a value function is required. This value function can either be a Q-function or a State value function. Moreover, the approximated value function needs to accommodate continuous states and actions. ?? outlines the environment, and due to the numerous state variables and actions available, discretizing either the action or state space (or both) would lead to a rapid increase in the dimensionality of the problem (curse of dimensionality). Hence a suitable approach would be the use of actor-critic or policy optimization methods.

All model-free algorithms presented in Figure A.1, except for (Vanilla) Policy Gradient, utilizes an approximated value function. Although A2C/A3C, PPO and TRPO are classified as policy optimization approaches, they are commonly used with critic-networks to reduce variance and increase learning

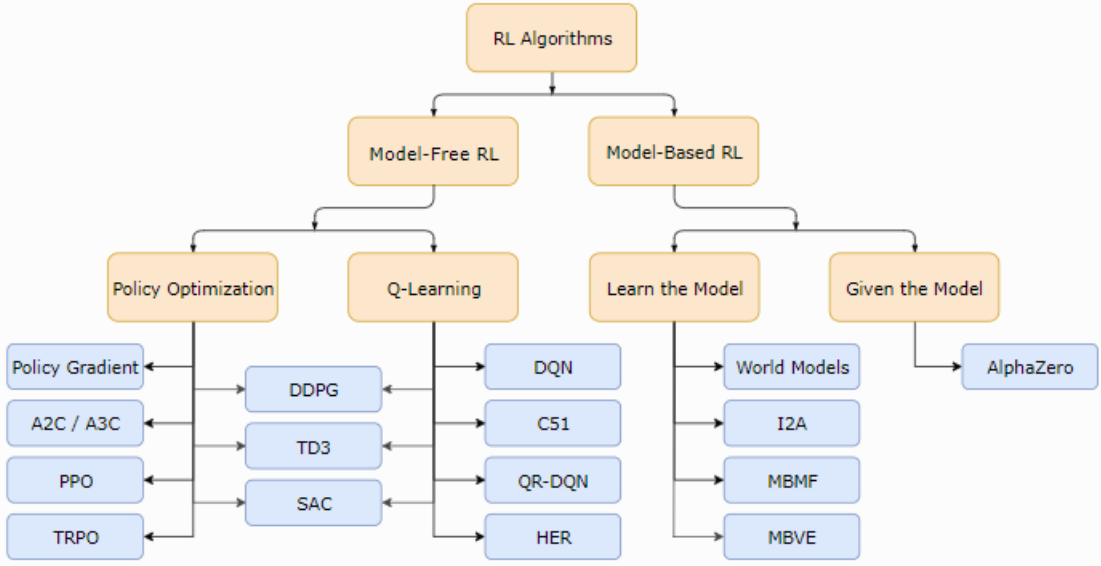


Figure A.1: Taxonomy of algorithms in modern RL

speed, as opposed to using monte-carlo sampling [47].

In recent developments, q-learning algorithms such as DQN (developed in 2013 [64]), originally designed for discrete actions [47], have been extended with Deterministic Policy Gradient approaches [65] to be capable of continuous action spaces. The resulting actor-critic algorithm, known as Deep Deterministic Policy Gradient (DDPG) [66], is an off-policy algorithm capable of both continuous state and action spaces and was developed in 2016.

Furthermore, a policy optimization method, TRPO, was released in 2015 [67] and improved upon the stability and learning speed of vanilla policy gradients by limiting the size of the policy update, although it is a challenging algorithm to implement. The Kullback Leibler (KL) Divergence is applied to ensure that the updated policy does not differ significantly from the previous policy.

In 2016, (Asynchronous) Advantage Actor-Critic A2C/A3C was published [64], whereby A3C is an asynchronous version of A2C. A2C/A3C is on-policy policy optimization algorithm, that uses a value function to optimize the policy gradients. A3C significantly reduces the time of learning by using multiple agents to gather experience to update the shared policy network. The gathered experience is more diverse which stabilizes training as compared to A2C. However, it was found empirically that A2C produces comparable performance to A3C while being more efficient [68].

Proximal Policy Optimization (PPO) was released to further improve on TRPO in 2017 [69]. Instead of using KL divergence to restrict the size of the policy update, first order methods are used to limit the update policy, allowing for easier implementation, faster learning and similar performance.

Finally, in 2018, two algorithms were released. Twin Delayed Deep Deterministic Policy Gradient (TD3) was introduced [70] and expands on the DDPG algorithm. TD3 uses additional Q-functions, delayed updates and policy smoothing to improve the performance and the stability of the DDPG algorithm. Moreover, Soft Actor-Critic (SAC) also extends the framework established by DDPG, but uses entropy regularization for agent exploration and removes the need for policy smoothing. Additional differences are in the way the agents actions are selected during learning, where TD3 uses the target policy, SAC uses the current policy. However, both algorithms are considered state-of-the-art algorithms and have similar performance, with SAC having a slightly faster convergence rate due to its entropy regularization.

Algorithms such as A2C/A3C [64], PPO [69] and TRPO [67], are on-policy methods, albeit state-of-the-art algorithms, have low sample efficiency and high computational cost. The greenhouse is a complex environment and the anticipated learning process for policies in such a complex setting is expected to be long, therefore opting for an off-policy method is deemed desirable. Both Twin-Delayed Deep

Deterministic Policy Gradient (TD3) [70] and Soft Actor-Critic (SAC) [71] are extensions of DDPG that result in a more stable Q-function and thus it was decided to use SAC.

### **A.3. Agent Training**

### **A.4. Value Function Training**

B

RL-MPC